6-2023

Design of a Solar Tracking System with Independent Sensing Unit

Nathan T. Constable
Union College - Schenectady, NY

Design of a Solar Tracking System with Independent Sensing Unit

Nathan Constable

Union College Mechanical Engineering Senior Thesis

2023

Professor William Keat

Abstract

A hybrid loop, dual axis solar tracking system was developed to increase the efficiency of a stationary solar panel by continuously tracking the highest solar radiation point of the sun. The design features two systems that work to find and track the sun vector, the independent sensing unit and main panel unit. The first detects the optimal point of the sun without expending energy moving the large solar panel. The sensing unit consists of 3D printed ASA plastic parts designed to hold and move single photovoltaic cells, ultraviolet sensors, and light dependent resistors. Once the sensing unit has accurately tracked the sun the optimal point is translated to the second unit for energy collection. The second unit, or main panel system, is made of 3003 Aluminum with 1045 steel shafts that control the movement. It collects solar energy using a 50W mono-crystalline photovoltaic panel and stores it in a 12V lithium polymer battery for self-sustaining operation. The motion is achieved using four Pololu gearbox motors for the elevation and azimuth control of both the sensor and main panel units. Worm gears are utilized on all four shafts to achieve a self-locking structure that can sustain winds up to 60 MPH. An Arduino Mega 2560 microcontroller implements a controller algorithm for accurate positional feedback and motion. The proposed system will begin data collection in the spring to determine the energy gain compared to a stationary panel. A 20% increase in energy collection is the expected minimum value that will result from the use of the independent sensing unit paired with the main panel system.

Table of Contents

1. Introduction

The development of solar tracking technology is critical in advancing the clean energy field. By 2050 it is estimated that 16% of the global energy supply could be provided from photovoltaic (PV) solar panels [1]. Changing climate conditions are also going to alter the availability of efficient solar energy conditions in different areas of the world. In the Indian subcontinent, China, parts of North America and Australia there is a projected decrease in solar energy potential over the coming decades [2]. Currently, a low energy conversion efficiency of about 9%-16% exists in stationary photovoltaic (PV) panels [1] [3]. Solar tracking technology can increase the energy conversion from anywhere between 15%-80% [4] and as a result will increase the potential for solar to be a solution to the energy crisis.

Solar tracking systems are designed to find the sun vector and communicate it to the electronic system for movement. Following the sun vector is accomplished by using one of three control methods, and one of two directional movements [5]. The sun vector is comprised of the azimuth and elevation angles which are defined in Figure 1 and as follows. The azimuth angle is measured parallel to the surface from north, and the elevation angle is measured from the surface of earth up to the sun in the sky.

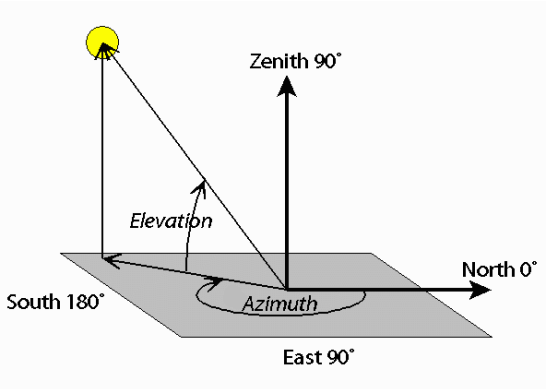

Figure 1: Azimuth and elevation angle diagram [6].

The three control methods for solar tracking are open-loop, closed-loop, and hybrid loop systems, each providing different forms of information to the electronic components for movement. Open-loop systems use a sun position algorithm to determine the sun vector at any given time of day [7]. Opposingly, closed-loop systems generate feedback on the position of the sun through various sensing devices [8]. These sensing devices often include light dependent resistors (LDR's) [8], ultraviolet (UV) sensors [9] and single PV cells [5]. Combining both open and closed loop generates a hybrid-loop system which tracks the sun by switching between the algorithm and the sensor system based upon the atmospheric conditions of the day [Safan - 10].

The mechanism that is controlled by the described loop systems can be separated into two groups, single and double axis trackers. Single-axis trackers rotate around either the azimuth angle or the elevation angle [4]. A limitation of single axis movement is that they require the other axis to be calibrated before energy collection can begin. If there is azimuth control, the elevation of the panel must be set manually, and vice versa. Dual-axis trackers rotate around both the azimuth and elevation axis which requires no calibration, but more complex components.

Multiple studies have been conducted on the effectiveness of open loop systems. Sidek developed an open-loop dual-axis tracker using the United States Naval Observatory sun trajectory patterns which produced a 26.9% increase in energy consumption compared to a stationary panel [11]. Another compared the effectiveness of the Sun Position Algorithm (SPA) to the Astronomical Almanac algorithm (AA) and found that the AA differs from the SPA by 0.4° but is less computationally expensive than the SPA [12]. The designed system also produced a 13.9% energy gain compared to a stationary panel.

Batayneh produced a tracker that moved to three optimal positions each day producing an energy collection of 91%-94% of what a continuously tracking system would produce [Batayneh -13].

Jamroen developed two different closed loop systems one using LDR's and one using UV sensors. The former produced an energy conversion gain of 44.89% while the latter showed a 36.67% gain [8] [9]. This difference goes against the comparison made in the same article where it was determined that the UV had a 12% higher energy gain compared to the LDR system. A single-axis closed-loop system was developed that produced an energy gain of 28.94% compared to the stationary panel, a large output for only one axis of movement [14]. One closed loop system ran for 128 days to determine that the proposed LDR system outperformed the stationary panel by between 17.2% and 31.1% based upon the atmospheric conditions of the day [15].

A hybrid loop system implemented the use of a real time clock module (RTC) and global positioning system (GPS) to determine the time of day and position of the panel. Both were communicated to an algorithm for calculation of the sun vector. An inclinometer was installed to produce an error value between the machine and the actual sun position. The system produced an energy efficiency gain of 38.72% [7]. Rubio and Zhang also used hybrid-loop controls to develop error tracking and analysis of their respective systems [16] [17]. Safan developed a solar tracker that implemented the use of the SPA for initial startup and poor weather tracking. The algorithm was then paired with sun sensors to develop an effective feedback control system [10] that produced an energy gain of 23.3%. The last hybrid loop system implemented the use of a voltage threshold to determine when to switch between open and closed loop systems [18].

2. Design Requirements

A few design requirements were set at the start of the project to guide it in the proper direction. The requirements can be seen in Table 1 and are labeled as want or need based upon importance. A functional decomposition of the overall system is featured in Figure 2.

Table 1: Design requirements and their descriptions.

Requirement	Want or Need	Description
Dual axis	Need	System will require no manual calibration.
Hybrid-loop	Need	Can perform startup without human assistance allowing the system to operate in any location.
Independent sensor system	Need	Will decrease the overall energy consumption of the unit.
Stable up to 60 MPH winds	Need	Highest recorded wind gusts in Schenectady are 60 MPH.
Self-locking mechanical units	Need	The system needs to hold its position when not moving.
Smart tracking	Want	Will increase the efficiency of the system by not tracking when no energy is being gained.
At least 20% energy increase	Want	If the system is below a 20% energy gain more tuning will be performed.
Self-contained energy storage	Want	The unit should recharge its on-board battery which will power the system.

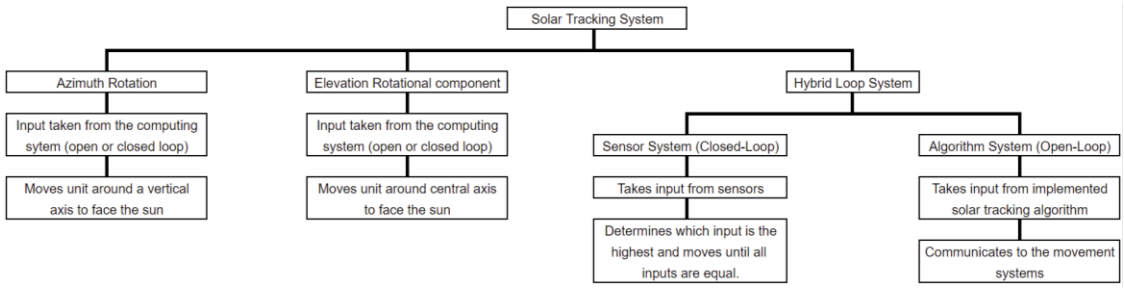

Figure 2: Functional decomposition of the system.

3. Design Overview

The final design (Figure 3) can be broken down into two main components, the sensor tracking system and the main panel system. The sensor tracking system features double-axis movement about the azimuth and elevation and contains a universal mount to hold three types of sensors. The axis movements are controlled by two Pololu DC gearmotors with encoders which power worm gear sets. The main panel system features one Pololu DC gearmotor that turns the same worm gear set as the sensor system. The input is translated to a spur gear train which transfers rotation to the main elevation shaft for panel movement. The main system then features a worm gear box motor with encoder to control the azimuth angle. Both systems feature 360° movement about the azimuth allowing for calibration of the system no matter where it is placed or what orientation it is in. The elevation shaft can rotate around 170° to account for the maximum height of the sun in the sky.

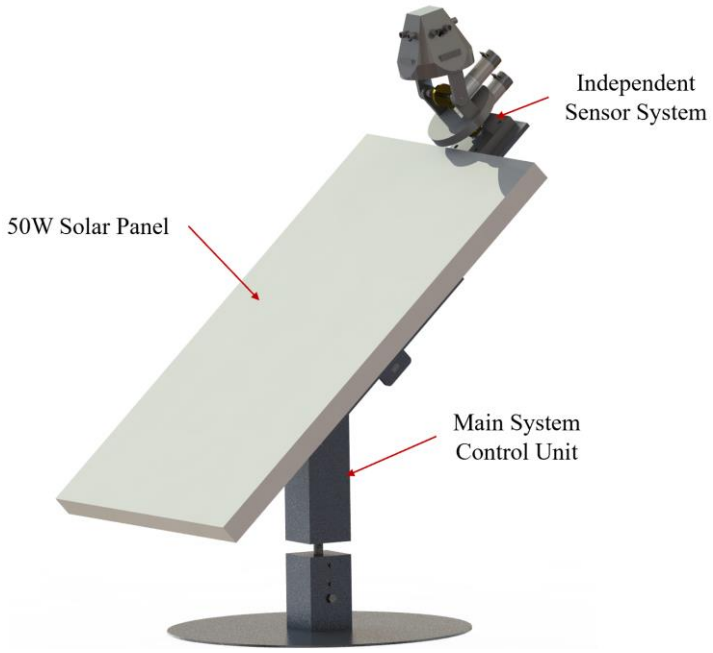

Figure 3: Full System with labeled components.

The sensor tracking subsystem can be seen in Figure 4 and is featured (in Figure 3) on a 6061-aluminum clamp that attaches to the back of the main panel. It moves independent of the main panel unit to decrease the overall energy consumption of the tracking motion. The four aligned sensors compare the feedback on opposing poles (N-S vs E-W) and when one is higher than the other, it moves the system until they are equal. The movement involves taking small steps back and forth until the sensors are reading the same amount. If the main panel were to be performing the same back-and-forth step motion it would consume a larger amount of energy than the sensor system. Another benefit is that the sensor system can communicate the optimal position to multiple panels at once.

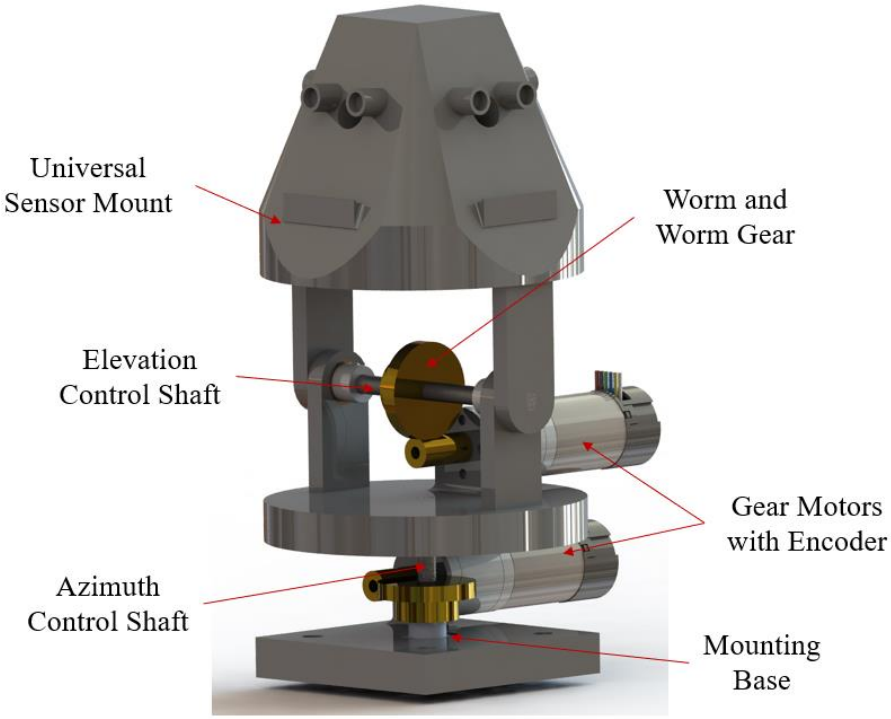

Figure 4: Sensor System with labeled components.

The main system (Figure 5) rests upon a 16 in diametral 5052 aluminum disk to provide a rigid surface for the system to move about. The structure holds a 50W HQST monocrystalline PV panel that has a maximum operating current of 2.3 A. The panel is

secured by two mounting brackets that hold the inside lip of the panel and attach it to the main system upright casing. The casing is made of 3003 aluminum sheets that were water jet and welded together using cut and groove features. The entire casing system rests upon the azimuth shaft that goes into a solid 6061 square aluminum hub. The hub then rests on a hollow piece of square 6061 aluminum tubing for material reduction and easy disassembly. The casing unit can be removed from the system so that work can be done on it independently. The square tubing was welded to the baseplate to provide the structure with a sturdy standing mount. The two shafts are made of ½ in 1045 steel rods.

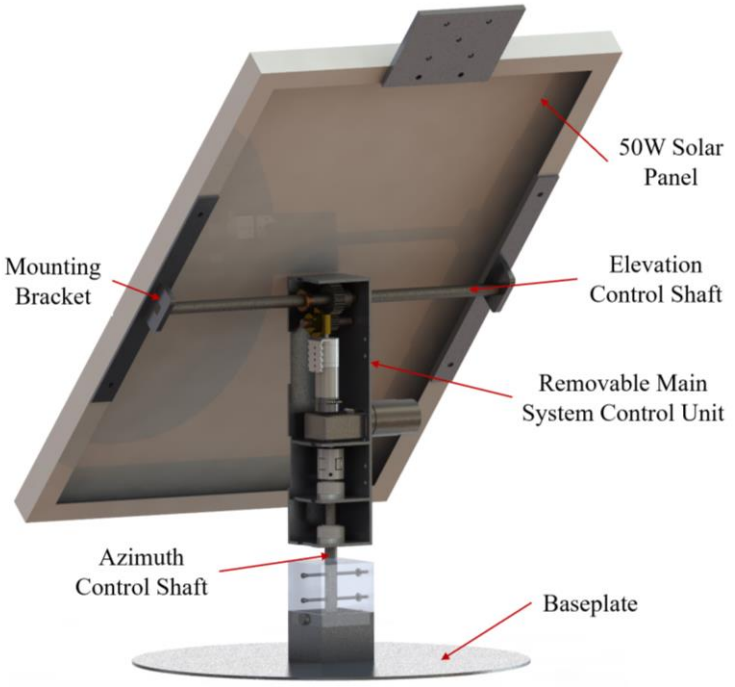

Figure 5: Back side of main panel system, note the removal of the sensor unit.

Once the sensor system has performed the necessary iterative movement to find the optimal tracking position it will send the locational feedback to the Arduino code. The code will translate this information to the specific step lengths that each main system axial motor will have to take to be in the same position as the sensor system. Once the amounts are

determined they are communicated to the main system for movement. Together the two systems create a fluid path for the main panel to efficiently travel about.

4. Detailed Design

The overall design of the system features four categories. The sensor, main, and electronics systems as well as the controller code. All systems function together to generate a fluid tracking motion.

4a. Sensor System

The sensor system features the universal sensor mount that can house LDR's, UV sensors, and single PV cells and is seen in Figure 6 below. All the wiring can flow through the hollow interior, down into the Arduino microcontroller. The single PV cells were the first to be implemented, and they rest upon the labeled shelf. Above the shelf two ¼ in neodymium magnets are attached to the inside of the circular extrusions. Two magnets were attached to the outside of each PV cell so that they could be easily secured to the sensor mount. Due to the unique geometry of the sensor mount, the final product was 3D printed out of ASA plastic. A detailed image of the universal sensor mount can be seen below.

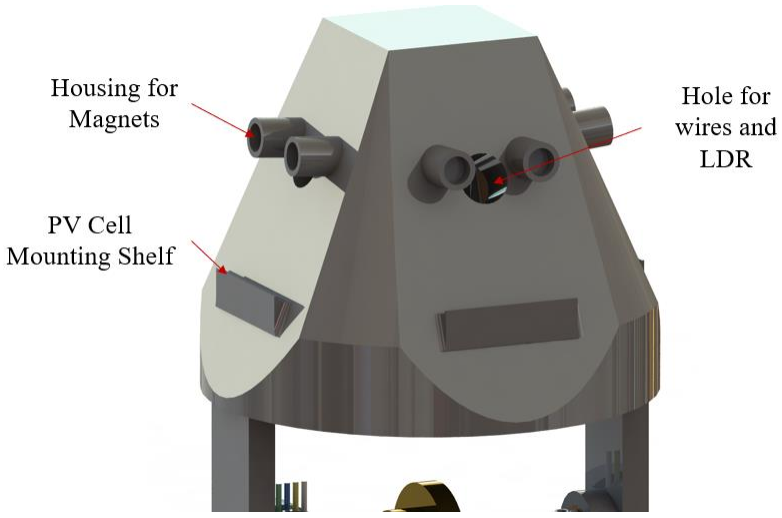

Figure 6: Detailed image of the universal sensor mount.

The universal mount rotates around the elevation control shaft (Figure 7) using a worm gear set and Pololu motor. The worm gear presents a 60:1 speed reduction to enable a low control speed of 0.2 rotations per minute (RPM). The required torque to move the universal sensor mount is 1.71 lb-in and the chosen motor with the worm gear set has a stall torque of 1614 lb-in. The calculations discussed can be seen in Appendix A. The 0.236 in (6 mm) elevation control shaft goes through two oil impregnated bushings before entering a press-fit, double D, hole on the outside arm of the universal sensor mount. The two flat surfaces that make up the double D shape will produce a surface to efficiently transmit torque about without slip. Two shaft collars with set screws secure the shaft axially. The worm gear is also secured with a set screw in the middle of the shaft to ensure proper alignment with the worm.

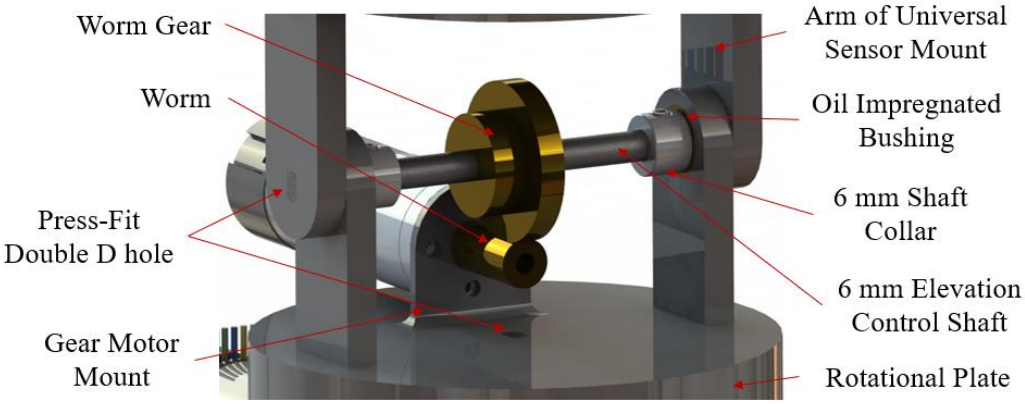

Figure 7: Detailed image of the elevation control system on the sensor unit.

The Pololu gearmotor used in this application was chosen for its low speed (12 RPM) and high positional accuracy (29,000 steps per revolution). The motor also features a 499:1 gear ratio which increases the torque and decreases the speed. The high torque of the motor is not useful for the sensor system, only the low speed, which is why the torque is higher than required. The worm gears were chosen over spur gears because of their self-locking capabilities. Since the system needs to maintain high positional accuracy self-

locking will ensure that the unit is not experiencing any unwanted movement that would require recalibration towards the optimal point.

The azimuth control shaft is powered by the same worm gear set with the same gearmotor to reduce the amount of setup required for the system. A detailed image of the azimuth shaft can be seen in Figure 8. Torque calculations were re-performed for the azimuth shaft using the same assumptions as the elevation shaft, resulting in a required torque of 3.46 lb-in (Appendix A). The speed reduction to 0.2 RPM is the same since the same worm gear set was implemented. The rotational plate that houses the elevation components is supported by a 0.236 in (6 mm) shaft. The shaft is secured to the rotational plate with the same double D flats and features a small plastic spacer to hold the unit up. The spacer rests on a thrust bearing that supports the axial load of the system while still allowing for rotation about the azimuth shaft. The entire system sits upon a square mounting plate which is secured to the aluminum mounting tab pictured in Figure 3. A final shaft collar supports the azimuth shaft from pulling out of the square mounting plate.

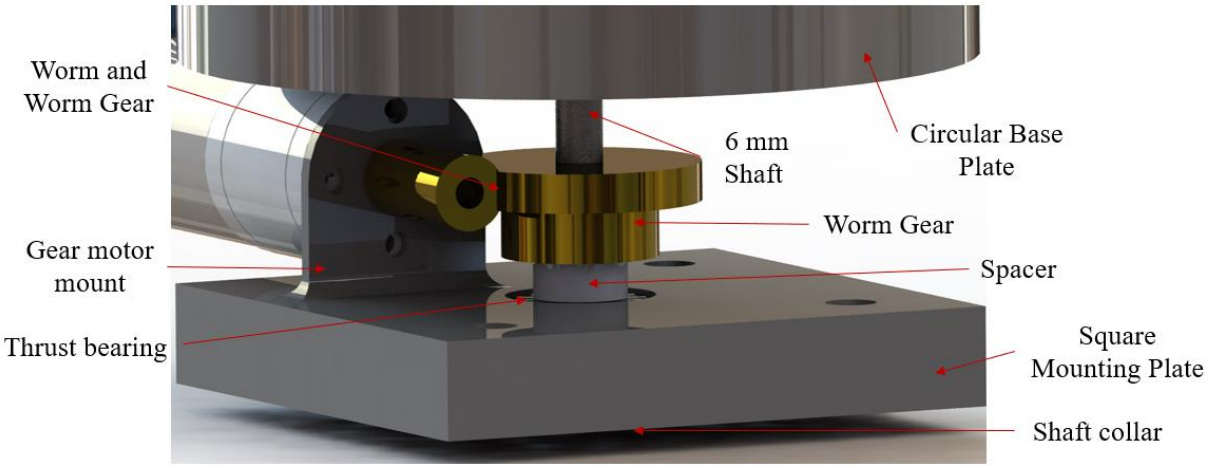

Figure 8: Detailed image of the azimuth control system on the sensor unit

4b. Main System

The main panel unit is responsible for the movement of the 50W solar panel and features similar control structures to that of the sensor system. The internals of the

removable main system control unit can be seen in Figure 5 and feature sets of movement and support components. A more detailed version of the elevation and azimuth control systems can be seen in Figures 9 and 10 respectively.

The elevation control shaft goes through two oil impregnated flanged bushings at the top of the casing unit. Bearings are often used in high-speed applications, so bushings were chosen instead for their low cost and easy installation. To control movement the same Pololu gear motor with a 60 tooth, 0.315in (8 mm) bore worm gear set was chosen. Since the worm gear set has the same tooth count as the sensor system, the same gear ratio was used to produce a speed reduction to 0.2 RPM and a stall torque of 1614 lb-in. The worm gear set now powers a 5/16 in stainless steel shaft that spins a 0.6 in spur gear. The 0.6 in spur gear is compounded to a 1.2 in spur gear to further decrease the speed and drive the elevation shaft. The spur gear set has a gear ratio of two so the new speed and torque are 0.1 RPM and 3228 lb-in (Appendix B) respectively. A compound spur gear set was implemented over a larger worm gear due to cost and size. To put a worm gear with a ½ in bore would not have allowed for clearance of the panel when it is at 90°. All three gears are attached to their respective shafts using set screws.

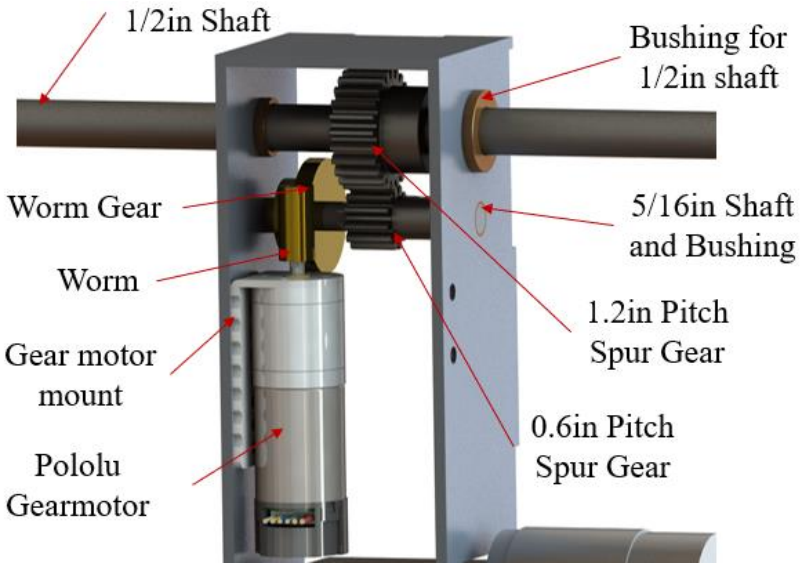

Figure 9: Detailed image of the elevation control system for the main panel.

The azimuth control shaft is featured in Figure 10 going into a flexible shaft coupling that attaches to a worm gearbox motor with encoder. The worm gear box motor has the same encoder pins as the Pololu gearmotor with the advantage of having preinstalled self-locking capabilities. The gear motor attaches to the azimuth control shaft through a flexible coupling to account for any misalignment between the motor and azimuth shafts. The azimuth shaft goes into two pillow block bearings that are mounted to a middle shelf, and the bottom of the casing unit. The shelf is cut and grooved into the left and back portions and held together with a tig weld. Since the shaft will be holding up the entire system, the pillow blocks are installed to support the moment arm created by any force applied on the solar panel, most commonly wind. The shaft sets into the solid aluminum hub for support, where two 1/8 in bolts are sent through for further stability. The hub rests in hollow square aluminum tubing where a ¼ in through bolt is added to hold the unit together. The square tubing decreases the overall material cost while allowing for easy removal of the hub for any adjustments. It is important to note that the removable main system control unit rotates about the stationary azimuth control shaft, the shaft does not

rotate. A final torque calculation was done with the new gearbox motor, and can be seen in Appendix B.

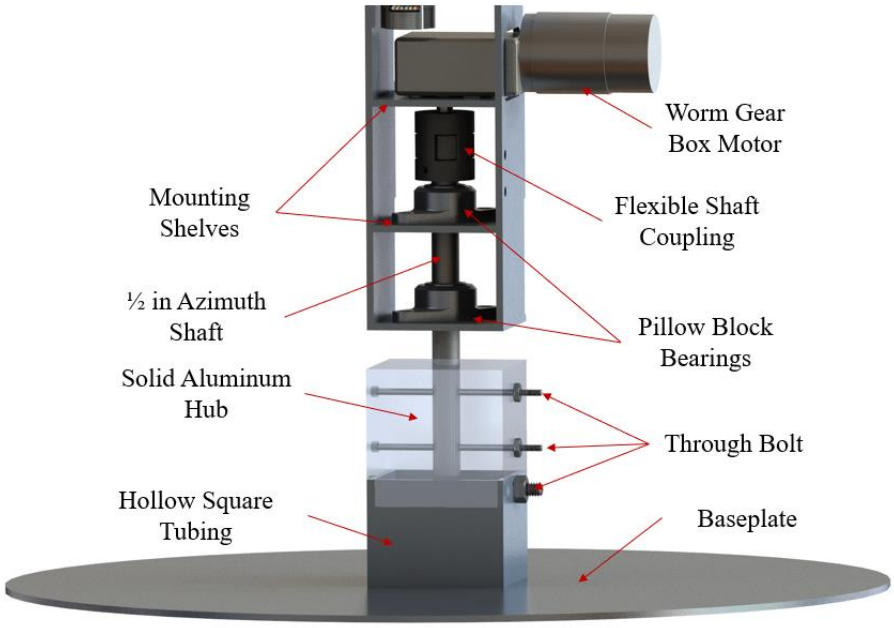

Figure 10: Inside view of the main system control unit with hidden case walls.

Structural Analysis

Hand calculations and finite element analysis (FEA) were performed to determine that the proposed system will not fail in winds up to 60 MPH. The maximum wind speed was chosen based upon the highest wind gust recorded in Schenectady NY during 2022 [19]. Six components at the highest risk for failure were analyzed and all hand calculations can be seen in Appendix C, and all FEA outputs in Appendix D.

To analyze the most critical parts of the system the force exerted on the panel was calculated based upon the uniform loading seen in Figure 11 below. The distributed load was normalized into a single force of drag component that was calculated using,

$$F_D = \frac{1}{2} C_D \rho V^2 A \quad (1)$$

where ρ is the density of air, V is the velocity of air, A is the cross-sectional area of the panel and C_D is the coefficient of drag found as 1.14 [20]. The resulting drag force was calculated as 36.03 lbf which is the driving load for the following calculations.

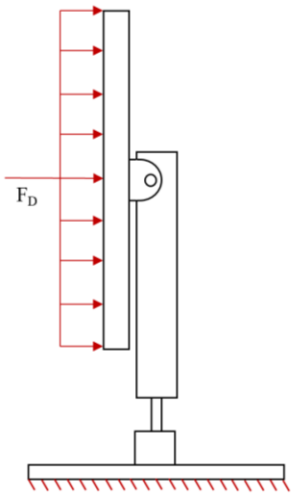

Figure 11: Assumed loading of the main system under a 60 MPH wind gust.

The azimuth control shaft is a critical component in supporting the casing unit and 50W panel. The part was analyzed using FEA for which the free body diagram is seen in Figure 12. For FEA setup the shaft was supported at the top, simulating its fixture to the motor. The resulting force produced by the 36.03 lbf load was applied to the through bolt holes located on the lower half of the azimuth shaft. The analysis produced a maximum stress concentration of 30,000 psi corresponding to a minimum factor of safety (FOS) of 2.57. The shaft experiences a maximum deflection of 0.0618, which can be seen in Appendix C. Additionally, the shaft was analyzed by hand and the solved moment was utilized to find a bending stress of 28,634 psi. Comparing this to the yield stress of 1045 alloy steel, the FOS was found to be 2.72. The calculation can be seen in Appendix C.

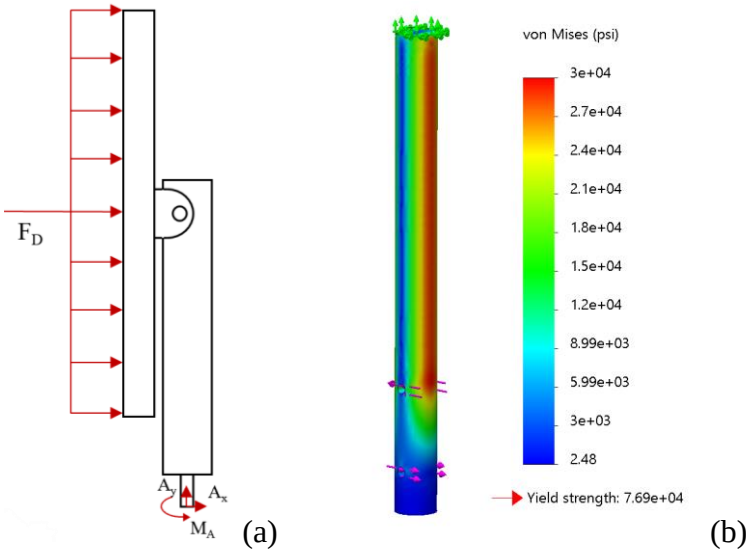

(a) (b)

Figure 12: Azimuth shaft (a) free body diagram and (b) FEA stress output.

The shaft tabs seen in Figure 5 were analyzed to produce an FEA FOS of 12.62. In the FEA setup the bottom extrusion and walls were secured as fixed points, and the 36.03 lbf load was placed on the double D hole. Due to the flats on the inside of the hole the stress concentration did not exceed 475 psi. A hand calculation was performed, note that it is assuming this hole is circular to implement the use of a bearing stress equation. The hand calculation resulted in a FOS of 2.32 ensuring that the part will not fail to either geometry. Figure D.3 and D.4 show the FEA results.

The entire casing unit was the next part to be analyzed in FEA. The unit was supported at the holes where the azimuth shaft interacts with the pillow block bearings. The 36.03 lbf load from the wind was applied where the elevation shaft rests against the two flanged bearings. The analysis produced a FOS of 2.06 and the bushings max load was verified at 370 lbf to ensure they would not crack. The absence of a front plate paired with the hole for the worm gear motor decreases the resistance to bending, however the FOS is still within an acceptable range. The maximum deflection for the part is 0.0146 in. No hand calculations were performed on the case.

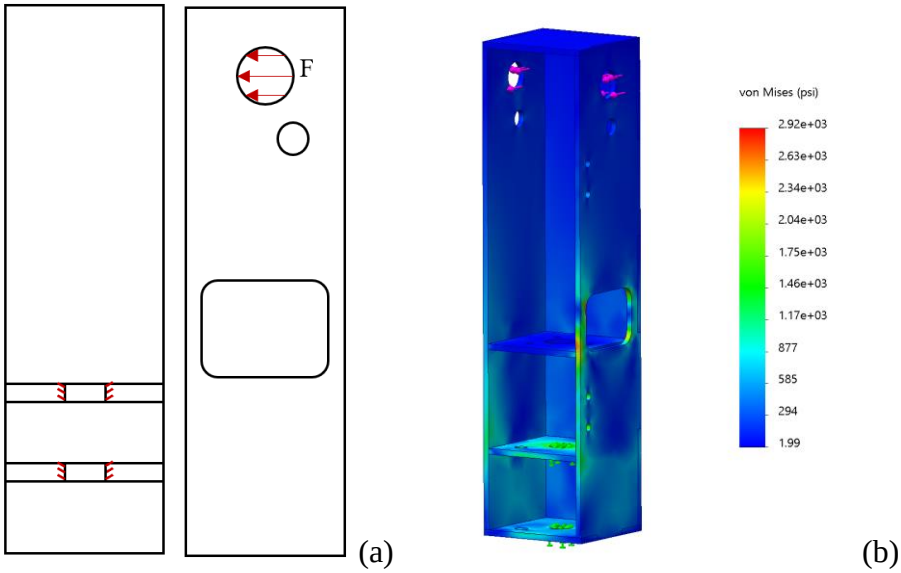

Figure 13: Full casing (a) free body diagram and (b) FEA stress output.

Two additional calculations were performed by hand. The first was a shear and moment diagram of the elevation shaft where two 36.05 lbf loads (force of wind on the panel) were applied on each end of the shaft, and two support loads were applied where the shaft sat in the bronze bushings. Two loads were applied for a conservative check of the part with the idea of even wind distribution across the face of the panel. The free body diagram can be seen in Figure 14 below. Analyzing the shear and moment diagrams of this shaft produced a FOS of 3.8, well above the acceptable limit. The full calculation can be seen in Appendix D.

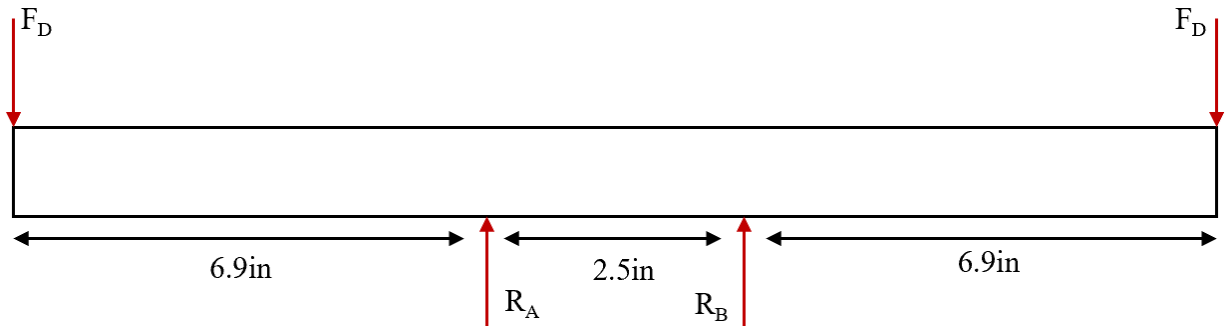

Figure 14: Free body diagram of elevation shaft.

The entire system was then analyzed to see if the circular 16 in 5052 Aluminum base was large enough to resist tipping in a 60 MPH wind gust. The analysis can be seen in Appendix D and observes how much the normal force against the bottom of the system will move when a force of 36.03 lbf is applied to it. The tipping calculation shows that normal force will move 27.28 in, which is above the allowable 8 in and proves that the system will tip in a 60 MPH gust. To overcome this, the final model will be weighted or bolted to the roof, depending upon the available hardware.

Table 2: Summary of factor of safety results from structural analysis.

Part	**FEA FOS**	**Hand Calculation FOS**
Azimuth Shaft	2.57	2.72
Shaft Tabs	12.62	2.32
Casing Unit	2.06	-
Elevation Shaft	-	3.80

A total of 30 drawings were generated to complete the assembly of the proposed design. The drawings include all parts that were water jetted out of sheet metal, all assembly drawings, all parts that were made by hand, and additional parts that were modified for the system. A complete list of all 30 drawings can be found in Appendix E. The nomenclature follows that CU is for drawings related to the casing unit, PM for panel mounting equipment, B for parts on the base, SS for parts on the sensor system and O for parts that were modified or simply did not have a place in another subsection.

4c. Electronics System

The electronics are responsible for automated movement of the solar tracking system. The unit is controlled by a code that takes inputs from the sensors and sun tracking algorithm. Together the optimal position of the sun is found and communicated to the

movement systems. The electronics schematic below shows how the system is wired to the Arduino Mega.

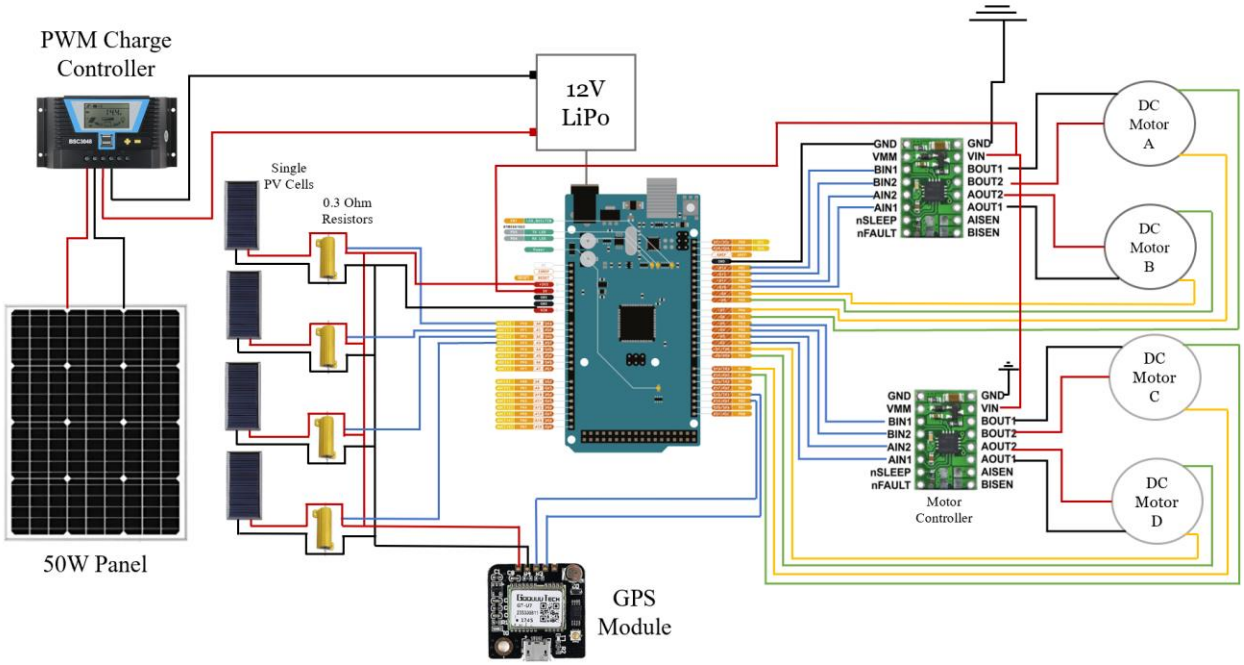

Figure 15: Electronics Schematic of the overall system.

The driving component of the electronics system is the Arduino Mega with an ATmega2560 microcontroller, and 54 DIO pins (of which 15 are PWM). The mega was chosen for its high computational power and large number of pins. It is also a well-documented and reliable component that can handle complex circuits like the one presented. It features 6 RX/TX pins that can be used for board copying, as well as serial information transferal, like that of the GPS module.

On the right of the schematic are the four motors that control the azimuth and elevation for both the sensor and main system. The two sets of motors are identical to each other and are powered from the 5V pin on the Arduino Mega. A Pololu DRV8833 Dual Drive Motor Carrier is responsible for powering the two motors at the designed intervals. The motor driver features two “in” pins and two “out” pins for both motor A and B. Setting

both pins to HIGH causes the motor to run whereas setting both pins to LOW causes the motor to stop. To control direction, pin 1 is set to HIGH and pin 2 is set to LOW, or vice versa. To control the speed, HIGH can be replaced with a numerical value between 0 and 255. Once the driver has sent current to the motors, the encoders obtain feedback on the system and translate it back to the board through the green and yellow wires. The feedback goes back into the microcontroller where the position of the motors can be determined and restricted to keep components from rotating into one another.

On the left of the system there are four single PV cells that are wired as the current sensing system. They are self-sustaining units and generate a voltage based upon the amount of solar radiation they are collecting at any given moment. The first step in controlling the sensor system is to accurately solve for the position of the sun. Four, 400 mA 1 V dual PV cell units were used to track the highest solar radiation point in the sky. To successfully track the sun, each PV cell was connected to a 0.3 ohm high sensitivity resistor. Since the PV cells draw a lower current, a low ohm resistor was used to accurately sense the changes in current. A standard IV curve (Current, Voltage) starts at a constant current for low voltage, and then drastically decreases in current as the voltage increases, as seen in Figure 16 below. To accurately track a change in current, the change needs to be observed during the large change in current (oval in Figure 16). To achieve this, a low ohm resistor that falls within the proper range needs to be utilized. For the 400 mA cell, the resistor value was about 0.3 ohm.

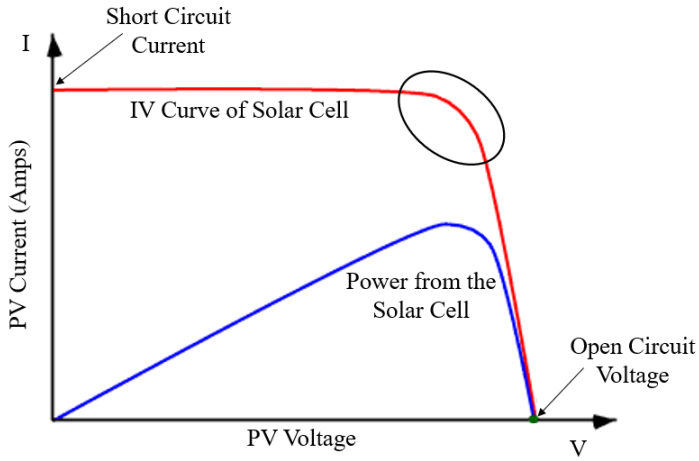

Figure 16: IV diagram of an average solar panel. Note that figure seen here is modified from the source, only the curves were kept [21].

The GPS module, seen in the bottom of Figure 15, operates using the serial RX and TX pins. The RX pin is used to receive data and the TX pin to transmit data. Together they create a loop that provides continuous information transfer. The module is connected to the 5V power from the board and is set to the common ground.

Further left is the main 50W solar panel which is connected to a pulse width modulation (PWM) charge controller. The main panel will be responsible for powering the system. The 12V battery will be dissipating energy to move the four motors and run the code. Power gained by the sun during tracking will be directed into the battery for charge. The battery only gains charge when the solar radiation is greater than the amount of energy expended by the motors. Through testing, it will be determined if the designed system will be efficient enough to gain energy while powering the motors. Lithium polymer (LiPo) batteries will be used for this design as they can handle consistent depletion and energy gain.

An additional encoder unit was added to the worm gear motor, as it did not come with one originally. An AS5600 encoder module was attached to a custom 3D printed part and added to the worm gear motor. Its code [22] runs separate from the main code and is

used to define the positional accuracy of the worm gear motor. The external magnet is less accurate compared to built in encoders, but still describes the motion of the motor.

Missing components from the electronics schematic include the LDR and UV sensor systems. They will be wired into the remaining pins on the left side of the Arduino and will be implemented onto the tracking system.

4d. Microcontroller Algorithm

The microcontroller runs off an Arduino IDE (C++) code that performs the calculations of the sun position and translates them to the system for panel movement. The code features a combination of functions that are called to perform the operating tasks. A logic flowchart can be seen in Figure 17 representing how the algorithm steps through the multiple inputs. The Arduino code was written to perform three main functions, sensor feedback, motor control, and feedback control. All three subsections feature a combination of setup, loop, and independent function logic to complete each respective task. The entire code can be found in Appendix F.

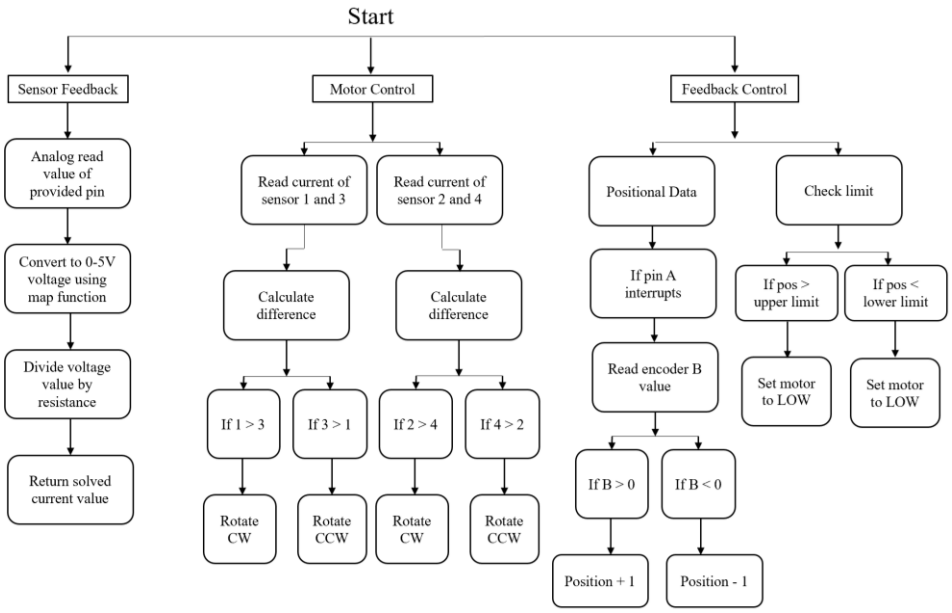

Figure 17: Logic flowchart for solar tracking code.

Sensor Feedback

To accurately track the current through the system, a small function was written. The *readCurrent* function takes a voltage input, converts it to a current, and returns the value to the loop function. Analog pins on the Arduino boards take values on a scale of 0 to 1023. The built in Arduino *map* function converts an analog value to a desired range. Since the board operates at 5 V the analog input read from the Arduino was mapped to a 0-5 voltage value. Once the analog value was converted to voltage, it was simply divided by the resistor value to find current. The main Arduino loop code calls *readCurrent* for each of the four PV cells wired in the system.

Motor Control

The motor control [23] section of the code (*setMotor*) is additionally broken down into two parts, input (motor control) and feedback (encoder control). The analog pins that were used for motor control were first defined in the Arduino code. All pin numbers can be found in the circuit schematic in Figure 15. Analog pins in the motor control are first set to output, and then set to either LOW or HIGH, to control direction and movement. With all pins assigned, and set to LOW, a function was created to determine the motor direction and speed according to the sensor results. The function takes the difference between the two sensors (N-S and E-W), and their respective motor pins as inputs. If the difference between the N-S or E-W cells are greater than zero, the motor was set to rotate one way, and if it is less than zero, it is set to rotate the other way. If the difference is equal to zero both motors stop as that shaft has been aligned. The function can then be utilized to control any of the motors with ease.

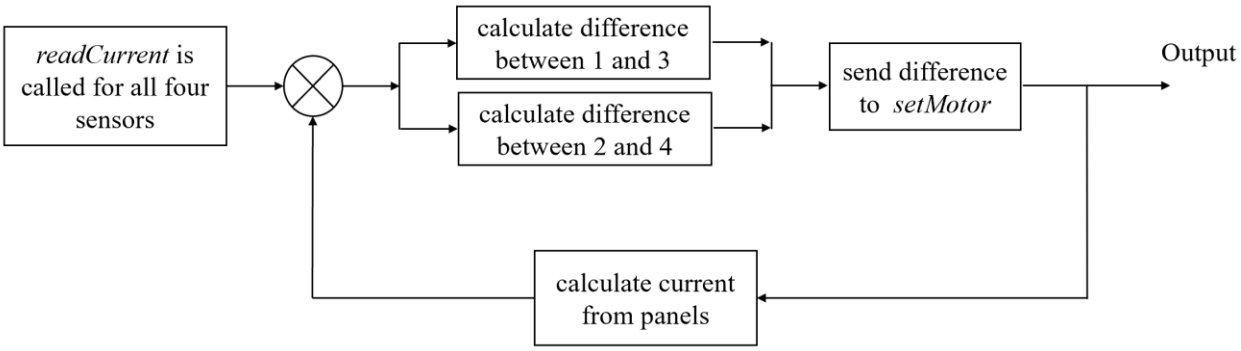

Figure 18: Closed loop control circuit diagram for the motors.

Feedback Control

The feedback control [24] consists of three individual functions that are referred to in the loop section of the Arduino code. To initialize the function *encoderFeedback* the encoder pins (A and B) are wired to analog pins for each of the four motors. The encoder pins are set to input as they are receiving data from the motor and once setup the direction of the motor is observed through the serial monitor. When rotating clockwise, the encoder for pin B is first to rise, whereas for counterclockwise the encoder for pin A rises first. The use of the *encoderFeedback* function is a check to ensure accurate data collection from the motor.

The *readEncoder* function paired with the *checkLimit* function, create an allowable range of motion that is updated every time the code loops. The entire system operates due to the Arduino function called *attachInterrupt* which can be applied to analog pins. To create the autonomous tracking system, the interrupt function was applied to the *readEncoder* function discussed above. The interrupt function is called every time the motor encoder adds or subtracts a step from its count. As a reminder the four gear motors that were implemented have a 29,000 step count per revolution. Each time the count is changed, the *readEncoder* function is called which adds or subtracts a step from the

positional variable. So, if motor A were to move 300 steps, the *attachInterrupt* function would call the *readEncoder* function which would add 300 steps to the positional variable.

Once the read encoder function was accurately counting the number of steps the *checkLimit* function was implemented to set bounds on the rotational limit of each motor. It was determined that the universal sensor mount can move about the elevation shaft 70° in the clockwise direction and 50° in the counterclockwise direction. The sensor unit can rotate about the azimuth shaft a full 720°. For the main system the panel can rotate a full 170° about the elevation and the same 720° about the azimuth. The limits were chosen based upon the average maximum angle of the sun in the sky and the system was designed around them. A figure of the rotation limits is seen below.

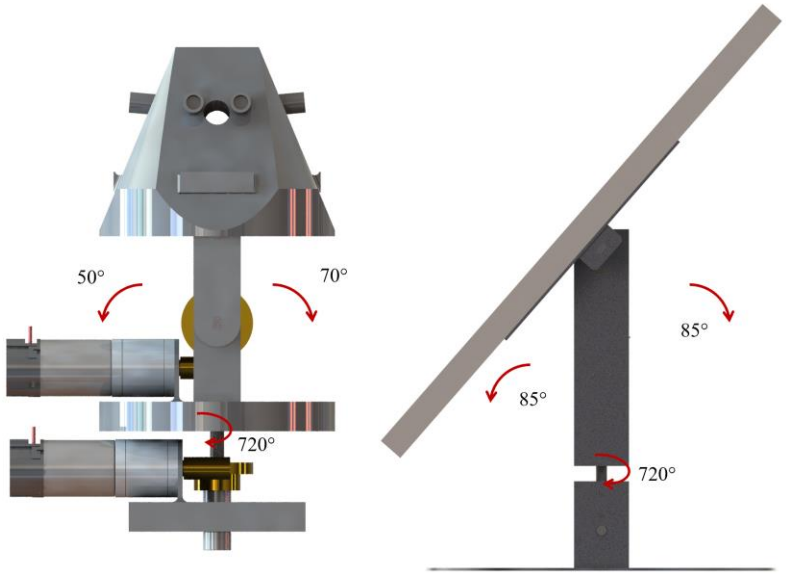

Figure 19: Labeled rotational limits of the axis.

With a gear ratio of 60:1 and knowing that one rotation of the worm corresponds to one tooth rotation of the worm gear, the total rotational limit could be translated from an angle to a step count. The elevation shaft is allowed to travel 260,000 steps in the clockwise direction and 158,042 steps in the counterclockwise direction. The azimuth is allowed to rotate a limit of 1,436,750 steps in both the clockwise and counterclockwise directions for

both the sensor and main systems. The main system is allowed to rotate 678,433 steps about the elevation shaft. The limits ensure that the machine will not crash into itself while attempting to track the sun.

5. Results

Due to time constraints the tracker was unfortunately not tested to determine its energy efficiency. The success of this project falls under the full design, manufacture and assembly of the sensor and main system. The sensor system is receiving feedback from the PV cells and calculating a difference required for movement of the motors. The motors are functioning for both the azimuth and elevation shafts, but require further debugging (detailed in section 7). The main system is fully assembled and was briefly tested to prove movement of the azimuth shaft, and partial movement of the elevation shaft. Both need to be properly scaled to the sensor system, as right now they are moving too quickly and for too long. This problem is arising due to the difference in gear ratios between the two systems. While it is disappointing to not have data to present, the project has reached a successful and conclusive end from the production and assembly. Small modifications need to be made to both the physical and electronic components, however all of that information is explained in section 7. Below is a series of pictures representing the final product for the solar tracking system.

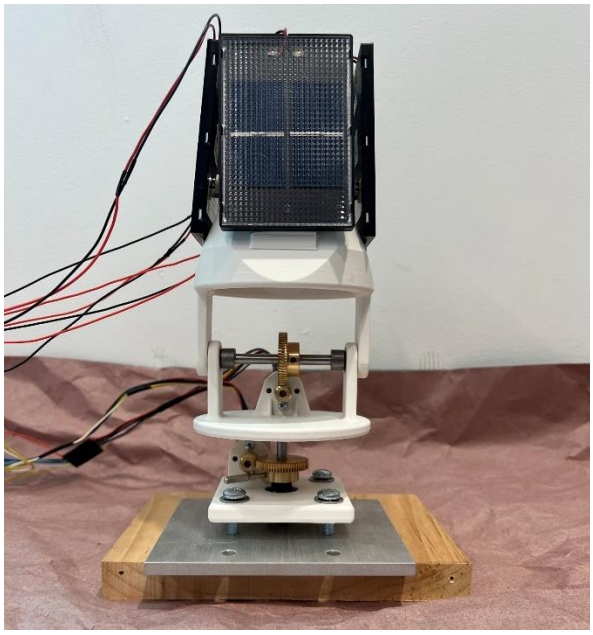

Figure 20: Assembled sensor system mounted on wooden platform.

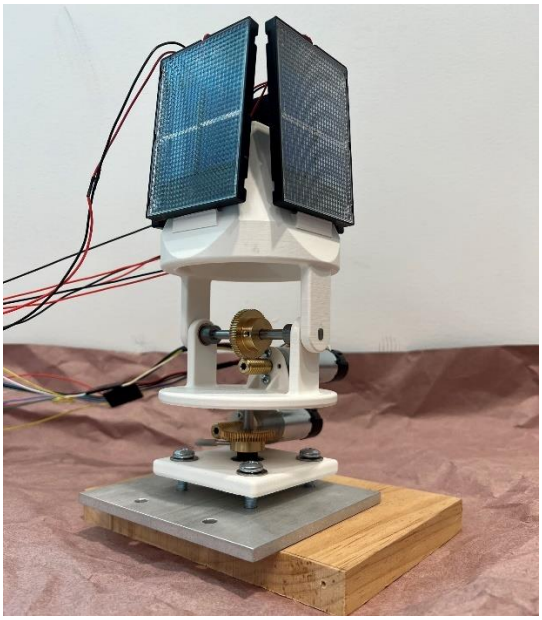

Figure 21: Assembled sensor system side view

Figure 22: Assembled main panel system front.

Figure 23: Assembled main panel system back.

Figure 24: Assembled main panel system side.

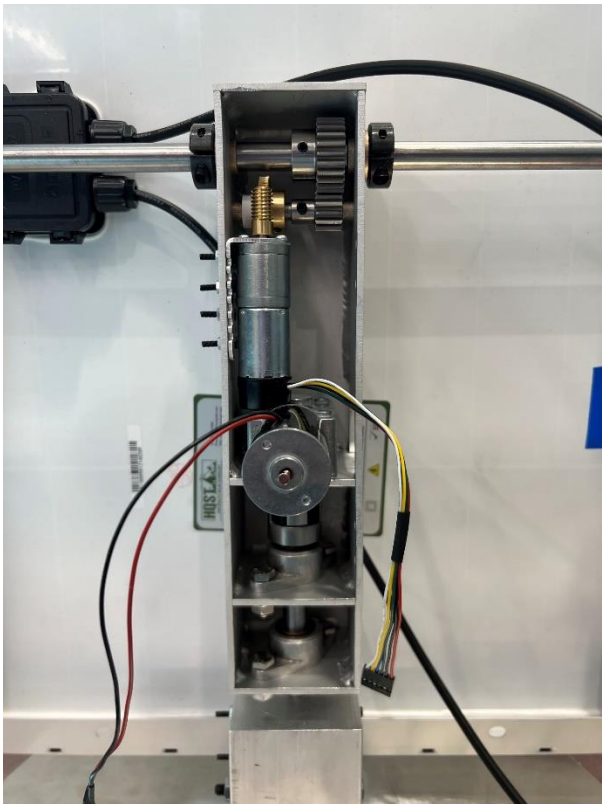

Figure 25: Assembled main panel close up

6. Conclusion

A solar tracking system with an independent sensing system has been successfully designed and created to decrease the amount of energy required to track the optimal point of the sun. The unique sensing system utilizes three different types of sensors to efficiently track the sun on a smaller scale before communicating to the main panel system for accurate movement. The system developed successfully tracks the location of highest light using four dual PV cell units. The short circuit current of the panels is read to increase the accuracy of the panels tracking. The worm gears used to drive the four shafts (elevation and azimuth of both systems) successfully provide self-locking capabilities for an overall stable structure. The main system is designed for wind gusts of up to 60MPH, where the lowest FOS component is the azimuth shaft at about 2.37.

Due to time constraints, energy conversion data was not collected to determine the success of the proposed system compared to a stationary panel. The success of this project is seen in the full design, manufacture, and assembly of the solar tracking system. While more work is required before a full day of testing, the system is close to its final form, and needs minimal modifications before it can be tested. The system will be donated to Professor Wilk in the Mechanical Engineering department where further fine tuning and research can be conducted with it.

7. Guidance for Additional Work

Unfortunately, too many problems arose in the final term to get to a full day of testing. In the hopes that a student or professor picks up this project, the following section will outline in detail, the work that needs to be done for this project to be completed. The first discussion will be of physical modifications and problems that currently exist, followed by predicted problems that may occur when testing. Then, the electronics and

code will be discussed in the same two-part fashion. Throughout this section the parts box is referred to. Inside of this box is the extent of parts ordered for the solar tracking system. A McMaster Car bag is inside labelled *parts for additional work* and contains critical parts discussed below. Any other parts in this box can and should be used to improve the system. The recommendation is that this section is read in vicinity to the solar tracking system, so that it can be easily followed.

7a. Physical Modifications

For the sensor tracking system, minimal changes need to be made. The biggest is to mount this tracker to the top of the main panel system after it has been tested successfully. Right now, it is roughly mounted to a wooden base. This can be replaced by a machined part if necessary since the current setup is relatively unstable. Either way, the first time the machine is tested the sensor system should be on the ground to see how it reacts.

A change *could* be made to the elevation shaft of the sensor system, if there is a scenario where modifications to it are necessary. Currently, two double D flats are cut into each end of the shaft. This prohibits the shaft from being able to be slide through one end of the universal sensor mount when assembling. To achieve this single sliding motion, a new shaft can be cut with only one flat along the entire face. This will both allow for easy assembly and disassembly, as well as provide a surface for the set screws to interact with.

The main system features more physical modifications, which require disassembly (explained further in this section). On the main system elevation control, there is a small shaft containing the 2:1 spur gear set. Currently, there are no shaft collars on the shaft, only spacers and gears. When the DC motor is supplying power to the shaft, the worm gear is being pushed to the right, and the press fit pushing is sliding out of its manufactured hole.

As a result, the elevation shaft is unable to move up or down. An image is seen below of the result of this phenomenon.

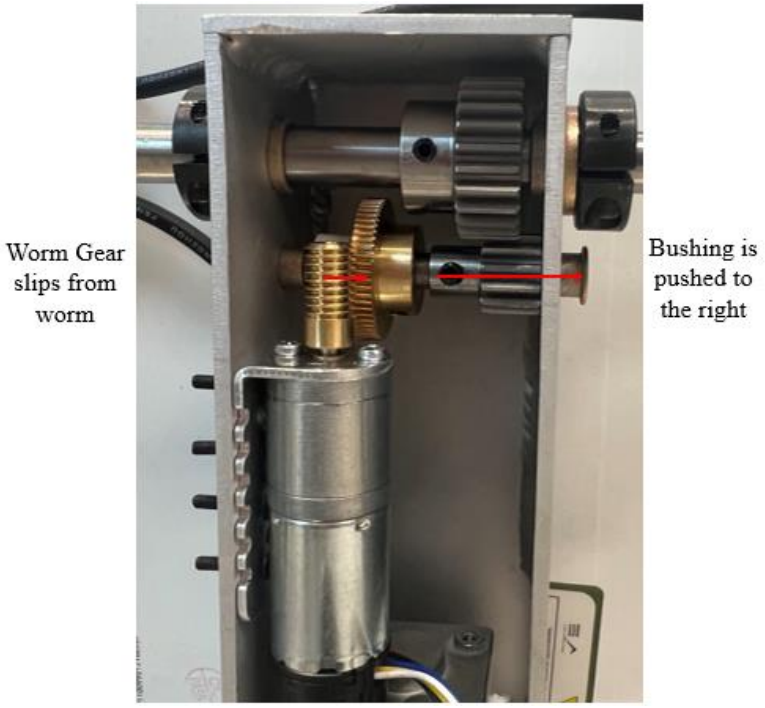

Figure 26: Result of bushing slip from worm gear movement right.

The easiest solution to this problem is to recut a new 8 mm shaft approximately 3.25-3.5 in long. This will allow for the attachment of shaft collars on the outside of the casing unit, which will prevent the rightward slip. Additionally, the gear could be slipping right if the worm is too close or tight to the worm gear. To fix this, the DC motor can be moved out towards the open wall, so that the worm is not too close to the worm gear. To achieve this, the mounting holes for the DC motor should be enlarged to allow for movement of the motor outwards. However larger washers would need to be used on the bolts. Additionally, this step would require disassembly of the system. Both of these solutions should fix this issue.

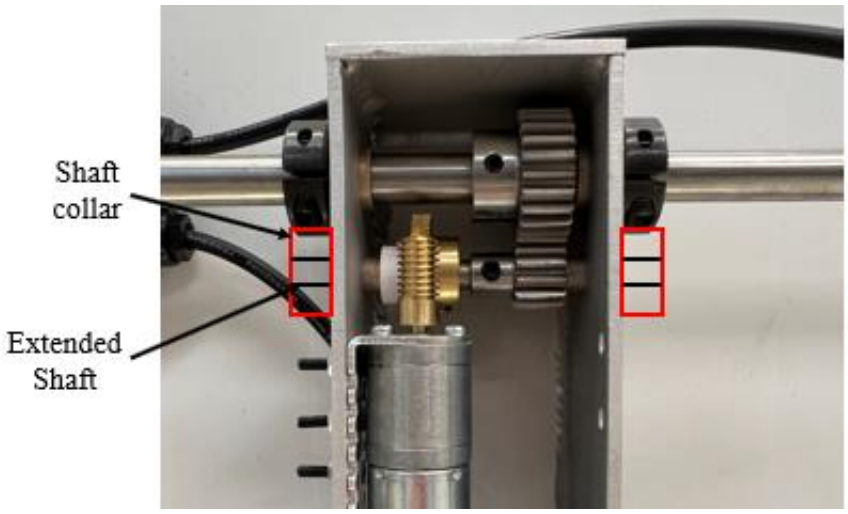

Figure 27: Drawing of modification with shaft collars

Another physical problem is that the small and large spur gears do not teeth perfectly. This allows for a relatively large fluctuation in the panel's rotation. This is challenging to fix, as the mounting holes for the gear set are already cut into the welded casing unit. Potential solutions that come to mind are to find a slightly larger spur gear for either shaft, or to somehow modify the openings so that the shafts can be set closer together. The first solution is the simplest, yet somewhat challenging and tedious to find such a gear. The second is harder conceptually but would result in a better outcome. There is no right solution, but these are the most prevalent at this stage.

Finally, the gear ratio of the worm gear motor that powers the azimuth shaft is currently unknown. Tests can be performed utilizing the encoder that is on the back of the motor and comparing the rotations to the output shaft. The current setup will tell you the number of rotations made by the motor, however not the number of rotations made by the output shaft. To count the output shaft rotations a second encoder can be placed upon it, or one can observe the shaft as it spins, since its rotation is relatively slow. An additional encoder is seen in the parts box. Either way, the gear ratio can be checked by removing the

outer casing and counting the teeth on each gear. A replica motor is also featured in the parts box, so the motor on the main system does not need to be removed.

7b. Predicted Physical Problems

The panel might play where the elevation shaft interfaces with the shaft tabs. Since the double D flats are longer than necessary it has the ability to move left and right slightly, but it will not fall off. Consider adding a 1/2in bore collar with a potential 3D printed spacer to keep the panel from moving at all, similar to the image below. Additionally, the set screws may slip as no geometry exists to interface with the shafts. Consider putting a long flat, or small holes in the shaft to account for this error.

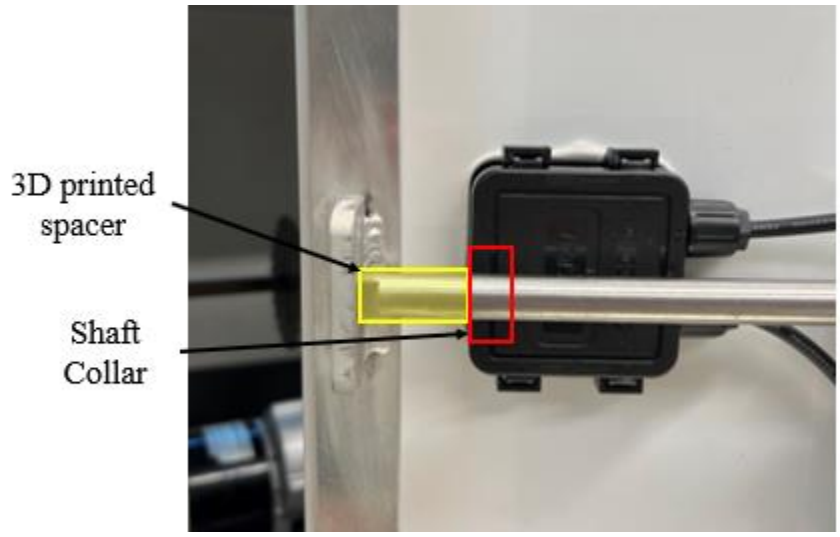

Figure 28: Potential solution for small movements of panel on the elevation shaft.

If the sensor tracking system falls, or is dropped, it will crack. The STL files are provided in the google drive link that Professor Keat has, just ensure to print them out of ASA plastic, as it is UV resistant. Feel free to talk to the 3D printing lab employees about printing with ASA. Outside of these problems the systems should operate according to plan. Of course, there are always unforeseen issues that will need to be handled accordingly.

7c. Electronics and Code Modification

There are two modifications to the existing code for the closed-loop tracking. The first is to determine why the written logic is not properly working. Before final assembly the motors were moving corresponding to the difference between the PV cells. After main assembly that system did not work much at all. There are three potential problems occurring right now. The existing code has a bug, and is not properly comparing the difference, or communicating movement. The only solution to this is to parse through the code to see exactly what is happening, using serial print cues for debugging. The second, potentially more real, issue is the wiring could be faulty from the microcontroller to the motor controllers. All wires were hand stripped and fastened to pins. There is a chance that some of them may have been assembled incorrectly. To sort through this issue, it is best to use a factory-made wire, and replace each hand-made wire, one at a time to see if anything changes. This is a tedious, but it will display where the error is occurring. Note all current wires on the system were crimped and cut by hand.

The next issue is scaling the motor movements between the sensor tracking system, and the main panel system. Currently, the movement speed for the main panel is too high, and not proportional to the angle change experienced by the sensor tracking system. The process for this is simply a relation of the gear ratios, and the root of this problem corresponds to the unknown ratio for the worm gear box motor. Once that gear ratio is known, the scale can be set for the speed at which the main panel motors move in relation to the sensor system motors.

To generate the hybrid-loop system, the open-loop code needs to be found and implemented into the already existing algorithm. The code is discussed above, and sources are provided to find the code. Implementation will be challenging, and will require external

research and work. However, the current setup will support open loop code implementation, especially if it is only applied for setup conditions (finding where the sun is before it breaks the horizon). To implement this, the GPS module found in the parts box is crucial for initial startup conditions. An additional RTC module will need to be added to use the current time for the open-loop code. An RTC module and source code can be easily found online. Those should be the only two inputs needed, however if more parts are required there is a large amount of PCB boards left over for use on this project.

Further down the line after sufficient debugging and testing the system can be made "smart". The initial idea for this project was to make a smart solar tracking system that would be able to shut off and remain stationary when tracking was not worth worthwhile. The base idea was to look at the energy expended to move versus the energy gained from the sun. If expended energy was lower than energy gained the panel would move to an optimal point and wait. If the difference was to flip, the panel would begin tracking again. This implementation on paper is not too difficult but will require sufficient knowledge of the system during coding.

Finally, the long-term goal is to test if the sensor system can be used to track the sun with multiple panels at once. If the same set of parts are used, and the scaling issue discussed is solved, then multiple tracking units could be built and powered off of one sensing system. This would increase the success of the sensing unit, and generate an efficient grid of hybrid loop tracking systems.

7d. Predicted Electronics/Code Problems

It is difficult to predict the multitude of problems that can arise one the electronics and code side. The biggest thing is the implementation of the hybrid loop system will come with a lot of challenging facets. To implement a long open loop code will require very

detailed and organized commenting within the existing algorithm. It will be difficult to add this in Arduino; however, it is possible to find examples of Arduino open loop codes Otherwise, the electronics process will be difficult, but will ultimately make the machine more efficient.

7e. Assembly/Disassembly Instructions

The current state of the solar tracking system is fully assembled. To dissemble it, the following steps should be taken. First remove the bolts from the mounting brackets that attach the panel to the elevation shaft.

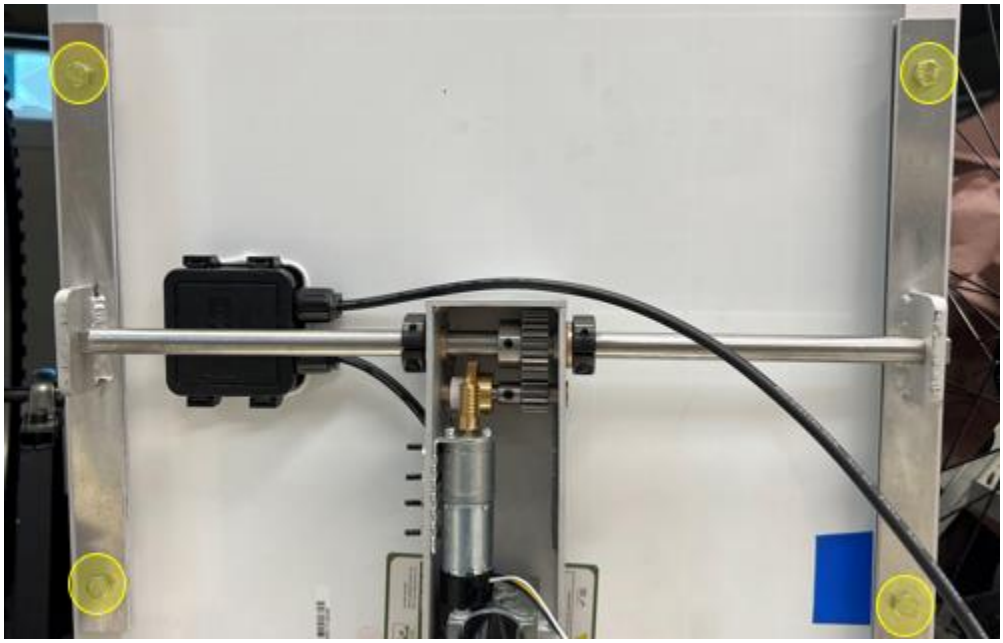

Figure 29: Highlighted bolts to remove to start disassembly.

Once those are removed, slide the brackets off the shaft, removing the panel from the system. Next, loosen the set screw on the lower half of the flexible shaft coupling and lift the main casing unit off of the azimuth shaft that is connected to the circular plate.

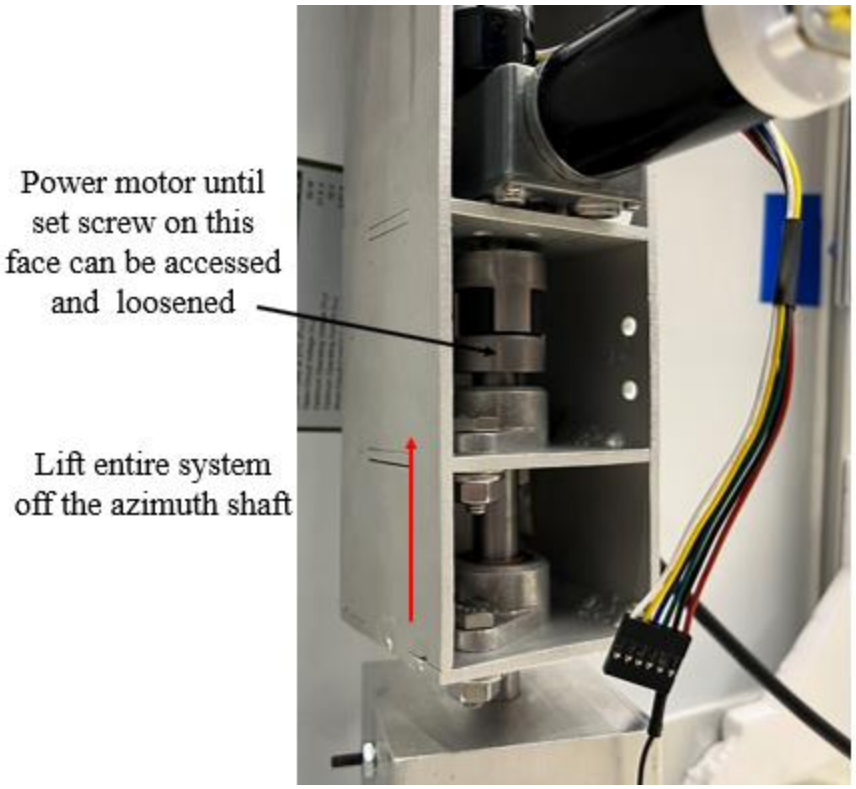

Figure 30: Removing the main casing system

Now the casing unit can be handled with ease for the remainder of disassembly. Remove the DC motor that is connected to the worm and worm gear set by loosening the bolts that hold the mounting bracket to the casing unit. This exposes the small shaft housing the small spur gear, and worm gear. Once the DC motor is removed, loosen the set screws on both the worm and spur gears, and pull the shaft out. Note the bushings will most likely come with the shaft as it is removed.

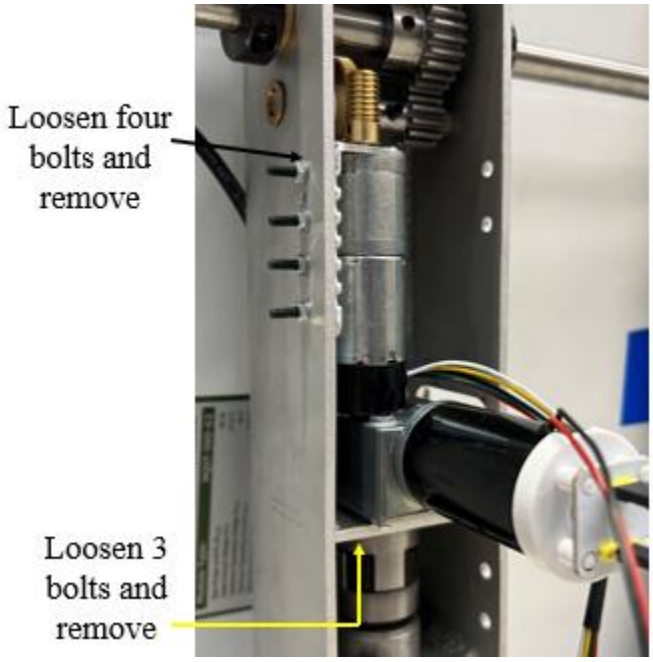

Figure 31: Removing the DC and worm gear motors

Loosen the set screw from the top half of the flexible shaft collar so that the worm gear motor can be removed. Using a socket wrench, or screw head bit with corresponding wrench, remove the three set screws that mount the worm gear motor to its shelf and take it out (this is relatively hard given the tight space). Finally, the pillow block bearings are removed by using a socket wrench to hold the head of the bolt, and loosening the lower nuts until the bolt can be removed. Since the system is compact, it is sometimes useful to wedge the bolt head with a wrench, and use the socket wrench on the other side. Either way it will eventually loosen to where you can do it by hand. Once that is removed the system is disassembled and modifications can be made accordingly. Do not make modifications with components inside, as chips and debris can ruin some of the parts.

Disassembly of the sensor system should be avoided if possible. The lower half, where the azimuth shaft connects base to the rotational plate, can be disassembled by loosening the set screw on the shaft collar and worm gear motor and pulling the top half out. The universal sensor mount cannot be removed in its current design without breaking.

The double D flats prohibit lateral movement of the elevation shaft making disassembly difficult. The only scenario this should occur is if there is a redesign imposed upon the sensor system, such as discussed above. The motors can always be easily removed by moving the worm gear, and loosening the screws holding the motors in place.

To wire the PWM charge controller to the 12V LiPo and PV panel first remove all components from the parts box and place them on the floor. As a general rule the battery should be connected to the PWM charge controller first, and then connect the panel. The charge controller is the component to the right of Figure 32 with the four wires entering. To start, connect the two wires to the battery terminals where brown goes to ground, and the brown wire with the attached fuse goes to positive. Then connect the other ends to the charge controller based on the labels (positive to positive ground to ground). Next, attach the black chords to the chords leaving the solar panel (male goes to female or vice versa). Attach black to ground and attach black with the added fuse to positive. The connectors have engraved indications of the polarity for an extra check. If all three green lights are on that means that everything is set up correctly. Additionally, there is a step by step guide in the parts box to follow along for the connection of the PWM charge controller. The 4A fuses are in the small casing on the red wires and replacements can also be found in the parts box.

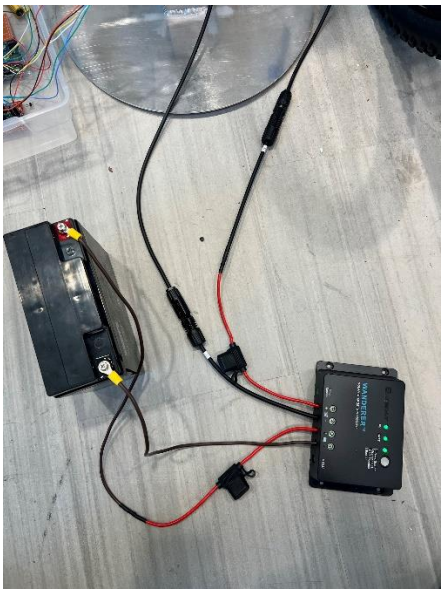

Figure 32: Battery and PV connection to charge controller.

Hopefully the information provided above is helpful in getting this project started again. If any questions arise please feel free to reach out at nconstable23@gmail.com.

Acknowledgements

I would like to thank Professor William Keat for advising me throughout the course of this challenging project. I would also like to thank Professor Richard Wilk and Professor David Hodgson for aiding me in the electronics design and experimentation. Special thanks go to the machinists Robert Harlan and Paul Tompkins for their contributions to my knowledge of machine design and physical work on my project. Finally, I would like to thank my family for their continued support throughout this project.

Sources

[1] R. Venkateswari and S. Sreejith, “Factors influencing the efficiency of photovoltaic system,” *Renewable and Sustainable Energy Reviews*, vol. 101, pp. 376–394, Mar. 2019.

[2] R. Dutta, K. Chanda, and R. Maity, “Future of solar energy potential in a changing climate across the world: A CMIP6 multi-model ensemble analysis,” *Renewable Energy*, vol. 188, pp. 819–829, 2022.

[3] D. C. Huynh, T. M. Nguyen, M. W. Dunnigan, and M. A. Mueller, “Comparison between open- and closed-loop trackers of a solar photovoltaic system,” *2013 IEEE Conference on Clean Energy and Technology (CEAT)*, 2013.

[4] W. Nsengiyumva, S. G. Chen, L. Hu, and X. Chen, “Recent advancements and challenges in solar tracking systems (STS): A Review,” *Renewable and Sustainable Energy Reviews*, vol. 81, pp. 250–279, Jan. 2018.

[5] G. Prinsloo and R. Dobson, *Solar Tracking, Sun Position, Sun Tracking, Sun Following*. Stellenbosch, South Africa: Stellenbosch: Solar Books, 2015.

[6] “What are the ‘azimuth and elevation’ of a satellite? Memorial Spaceflights,” *What are the "azimuth and elevation" of a satellite? | Memorial Spaceflights*. [Online]. Available: https://www.celestis.com/resources/faq/what-are-the-azimuth-and-elevation-of-a-satellite/. [Accessed: 21-Nov-2022]. 3

[7] C.-H. Wu, H.-C. Wang, and H.-Y. Chang, “Dual-axis solar tracker with satellite compass and inclinometer for automatic positioning and tracking,” *Energy for Sustainable Development*, vol. 66, pp. 308–318, Feb. 2022.

[8] C. Jamroen, P. Komkum, S. Kohsri, W. Himananto, S. Panupintu, and S. Unkat, “A low-cost dual-axis solar tracking system based on Digital Logic Design: Design and Implementation,” *Sustainable Energy Technologies and Assessments*, vol. 37, p. 100618, 2020.

[9] C. Jamroen, C. Fongkerd, W. Krongpha, P. Komkum, A. Pirayawaraporn, and N. Chindakham, “A novel UV sensor-based dual-axis solar tracking system: Implementation and performance analysis,” *Applied Energy*, vol. 299, p. 117295, 2021.

[10] Y. M. Safan, S. Shaaban, and M. I. Abu El-Sebah, “Performance evaluation of a multi-degree of freedom hybrid controlled dual axis solar tracking system,” *Solar Energy*, vol. 170, pp. 576–585, Aug. 2018.

[11] M. H. M. Sidek, N. Azis, W. Z. W. Hasan, M. Z. A. Ab Kadir, S. Shafie, and M. A. M. Radzi, “Automated positioning dual-axis solar tracking system with precision elevation and Azimuth Angle Control,” *Energy*, vol. 124, pp. 160–170, Apr. 2017.

[12] M. E. Chowdhury, A. Khandakar, H. Belayat, and R. Abouhasera, “A low-cost closed-loop solar tracking system based on the sun position algorithm,” *Journal of Sensors*, vol. 2019, pp. 1–11, 2019.

[13] W. Batayneh, A. Bataineh, I. Soliman, and S. A. Hafees, “Investigation of a single-axis discrete solar tracking system for reduced actuations and Maximum Energy Collection,” *Automation in Construction*, vol. 98, pp. 102–109, Feb. 2019.

[14] K. Vijaya Bhaskar Reddy, S. Vijaya Kumar, C. Subba Rami Reddy, and A. Hanumantha Rao, “Enhanced performance of Automatic Single-axis Solar Tracking system fed Induction Motor Drive,” *Turkish Journal of Computer and Mathematics Education*, vol. 12, no. 12, pp. 4554–4560, 2021.

[15] F. M. Hoffmann, R. F. Molz, J. V. Kothe, E. O. B. Nara, and L. P. C. Tedesco, “Monthly profile analysis based on a two-axis solar tracker proposal for photovoltaic panels,” *Energy*, vol. 115, pp. 750–759, Jan. 2018.

[16] F. R. Rubio, M. G. Ortega, F. Gordillo, and M. López-Martínez, “Application of new control strategy for Sun Tracking,” *Energy Conversion and Management*, vol. 48, no. 7, pp. 2174–2184, Feb. 2007.

[17] J. Zhang, Z. Yin, and P. Jin, “Error analysis and auto correction of hybrid solar tracking system using photo sensors and orientation algorithm,” *Energy*, vol. 182, pp. 585–593, Sep. 2019.

[18] I. Abadi, E. H. Setyawan, and M. Ardiansyah, “Design of automatic switching system and data acquisition on mobile hybrid solar tracking system for standalone small PV with reflector,” *IOP Conference Series: Earth and Environmental Science*, vol. 520, no. 1, p. 012001, 2020.

[19] “Latham, NY Weather History,” *Weather Underground*, 2023. [Online]. Available: https://www.wunderground.com/history/monthly/us/ny/schenectady/KALB/date. [Accessed: 05-Mar-2023].

[20] Y. A. Cengel and J. M. Cimbala, “External Flow: Drag and Lift,” in *Fluid Mechanics: Fundamentals and Applications*, 3rd ed., New York, NY: McGraw Hill, 2014, pp. 619–621.

[21] C. Honsberg and S. Bowden, “Open-circuit voltage,” *PVEducation*, 2019. [Online]. Available: https://www.pveducation.org/pvcdrom/solar-cell-operation/open-circuit-voltage. [Accessed: 09-Mar-2023].

[22] C. Scientist, “AS5600 Magnetic Encoder a Practical Example,” curiousscientist.tech,

[23] G. Zeglin, “2.1.20. exercise: Drv8833 dual DC motor driver,” *2.1.20. Exercise: DRV8833 Dual DC Motor Driver - 16-223 Introduction to Physical Computing*, 2016. [Online]. Available: https://courses.ideate.cmu.edu/16-223/f2016/text/ex/Arduino/DRV8833-motor-driver/DRV8833-motor-driver.html. [Accessed: 09-Mar-2023].

[24] E. Hartnett, “Pololu - video from content creator curio res: How to control a DC motor with encoder,” *Pololu Robotics & Electronics*, 2021. [Online]. Available: https://www.pololu.com/blog/900/video-from-content-creator-curio-res-how-to-control-a-dc-motor-with-encoder. [Accessed: 09-Mar-2023].

Appendices

Appendix A: Sensor System Motor Calculations

Nathan Constable | Sensor Elevation Motor Calculation | Thesis

Goal

Determine required motor power for the rotation of the small sensor mount

Analysis

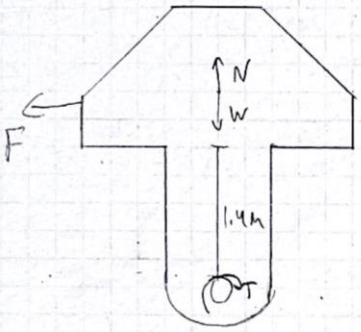

The volume of the unit was determined from solidworks CAD

$V = 13.68 in^3$

and the density of pla is $0.051 \frac{lb}{in^3}$

$W = 13.68 in^3 \cdot 0.051 \frac{lb}{in^3}$

$W = 0.698 lbs$

1 - mini PV panel ~ 0.131bs ~ 0.52lbs for 4 PV cells

$W_T = 0.698 + 0.52 = 1.22 lbs$

Required torque $T = F \cdot r$

$= 1.22 lbs \cdot 1.4 in$

$= 1.71 lbs\text{-}in$

Rotational speed:

Sun moves @ $\frac{15^\circ}{hr} \cdot \frac{1hr}{60min} \cdot \frac{1min}{60s} = 0.00417°/s$

Required power: $P = T \cdot \omega$

$= 1.71 lbs\text{-}in \cdot 0.00417°/s$

$= .00709 \frac{lb\text{-}in}{s}$

Convert to $\frac{g\text{-}cm\ rev}{min}$

$P = 0.00709 \frac{lb\text{-}in}{s} \left(\frac{2.54cm}{1in}\right)\left(\frac{454g}{1lb}\right)\left(\frac{60s}{min}\right)\left(\frac{1rev}{360°}\right) = 1.36 \frac{g\text{-}cm\ rev}{min}$

No motor supplies enough torque at the right spec. going to use a worm gear to accomplish this.

$GR_{worm} = \frac{N_g}{N_w}$ - # of teeth on worm gear / # of threads on worm

$GR = \frac{60 \text{ teeth}}{1 \text{ thread}} = 60$

To calculate the new torque

$GR = \frac{T_{in}}{T_m}$ $T_h = T_m(60) = 26.99 \text{ lbs-in} \cdot 60 = 1619 \text{ lbs-in}$ ✓

much more than needed
↳ recalculate speed

$\frac{\text{Worm-load speed}}{60} = \frac{12 \text{ RPM}}{60} = .2 \text{ rpm}$ with 23,945 seconds per revolution

Conclusion:

Lowest speed 60:1 gear motor runs with chosen worm gear ratio. It fits into the system and provides necessary holding torque for the sensor mount

Pattern Construct | Sensor Azimuth Motor Calculations | Thesis

Goal

Determine required motor torque and speed for the rotation of the bottom table

Analysis

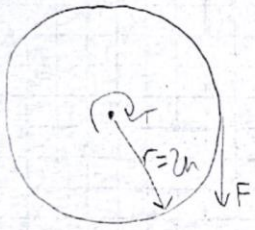

Total weight of the top unit was found to be

$.64 + .36 + .031 + 4(.13) + .01 + .12$

$W_{Total} = 1.73 lbs$

Required Torque $T = F \cdot r$

$= 1.73 lbs \cdot 2in$

$= 3.46 lbs \cdot in$

Rotational speed remains as $\omega = 0.00417$ %

Required power $= T \cdot \omega$

$= 3.46 lbs\text{-}in \cdot .00417$

$= 0.0144 \frac{lb \cdot in}{s}$ or $2.77 \frac{gram\ cm\ per}{min}$

Worm gear ratio

$GR = \frac{\text{no teeth}}{\text{no threads}} \quad \frac{60}{1} = 60$

$\frac{\text{No load speed}}{60} = \frac{12 RPm}{60} = 0.2 RPm$

New torque

$T_n = T_m(60) = 26.4 lbs\text{-}in \cdot 60 = 1614 lbs\text{-}in$

Conclusion

Some motor as sensor mount will work for this application.

Appendix B: Main System Motor Calculations

Nathan Constable | Main Panel Elevation motor calculation | Thesis Functional Torque

Goal

Determine required motor torque to change the elevation of the main panel system.

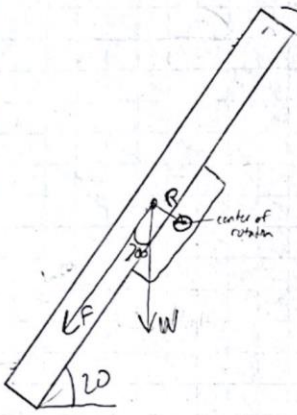

Weight of panel with attachments is

$9.63 + 2(.2516) + 2(.04)$

$W = 10.2116 lbm$

Where $R = 1.64$

Spur gear reduction GR

$GR = \frac{F_{out}}{F_{in}} = \frac{10}{.16} = 2.0$

$W = \frac{.12 RPM}{2.0} = .01 RPM$

Required torque $\Rightarrow T = F \cdot R$

$GR = \frac{T_{in}}{T_m} \Rightarrow T_{in} = (1.64)(2)$

$T_{in} = 3.228$

Translate weight into a + force

$\cos(70) = \frac{W}{F}$ $\quad F = \frac{W}{\cos(20)}$

$F = \frac{10.2116}{\cos(20)} = 29.8516$

$T = 29.8516 \cdot 1.64m$

$T = 31.5416 \cdot m$

Now lets add an extreme wind force say 5.5 lbf, How much torque will it take to continue rotating

assuming rotation about CG

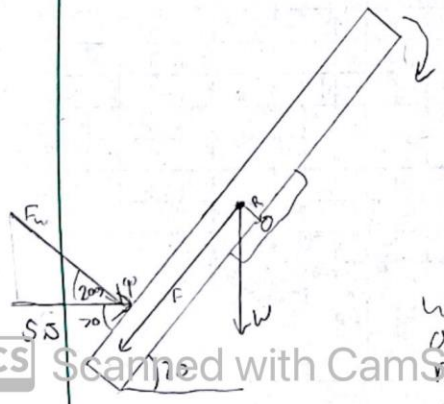

$\cos(20) = \frac{5.5}{F_w}$ $\quad F_w = \frac{5.5}{\cos(20)} = 5.85 lbf$

Torque required to overcome this will be

$T = 5.8516 \cdot 13.2m$

$T = 77.1516 \cdot m$

With a motor + gear ratio that provides 2691 lb-in of torque we still have enough, the chosen motor is fine for this application

Goal

Determine if the worm gear box motor has enough torque to move the entire system.

Analysis

The total weight of the system can be estimated as.

$$W = W_{metal} + W_{panel} + W_{motors} + W_{beams} + W_{coupling} + W_{gears}$$

$$= 3.0016 + 9.6816 + .25lb + .5lb + 2(.10) + (.03) + .10 + .10 + .07$$

$$= 13.8961 bs.$$

Assume that the rotation is about the center point

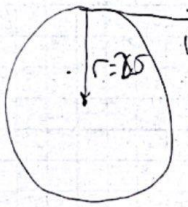

Most of the mass is about .25m off center

$$T = W \cdot R$$

$$T = 13.8948 \times .25m$$

$$T = 3.474 \, lb\text{-}ft$$

Worm gear box motor has a stall torque of 70kg-cm which is equivalent to 60.75 lb-in. We have double the torque required to rotate

Appendix C: Hand Calculations for Main System Analysis

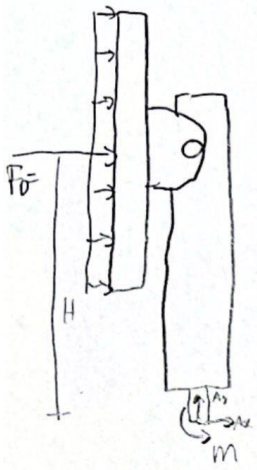

$F_D = C_D \tfrac{1}{2} \rho V^2 A$

$= 1.14 \tfrac{1}{2}(.0763 \tfrac{lb}{ft^3})(92.4 \tfrac{ft}{s})^2 (\tfrac{26.375}{12} \cdot \tfrac{12.0625}{12})$

$= 8064.51 \tfrac{lb\,ft}{s^2} \cdot (\tfrac{1\ lbf}{32.2 \tfrac{lb\,ft}{s^2}})$

$F_D = 36.03\ lbf$

Find Reactions

$(+\circlearrowleft \Sigma M_A = F_D(h)$

$= 36.03(9.75)$

$M_A = 351.4\ lbf\text{-}in$

$\sigma = \frac{Mc}{I} = \frac{351.4\ lbf\text{-}in \cdot .25in}{\frac{\pi}{64}(.5)^4}$

$\sigma = 28,634.6\ psi$

$n = \frac{S_y}{\sigma} = \frac{60,000\ psi}{28634.6} = \boxed{2.1}$ ✓

Failure of Tabs

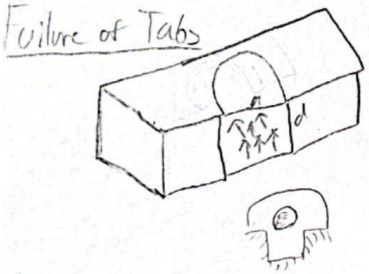

$\sigma_B = \frac{P_B}{ad} = \frac{36.03\ lbf}{.25in(.5in)} = 288.2\ psi$

from Fea $n = \frac{60,000}{[illegible]} = \boxed{2.32}$

Will it tip?

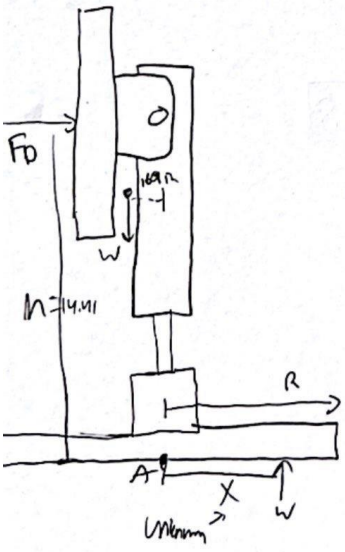

$(+\circlearrowleft \Sigma M_A \Rightarrow W(.69) + F_W(14.41) + N(X) = 0$

$N(X) = F_W(14.41in) - W(.69)$

$X = \frac{36.03lbf(14.41in) + 25lbf(.69in)}{25lbf}$

$X = 27.28in$ ← Guess for X

if X > R it tips

Elevator Shaft

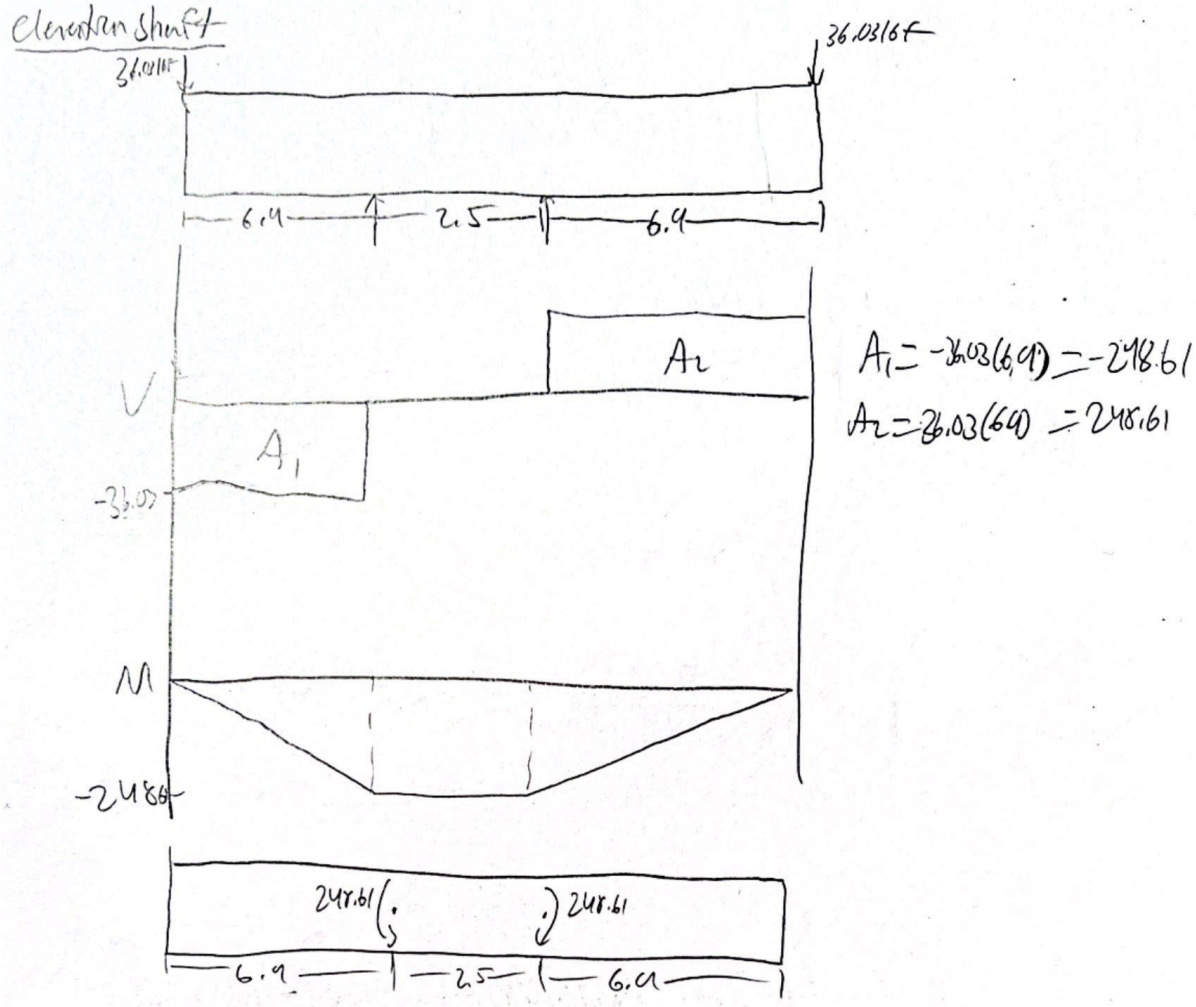

$A_1 = -36.03(6.9) = -248.61$

$A_2 = 36.03(6.9) = 248.61$

$$\sigma = \frac{Mc}{I} = \frac{248.61 \cdot (.125)}{\frac{\pi}{64}(.5)^4} = 20{,}258.6 \text{ psi} \qquad n = \frac{60{,}000 \text{ psi}}{20{,}258.6 \text{ psi}} = \boxed{3.8}$$

Appendix D: FEA Output for Main System Analysis

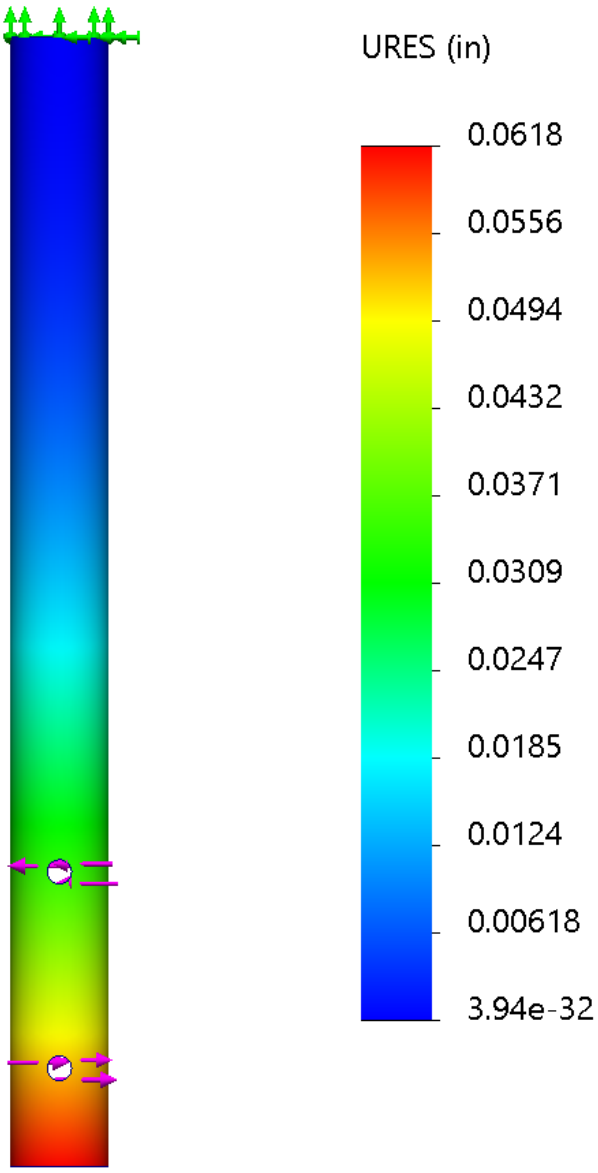

Figure D.1: Displacement of Azimuth Shaft.

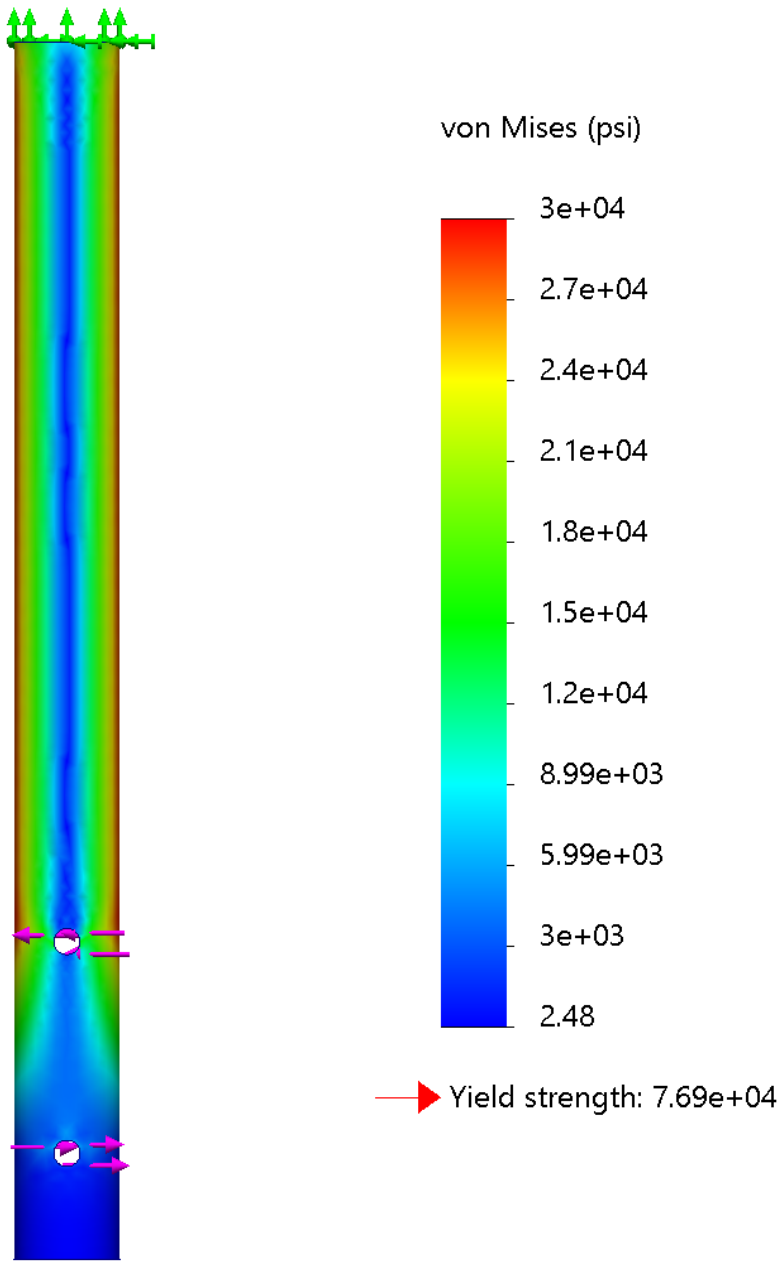

Figure D.2: Stress on Azimuth Shaft.

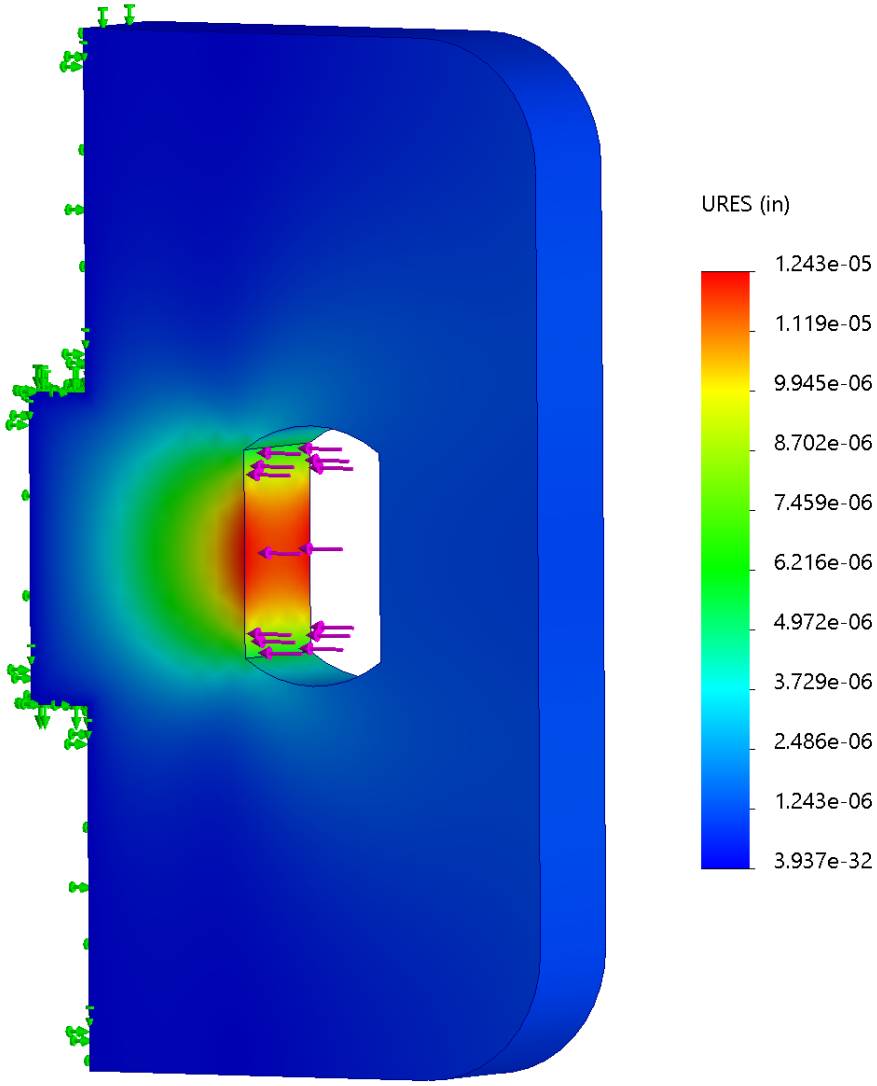

Figure D.3: Displacement of Shaft Tab

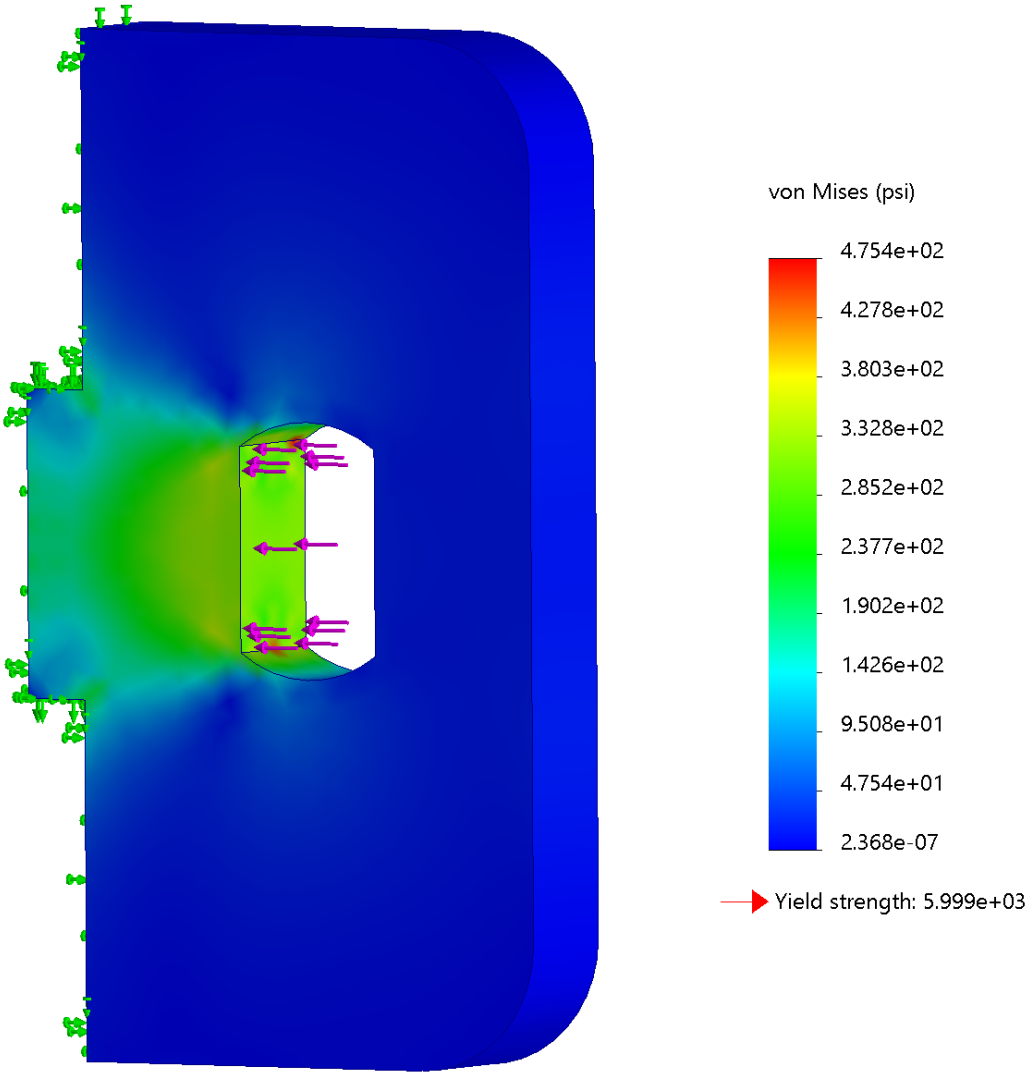

Figure D.4: Stress on Shaft Tab

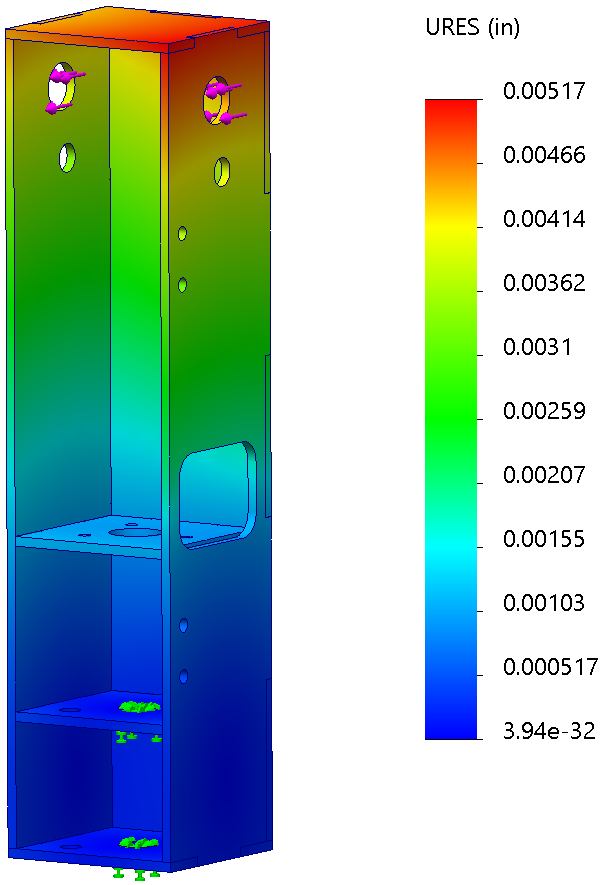

Figure D.5: Displacement of Casing system.

Appendix E: Complete Drawings list.

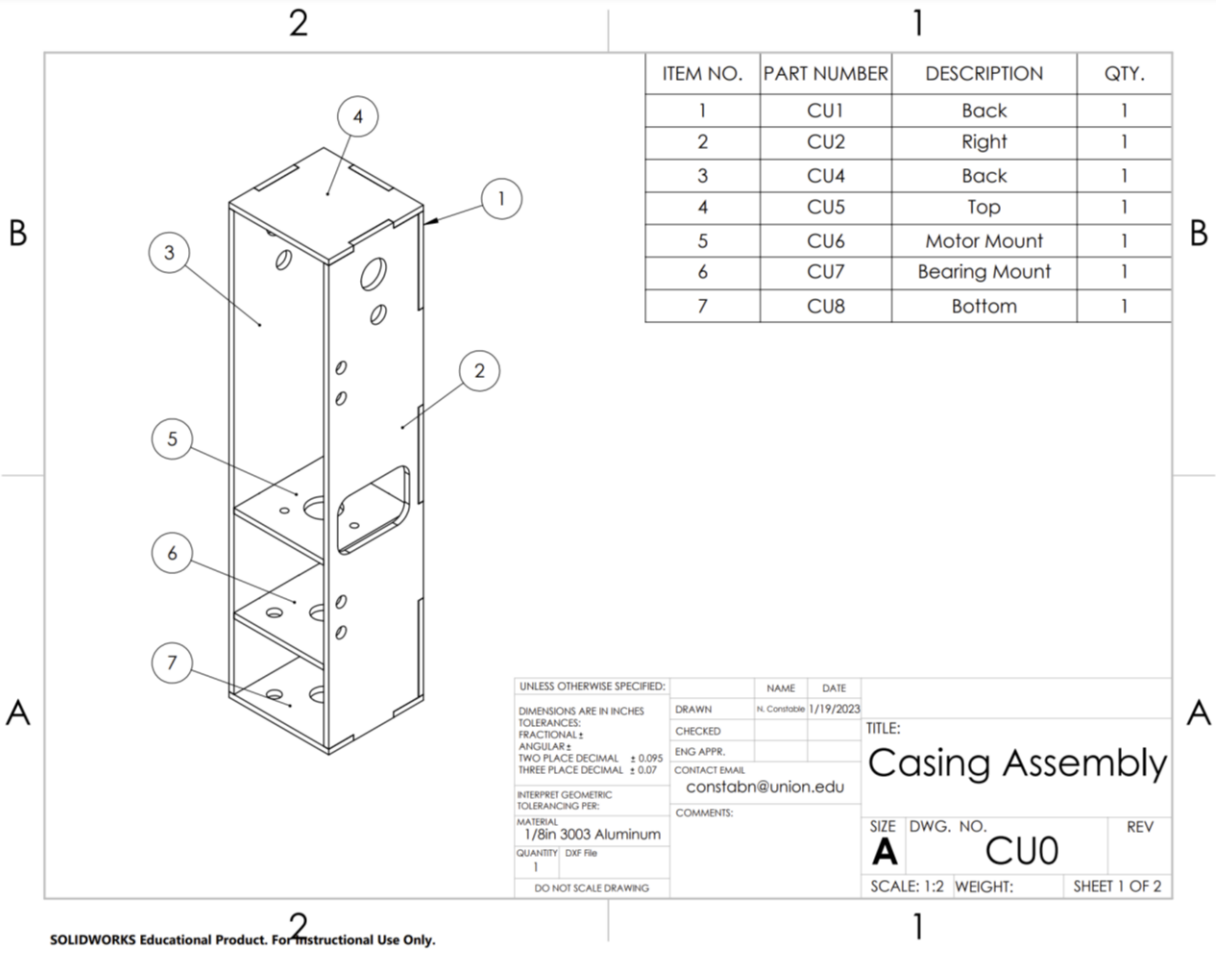

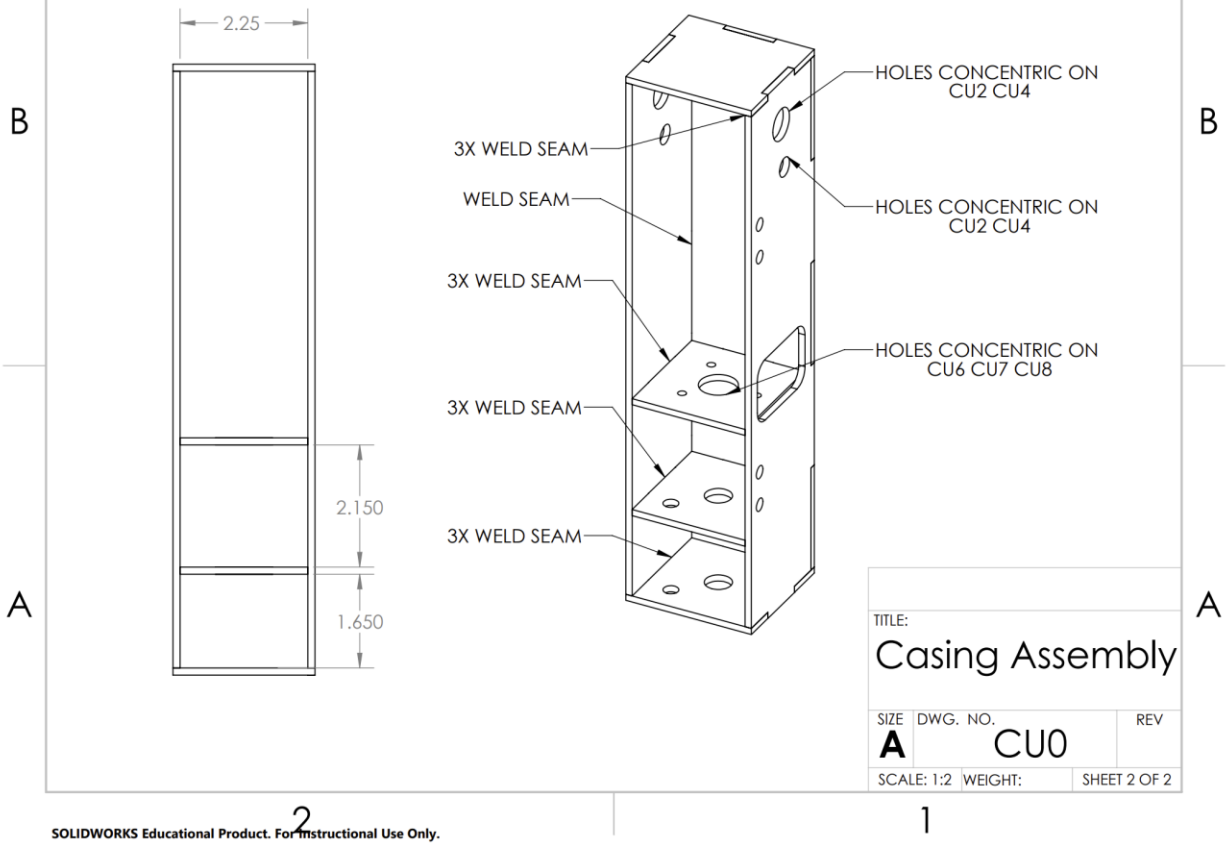
2.25
2.150
1.650
3X WELD SEAM
WELD SEAM
3X WELD SEAM
3X WELD SEAM
3X WELD SEAM
HOLES CONCENTRIC ON CU2 CU4
HOLES CONCENTRIC ON CU2 CU4
HOLES CONCENTRIC ON CU6 CU7 CU8
TITLE:
Casing Assembly
SIZE A
DWG. NO. CU0
REV
SCALE: 1:2
WEIGHT:
SHEET 2 OF 2
SOLIDWORKS Educational Product. For Instructional Use Only.

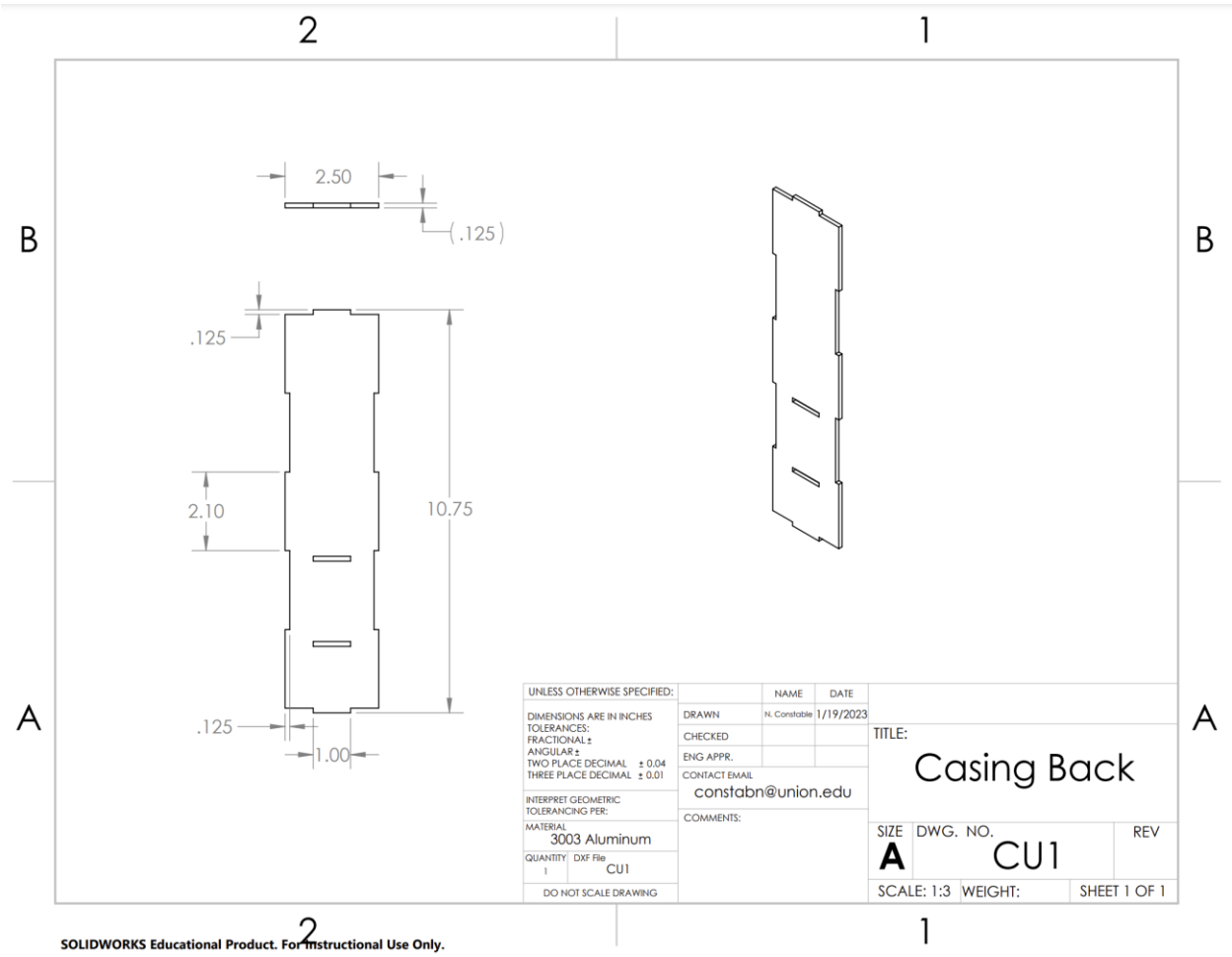
2
1
B
A
2.50
.125
.125
2.10
10.75
.125
1.00
UNLESS OTHERWISE SPECIFIED:
DIMENSIONS ARE IN INCHES
TOLERANCES:
FRACTIONAL ±
ANGULAR ±
TWO PLACE DECIMAL ± 0.04
THREE PLACE DECIMAL ± 0.01
INTERPRET GEOMETRIC TOLERANCING PER:
MATERIAL
3003 Aluminum
QUANTITY 1
DXF File CU1
DO NOT SCALE DRAWING
NAME
DATE
DRAWN N. Constable 1/19/2023
CHECKED
ENG APPR.
CONTACT EMAIL
constabn@union.edu
COMMENTS:
TITLE:
Casing Back
SIZE A
DWG. NO. CU1
REV
SCALE: 1:3
WEIGHT:
SHEET 1 OF 1
SOLIDWORKS Educational Product. For Instructional Use Only.

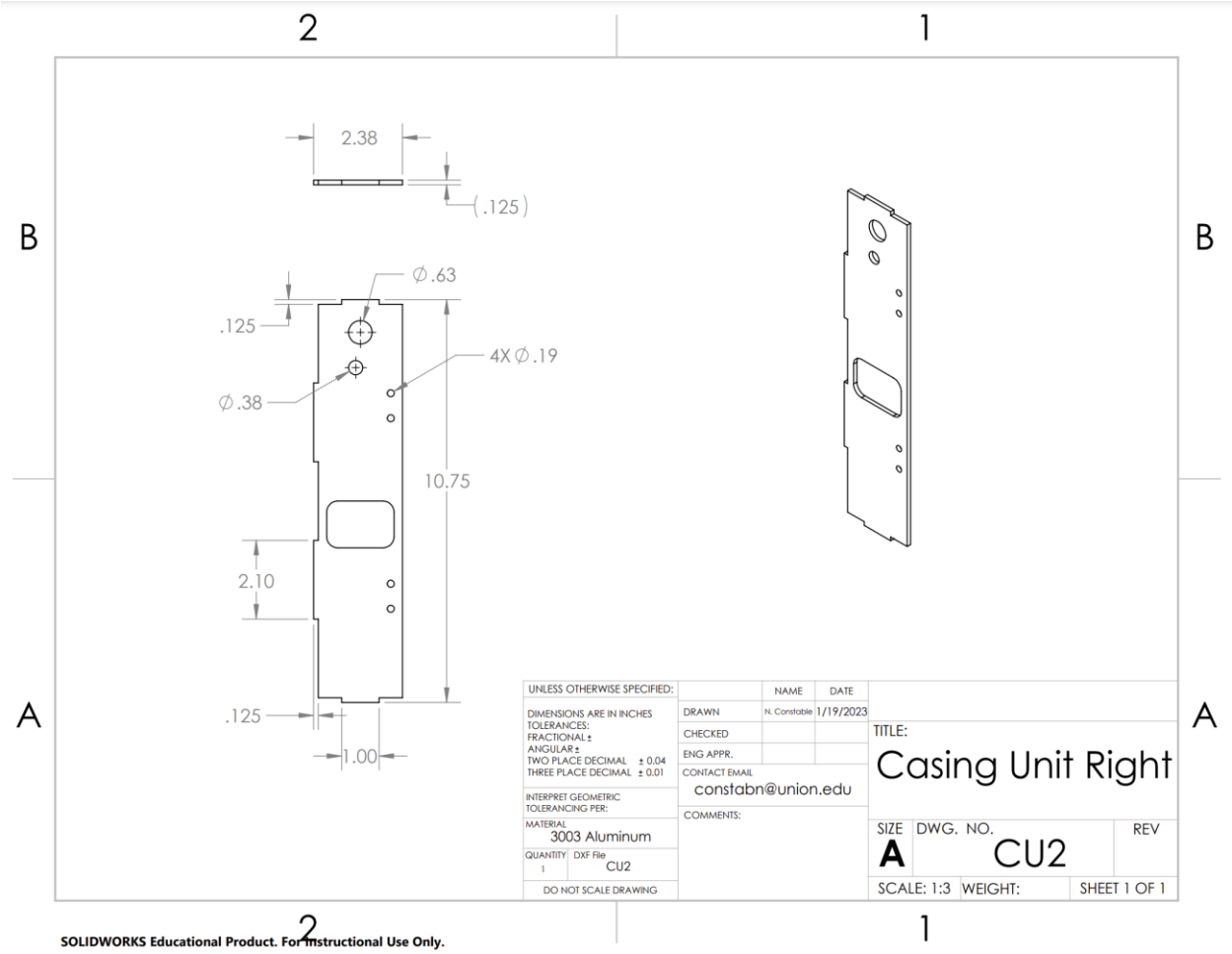
2
1
B
A
2.38
(.125)
Ø.63
.125
4X Ø.19
Ø.38
10.75
2.10
.125
1.00
UNLESS OTHERWISE SPECIFIED:
DIMENSIONS ARE IN INCHES
TOLERANCES:
FRACTIONAL ±
ANGULAR ±
TWO PLACE DECIMAL ± 0.04
THREE PLACE DECIMAL ± 0.01
INTERPRET GEOMETRIC TOLERANCING PER:
MATERIAL
3003 Aluminum
QUANTITY 1
DXF File CU2
DO NOT SCALE DRAWING
NAME
DATE
DRAWN
N. Constable
1/19/2023
CHECKED
ENG APPR.
CONTACT EMAIL
constabn@union.edu
COMMENTS:
TITLE:
Casing Unit Right
SIZE A
DWG. NO. CU2
REV
SCALE: 1:3
WEIGHT:
SHEET 1 OF 1
SOLIDWORKS Educational Product. For Instructional Use Only.

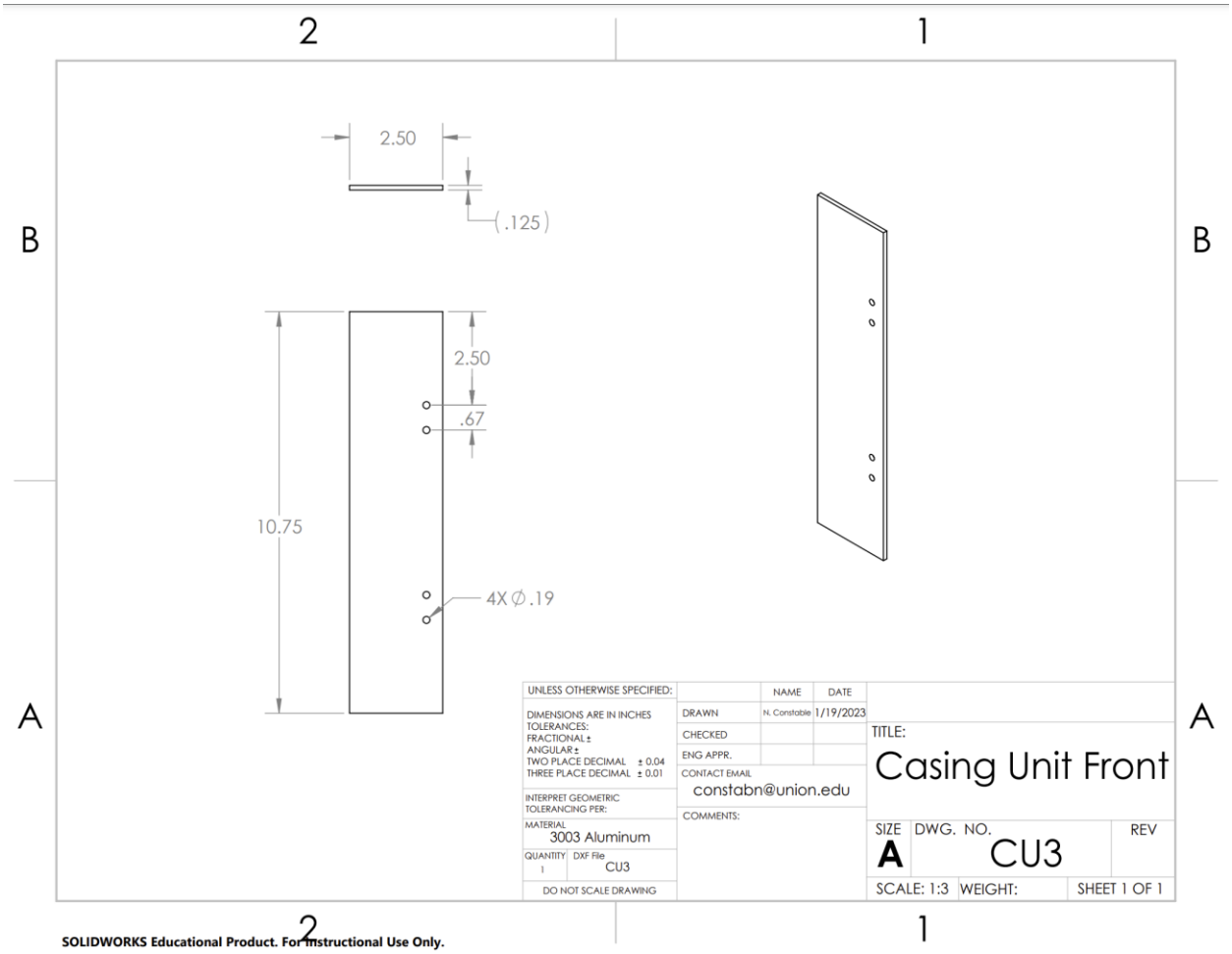
2
1
B
A
2.50
(.125)
2.50
.67
10.75
4X Ø .19
UNLESS OTHERWISE SPECIFIED:
DIMENSIONS ARE IN INCHES
TOLERANCES:
FRACTIONAL ±
ANGULAR ±
TWO PLACE DECIMAL ± 0.04
THREE PLACE DECIMAL ± 0.01
INTERPRET GEOMETRIC TOLERANCING PER:
MATERIAL
3003 Aluminum
QUANTITY 1
DXF File CU3
DO NOT SCALE DRAWING
NAME
DATE
DRAWN
N. Constable
1/19/2023
CHECKED
ENG APPR.
CONTACT EMAIL
constabn@union.edu
COMMENTS:
TITLE:
Casing Unit Front
SIZE A
DWG. NO. CU3
REV
SCALE: 1:3
WEIGHT:
SHEET 1 OF 1
SOLIDWORKS Educational Product. For Instructional Use Only.

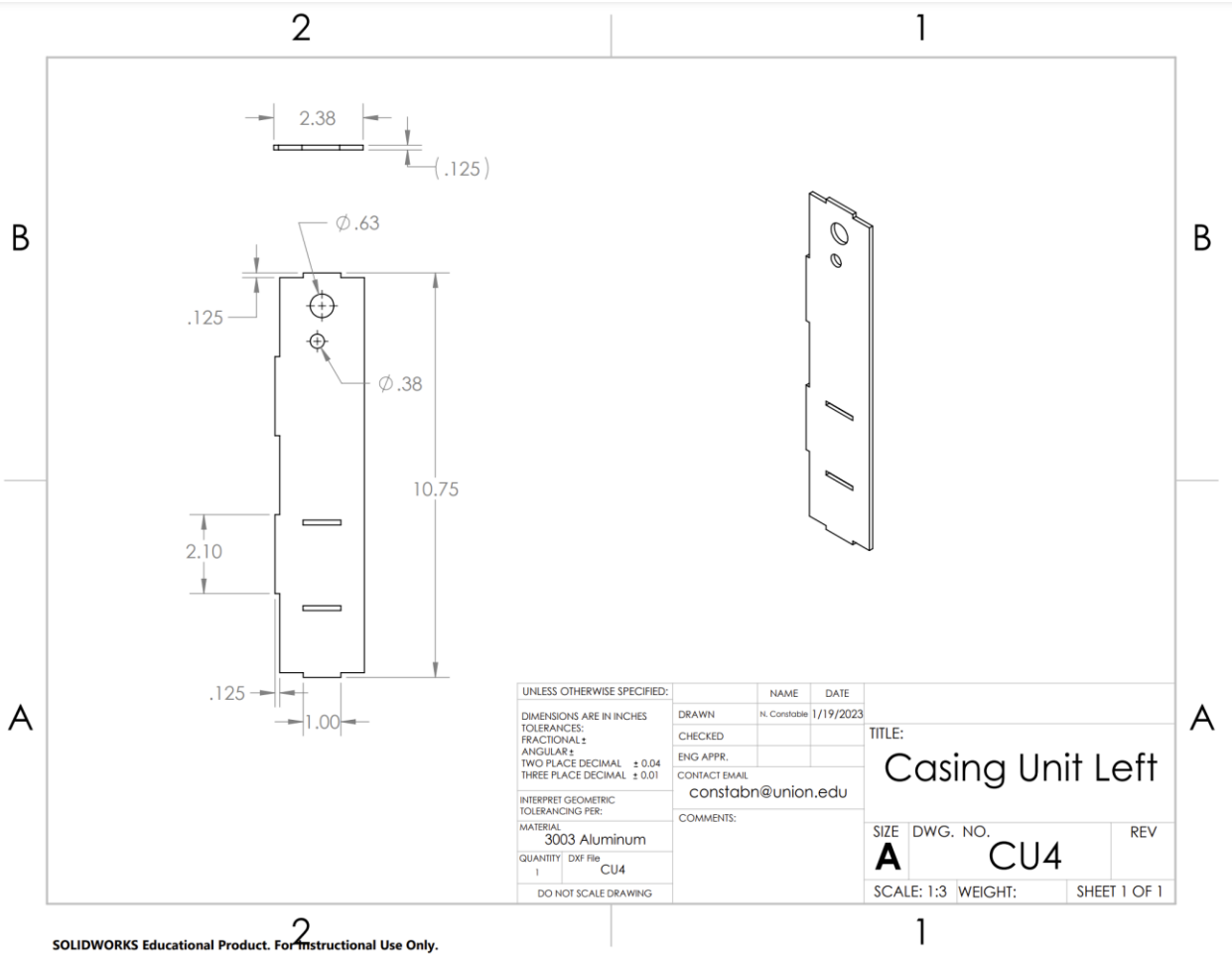
2
1
B
A
2.38
.125
Ø.63
.125
Ø.38
10.75
2.10
.125
1.00
UNLESS OTHERWISE SPECIFIED:
DIMENSIONS ARE IN INCHES
TOLERANCES:
FRACTIONAL ±
ANGULAR ±
TWO PLACE DECIMAL ± 0.04
THREE PLACE DECIMAL ± 0.01
INTERPRET GEOMETRIC TOLERANCING PER:
MATERIAL
3003 Aluminum
QUANTITY 1
DXF File CU4
DO NOT SCALE DRAWING
NAME
DATE
DRAWN
N. Constable 1/19/2023
CHECKED
ENG APPR.
CONTACT EMAIL
constabn@union.edu
COMMENTS:
TITLE:
Casing Unit Left
SIZE A
DWG. NO. CU4
REV
SCALE: 1:3
WEIGHT:
SHEET 1 OF 1
SOLIDWORKS Educational Product. For Instructional Use Only.

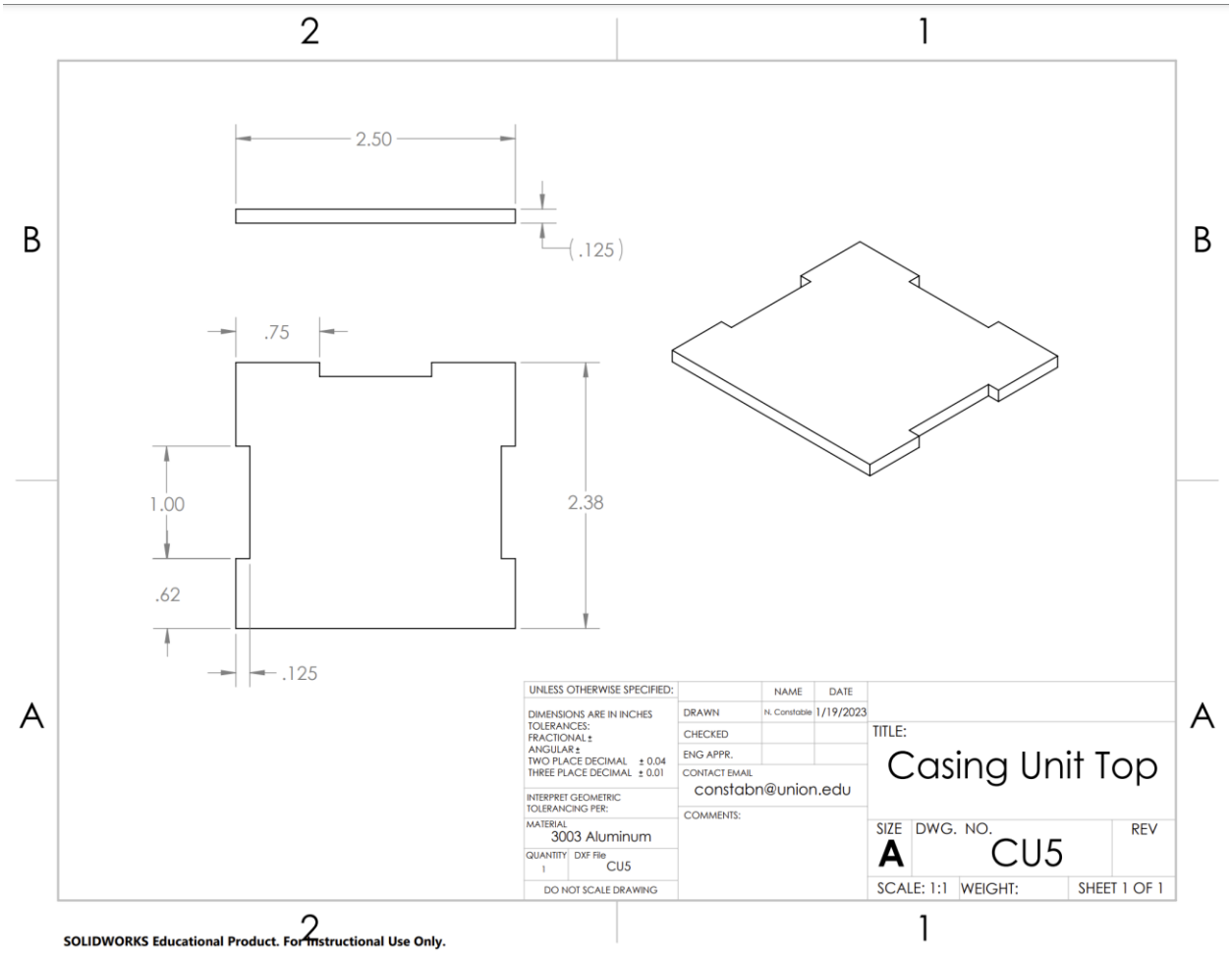
2
1
B
A
2.50
.125
.75
1.00
2.38
.62
.125
UNLESS OTHERWISE SPECIFIED:
DIMENSIONS ARE IN INCHES
TOLERANCES:
FRACTIONAL ±
ANGULAR ±
TWO PLACE DECIMAL ± 0.04
THREE PLACE DECIMAL ± 0.01
INTERPRET GEOMETRIC TOLERANCING PER:
MATERIAL
3003 Aluminum
QUANTITY 1
DXF File CU5
DO NOT SCALE DRAWING
NAME
DATE
DRAWN N. Constable 1/19/2023
CHECKED
ENG APPR.
CONTACT EMAIL
constabn@union.edu
COMMENTS:
TITLE:
Casing Unit Top
SIZE A
DWG. NO. CU5
REV
SCALE: 1:1
WEIGHT:
SHEET 1 OF 1
SOLIDWORKS Educational Product. For Instructional Use Only.

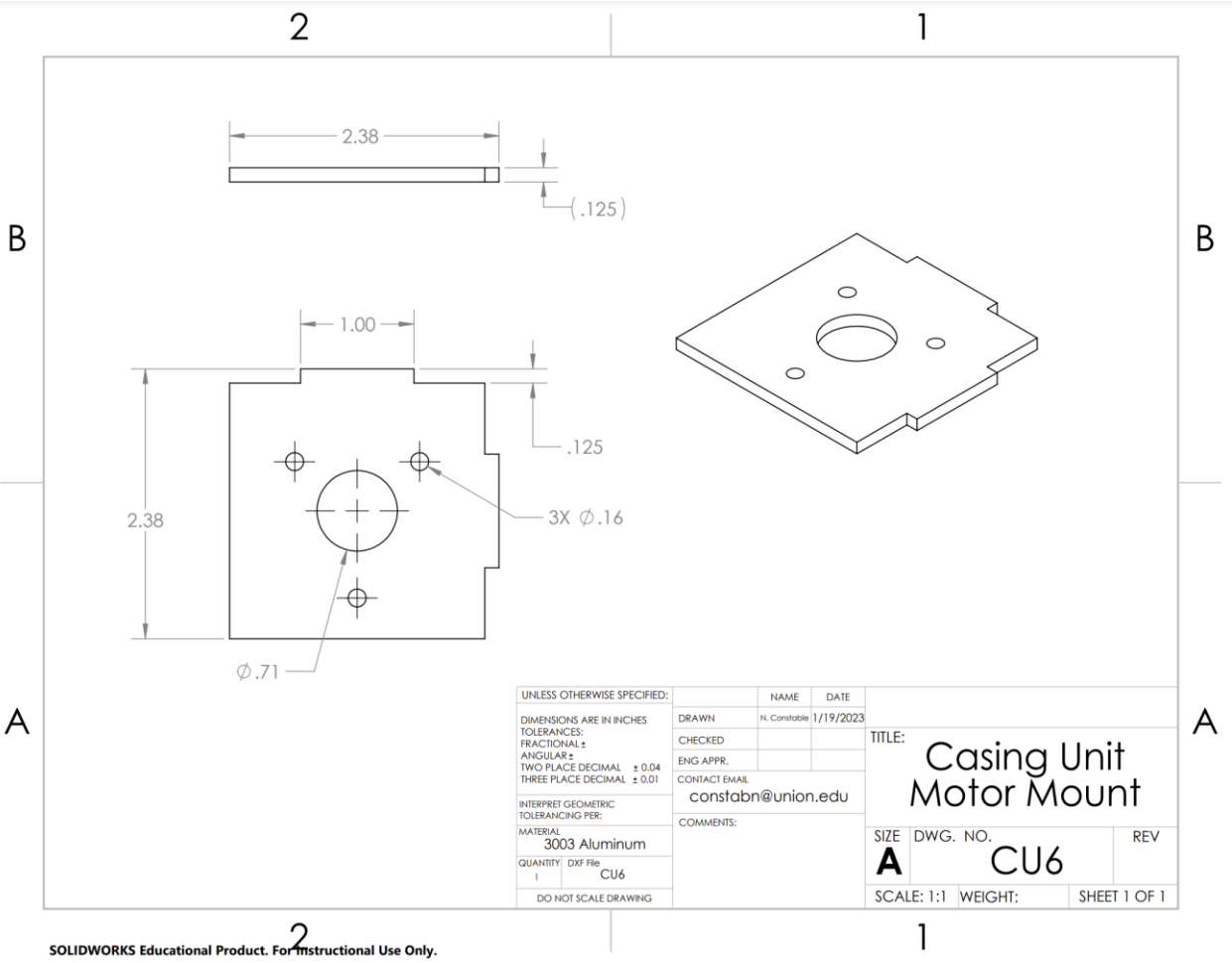
2
1
B
A
2.38
.125
1.00
.125
2.38
3X ∅.16
∅.71
UNLESS OTHERWISE SPECIFIED:
DIMENSIONS ARE IN INCHES
TOLERANCES:
FRACTIONAL ±
ANGULAR ±
TWO PLACE DECIMAL ± 0.04
THREE PLACE DECIMAL ± 0.01
INTERPRET GEOMETRIC TOLERANCING PER:
MATERIAL
3003 Aluminum
QUANTITY 1
DXF File CU6
DO NOT SCALE DRAWING
NAME
DATE
DRAWN N. Constable 1/19/2023
CHECKED
ENG APPR.
CONTACT EMAIL
constabn@union.edu
COMMENTS:
TITLE:
Casing Unit
Motor Mount
SIZE A
DWG. NO. CU6
REV
SCALE: 1:1
WEIGHT:
SHEET 1 OF 1
SOLIDWORKS Educational Product. For Instructional Use Only.

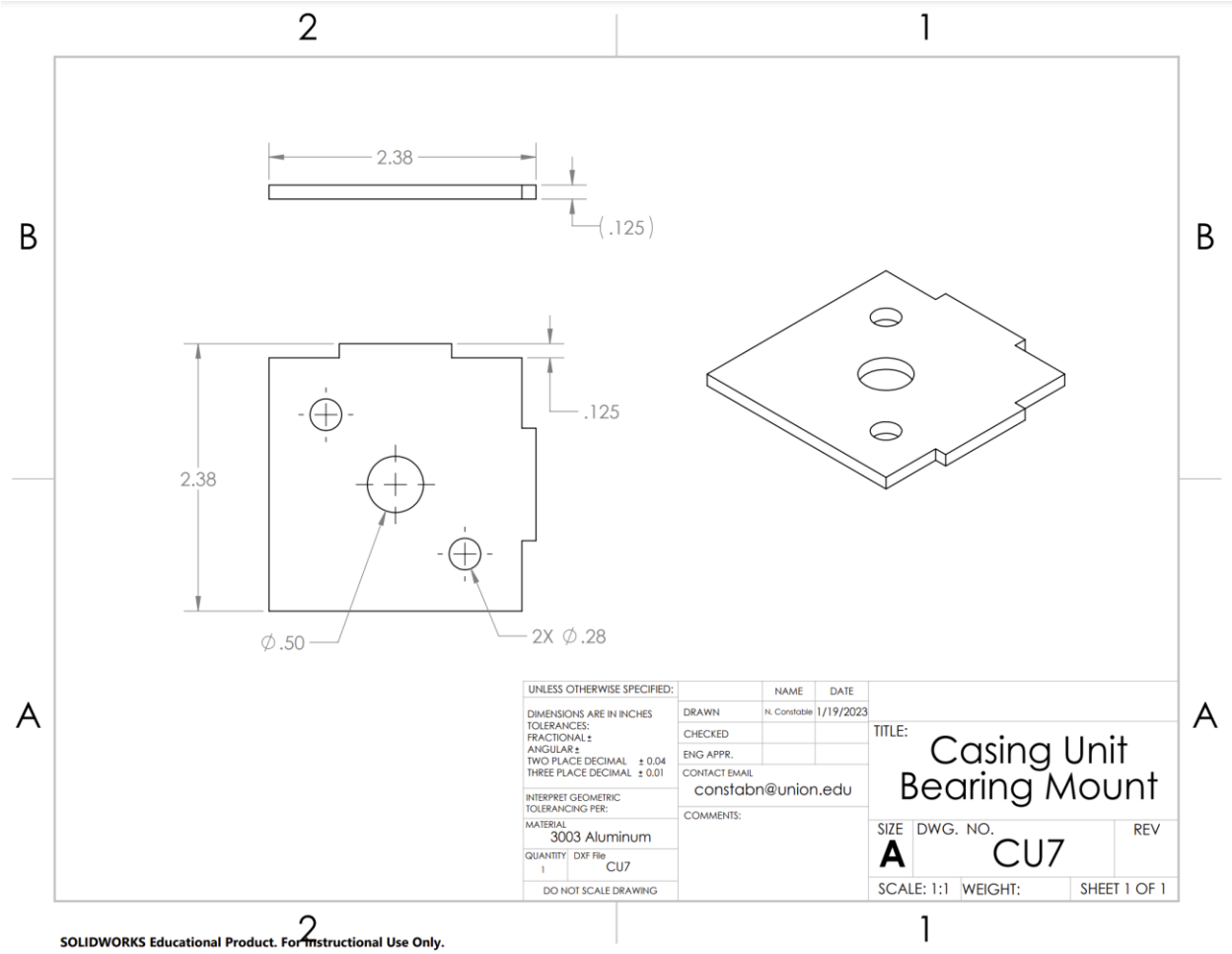
2
1
B
A
2.38
.125
2.38
.125
∅.50
2X ∅.28
UNLESS OTHERWISE SPECIFIED:
DIMENSIONS ARE IN INCHES
TOLERANCES:
FRACTIONAL ±
ANGULAR ±
TWO PLACE DECIMAL ± 0.04
THREE PLACE DECIMAL ± 0.01
INTERPRET GEOMETRIC TOLERANCING PER:
MATERIAL
3003 Aluminum
QUANTITY 1
DXF File CU7
DO NOT SCALE DRAWING
NAME
DATE
DRAWN N. Constable 1/19/2023
CHECKED
ENG APPR.
CONTACT EMAIL
constabn@union.edu
COMMENTS:
TITLE:
Casing Unit Bearing Mount
SIZE A
DWG. NO. CU7
REV
SCALE: 1:1
WEIGHT:
SHEET 1 OF 1
SOLIDWORKS Educational Product. For Instructional Use Only.

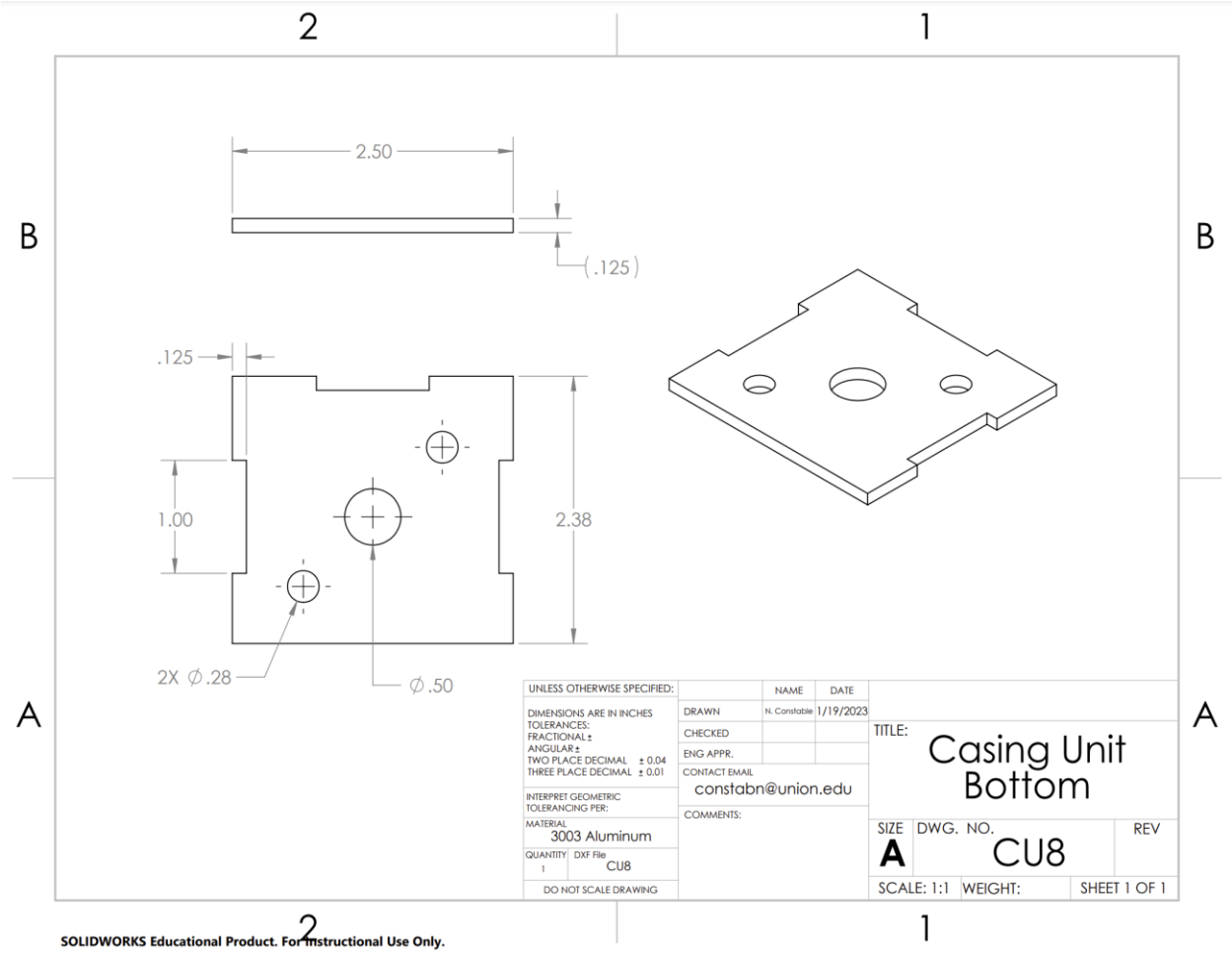
2
1
B
A
2.50
(.125)
.125
1.00
2.38
2X ∅.28
∅.50
UNLESS OTHERWISE SPECIFIED:
DIMENSIONS ARE IN INCHES
TOLERANCES:
FRACTIONAL ±
ANGULAR ±
TWO PLACE DECIMAL ± 0.04
THREE PLACE DECIMAL ± 0.01
INTERPRET GEOMETRIC TOLERANCING PER:
MATERIAL
3003 Aluminum
QUANTITY 1
DXF File CU8
DO NOT SCALE DRAWING
NAME
DATE
DRAWN
N. Constable 1/19/2023
CHECKED
ENG APPR.
CONTACT EMAIL
constabn@union.edu
COMMENTS:
TITLE:
Casing Unit Bottom
SIZE A
DWG. NO. CU8
REV
SCALE: 1:1
WEIGHT:
SHEET 1 OF 1
SOLIDWORKS Educational Product. For Instructional Use Only.

ITEM NO.	PART NUMBER	DESCRIPTION	QTY.
1	PM1	Panel Mount	1
2	PM5	Shaft Tab	1

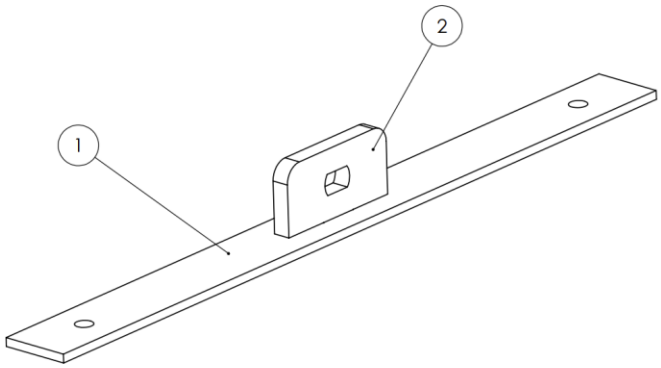

UNLESS OTHERWISE SPECIFIED:		NAME	DATE
DIMENSIONS ARE IN INCHES TOLERANCES: FRACTIONAL ± ANGULAR ± TWO PLACE DECIMAL ± 0.04 THREE PLACE DECIMAL ± 0.01	DRAWN	N. Constable	1/19/2023
	CHECKED		
	ENG APPR.		
	CONTACT EMAIL constabn@union.edu		
INTERPRET GEOMETRIC TOLERANCING PER:	COMMENTS:		
MATERIAL Aluminum			
QUANTITY 2 / DXF File			
DO NOT SCALE DRAWING			

TITLE: Shaft Tab Assembly

SIZE	DWG. NO.	REV
A	PM0	
SCALE: 1:1.5	WEIGHT:	SHEET 1 OF 2

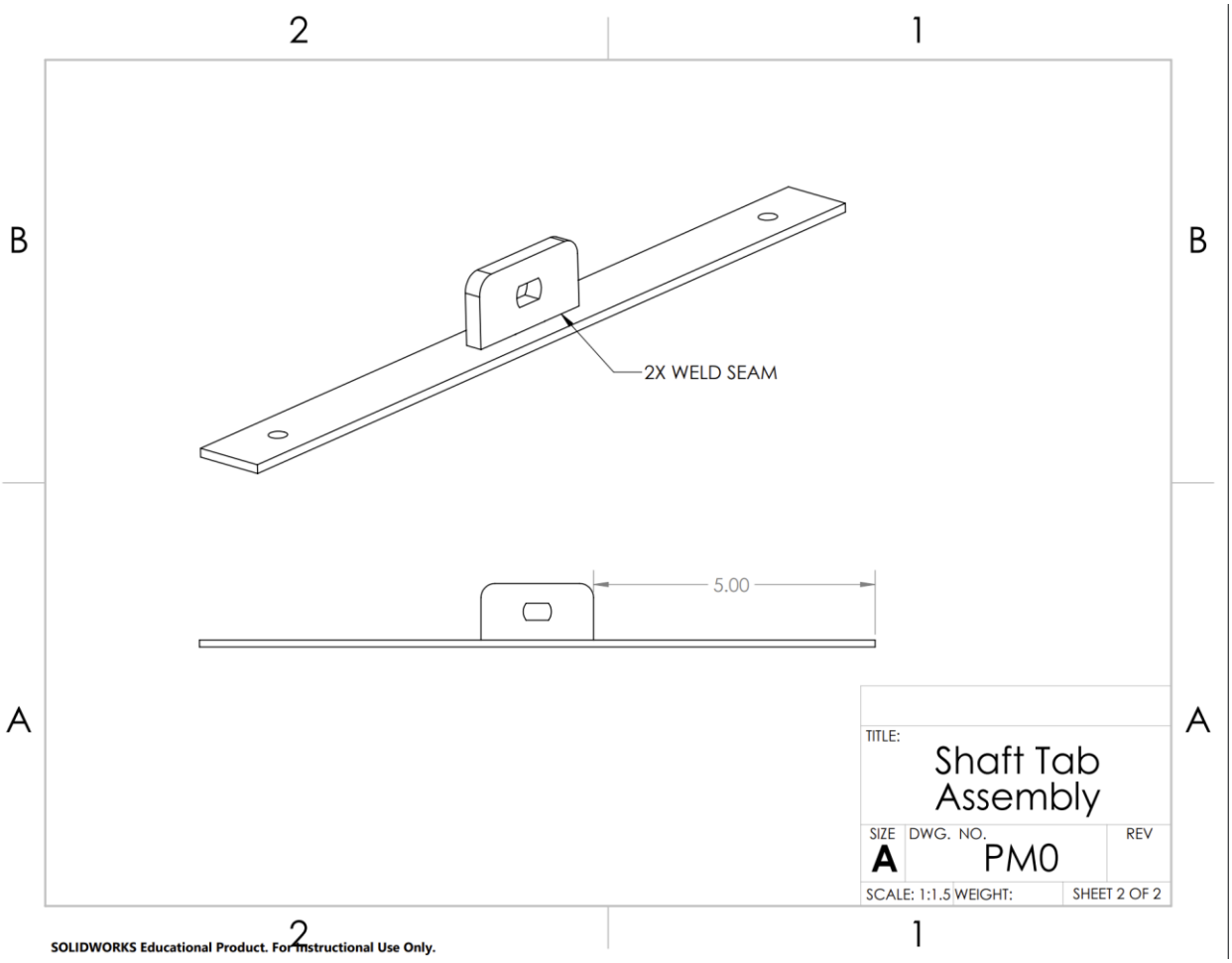
2
1
B
B
2X WELD SEAM
5.00
A
A
TITLE:
Shaft Tab Assembly
SIZE
A
DWG. NO.
PM0
REV
SCALE: 1:1.5
WEIGHT:
SHEET 2 OF 2
2
1
SOLIDWORKS Educational Product. For Instructional Use Only.

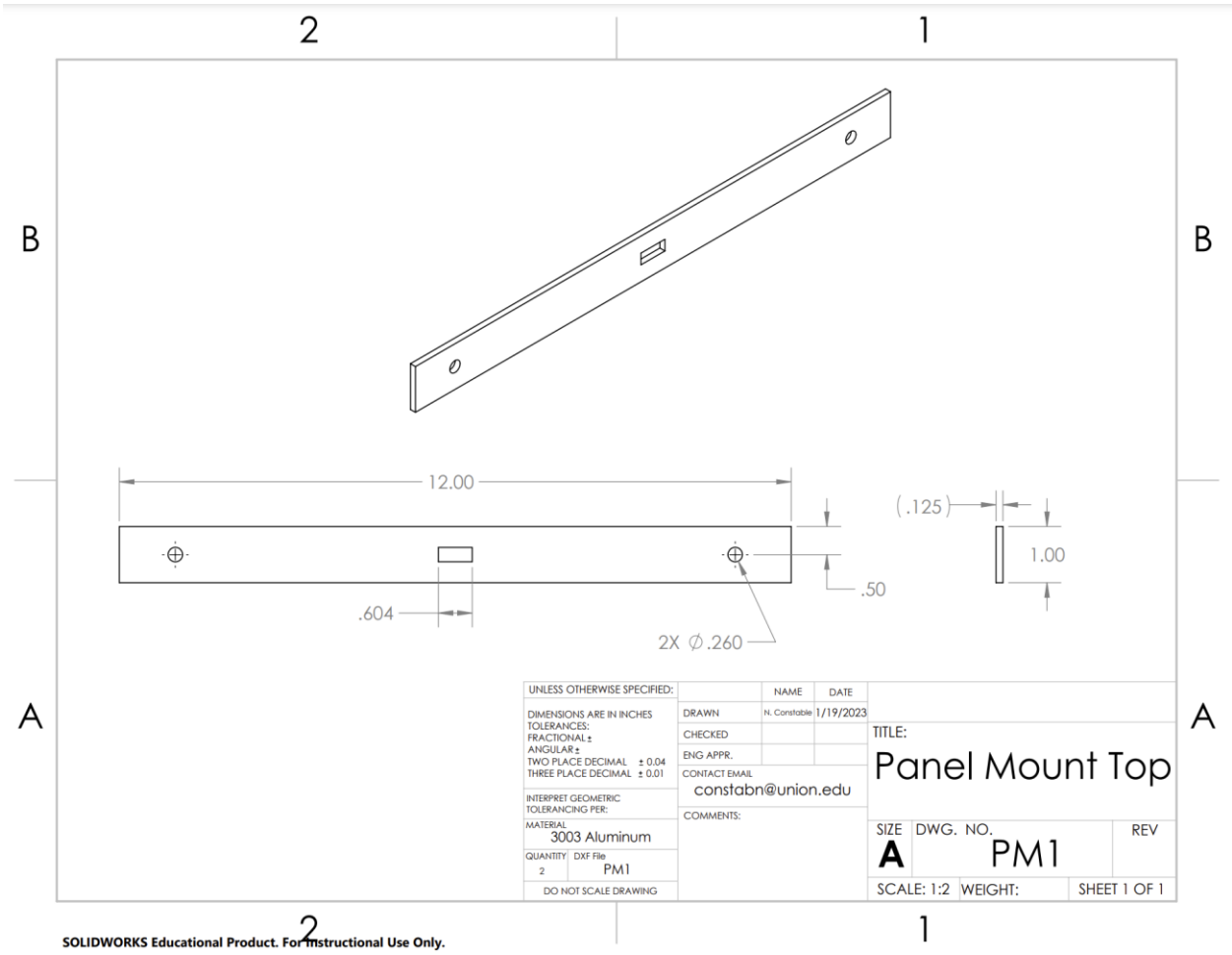
2
1
B
B
12.00
(.125)
1.00
.50
.604
2X ∅.260
A
A
UNLESS OTHERWISE SPECIFIED:
DIMENSIONS ARE IN INCHES
TOLERANCES:
FRACTIONAL ±
ANGULAR ±
TWO PLACE DECIMAL ± 0.04
THREE PLACE DECIMAL ± 0.01
INTERPRET GEOMETRIC TOLERANCING PER:
MATERIAL
3003 Aluminum
QUANTITY 2
DXF File PM1
DO NOT SCALE DRAWING
NAME
DATE
DRAWN N. Constable 1/19/2023
CHECKED
ENG APPR.
CONTACT EMAIL
constabn@union.edu
COMMENTS:
TITLE:
Panel Mount Top
SIZE A
DWG. NO. PM1
REV
SCALE: 1:2
WEIGHT:
SHEET 1 OF 1
2
1
SOLIDWORKS Educational Product. For Instructional Use Only.

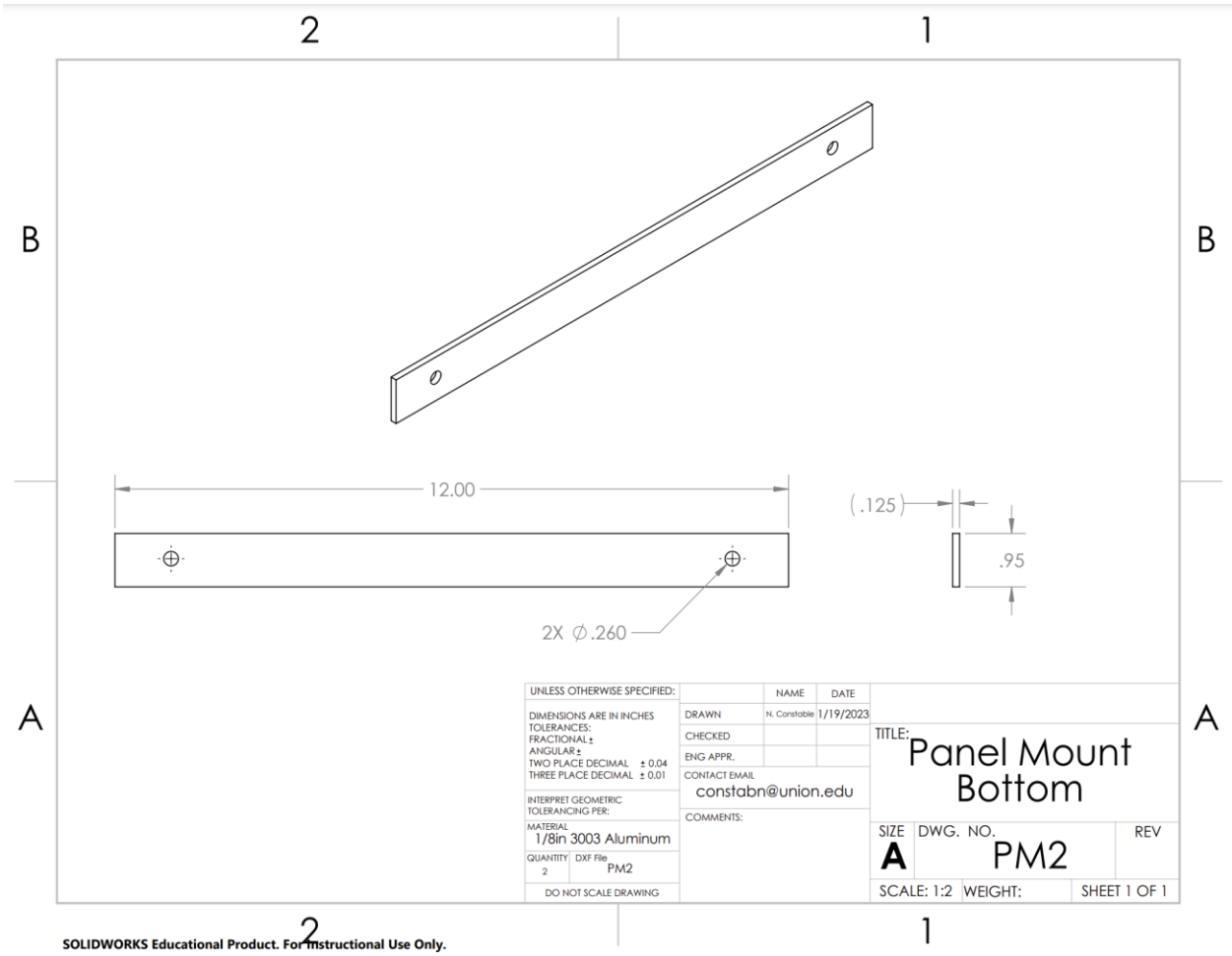
2
1
B
B
12.00
(.125)
.95
2X ∅.260
A
A
UNLESS OTHERWISE SPECIFIED:
DIMENSIONS ARE IN INCHES
TOLERANCES:
FRACTIONAL ±
ANGULAR ±
TWO PLACE DECIMAL ± 0.04
THREE PLACE DECIMAL ± 0.01
INTERPRET GEOMETRIC TOLERANCING PER:
MATERIAL
1/8in 3003 Aluminum
QUANTITY 2
DXF File PM2
DO NOT SCALE DRAWING
NAME
DATE
DRAWN N. Constable 1/19/2023
CHECKED
ENG APPR.
CONTACT EMAIL
constabn@union.edu
COMMENTS:
TITLE:
Panel Mount Bottom
SIZE A
DWG. NO. PM2
REV
SCALE: 1:2
WEIGHT:
SHEET 1 OF 1
2
1
SOLIDWORKS Educational Product. For Instructional Use Only.

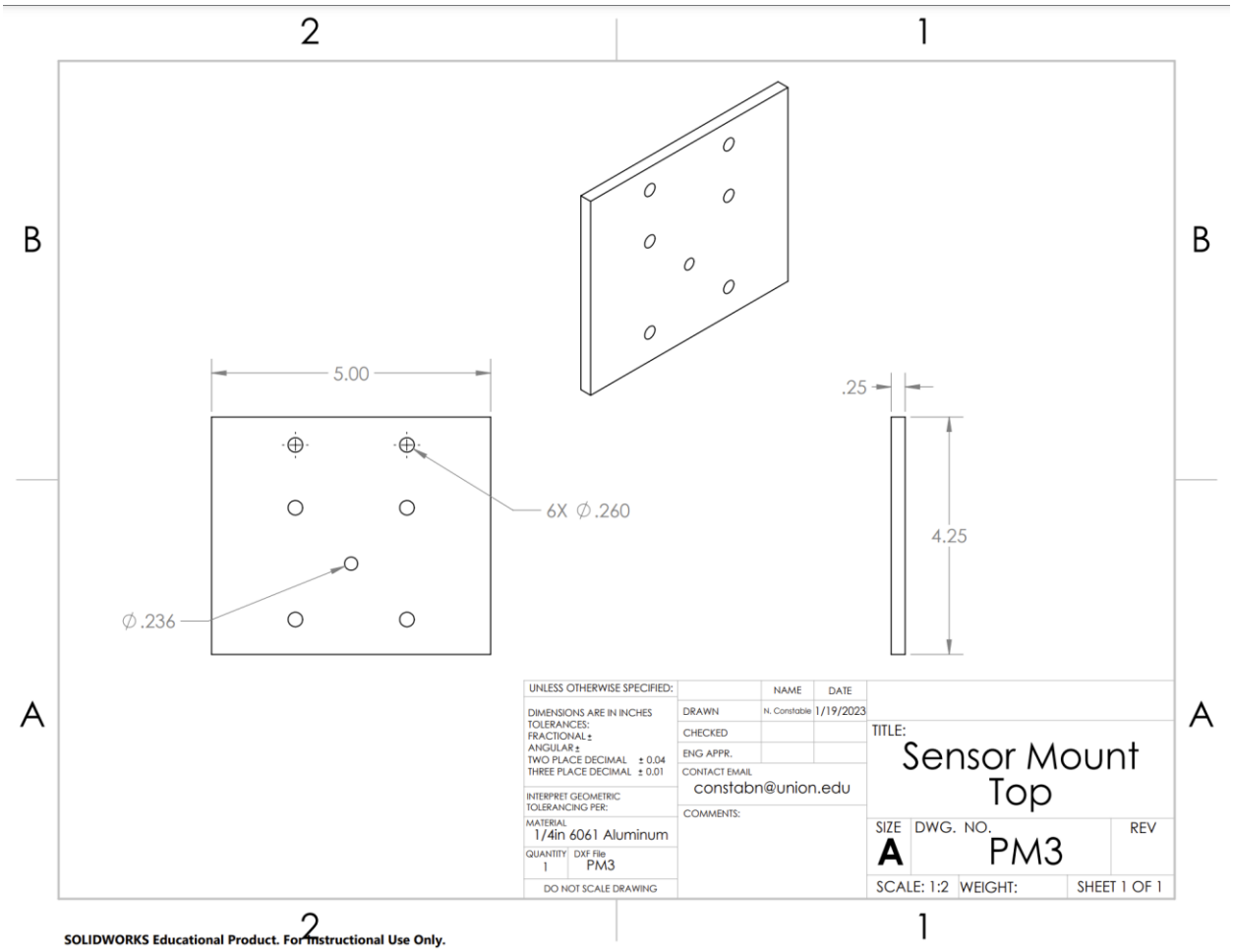
2
1
B
B
A
A
5.00
.25
6X ∅.260
4.25
∅.236
UNLESS OTHERWISE SPECIFIED:
DIMENSIONS ARE IN INCHES
TOLERANCES:
FRACTIONAL ±
ANGULAR ±
TWO PLACE DECIMAL ± 0.04
THREE PLACE DECIMAL ± 0.01
INTERPRET GEOMETRIC TOLERANCING PER:
MATERIAL
1/4in 6061 Aluminum
QUANTITY 1
DXF File PM3
DO NOT SCALE DRAWING
NAME
DATE
DRAWN
N. Constable 1/19/2023
CHECKED
ENG APPR.
CONTACT EMAIL
constabn@union.edu
COMMENTS:
TITLE:
Sensor Mount Top
SIZE A
DWG. NO. PM3
REV
SCALE: 1:2
WEIGHT:
SHEET 1 OF 1
SOLIDWORKS Educational Product. For Instructional Use Only.

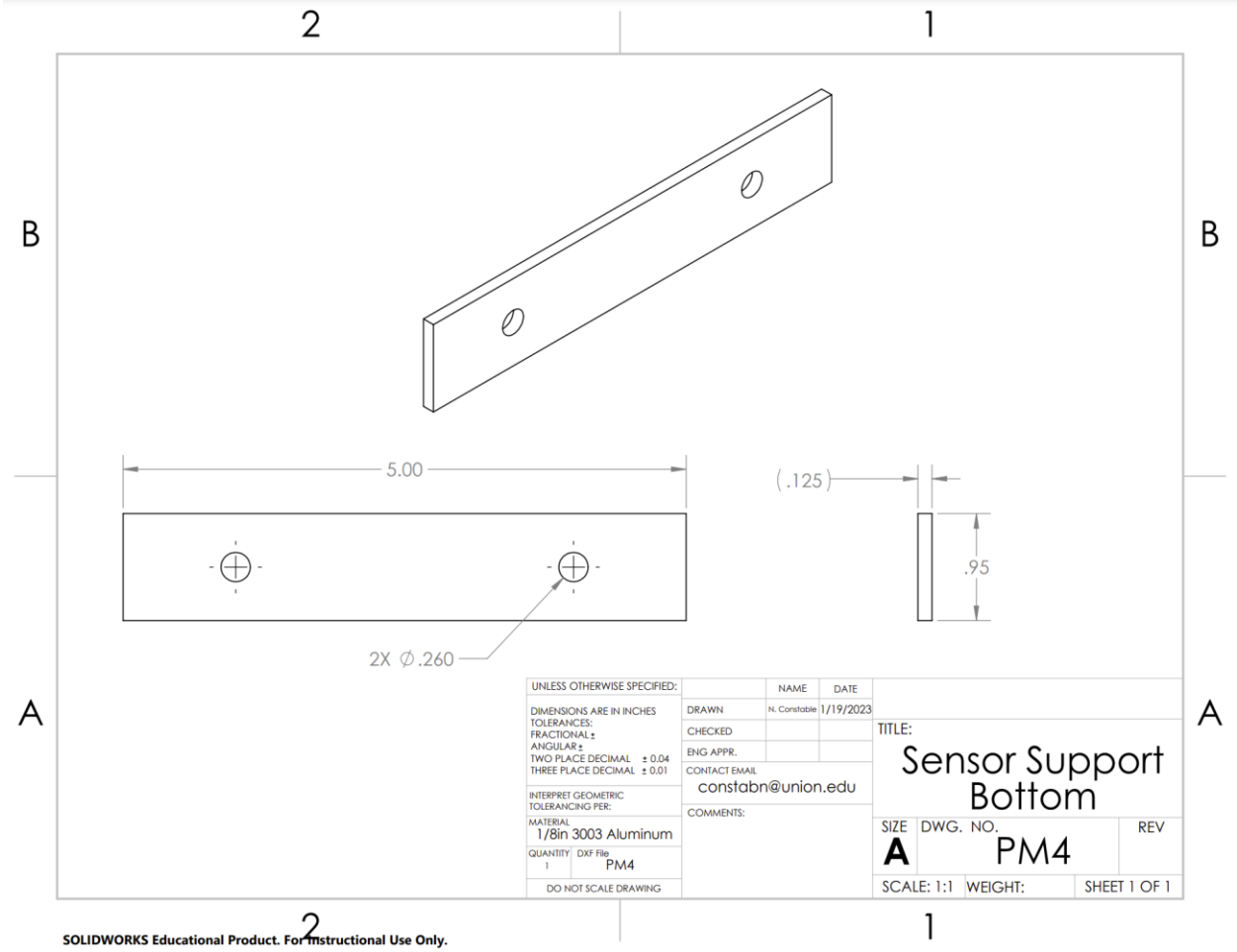
2
1
B
B
5.00
(.125)
.95
2X ∅.260
A
A
UNLESS OTHERWISE SPECIFIED:
DIMENSIONS ARE IN INCHES
TOLERANCES:
FRACTIONAL ±
ANGULAR ±
TWO PLACE DECIMAL ± 0.04
THREE PLACE DECIMAL ± 0.01
INTERPRET GEOMETRIC TOLERANCING PER:
MATERIAL
1/8in 3003 Aluminum
QUANTITY
1
DXF File
PM4
DO NOT SCALE DRAWING
NAME
DATE
DRAWN
N. Constable
1/19/2023
CHECKED
ENG APPR.
CONTACT EMAIL
constabn@union.edu
COMMENTS:
TITLE:
Sensor Support Bottom
SIZE
A
DWG. NO.
PM4
REV
SCALE: 1:1
WEIGHT:
SHEET 1 OF 1
2
1
SOLIDWORKS Educational Product. For Instructional Use Only.

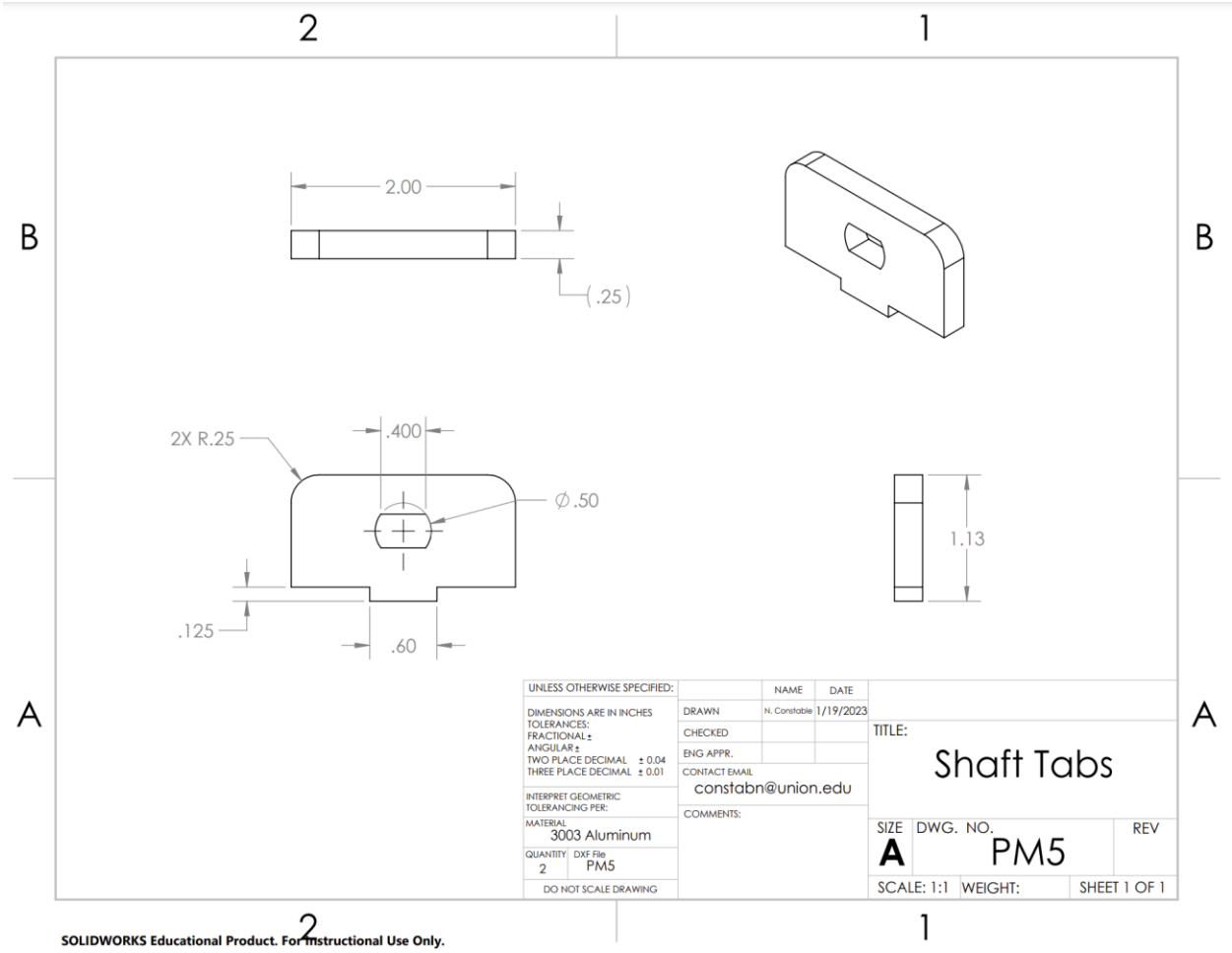
2
1
B
A
2.00
(.25)
2X R.25
.400
Ø.50
.125
.60
1.13
UNLESS OTHERWISE SPECIFIED:
DIMENSIONS ARE IN INCHES
TOLERANCES:
FRACTIONAL ±
ANGULAR ±
TWO PLACE DECIMAL ± 0.04
THREE PLACE DECIMAL ± 0.01
INTERPRET GEOMETRIC TOLERANCING PER:
MATERIAL
3003 Aluminum
QUANTITY 2
DXF File PM5
DO NOT SCALE DRAWING
NAME
DATE
DRAWN N. Constable 1/19/2023
CHECKED
ENG APPR.
CONTACT EMAIL
constabn@union.edu
COMMENTS:
TITLE:
Shaft Tabs
SIZE A
DWG. NO. PM5
REV
SCALE: 1:1
WEIGHT:
SHEET 1 OF 1
SOLIDWORKS Educational Product. For Instructional Use Only.

ITEM NO.	PART NUMBER	DESCRIPTION	QTY.
1	B1	Main Upright	1
2	B2	Main Rotational Plate	1

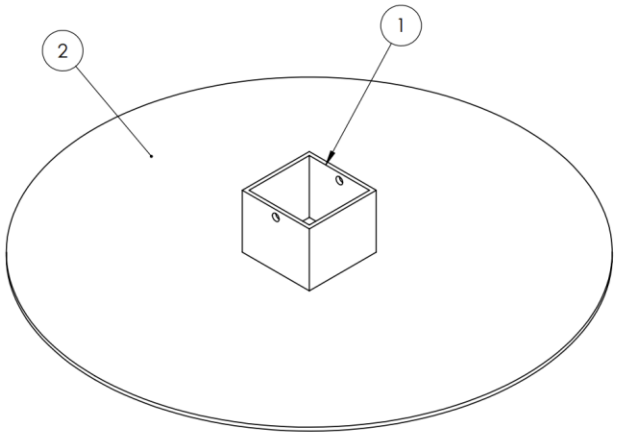

UNLESS OTHERWISE SPECIFIED:		NAME	DATE
DIMENSIONS ARE IN INCHES TOLERANCES: FRACTIONAL ± ANGULAR ± TWO PLACE DECIMAL ± 0.02 THREE PLACE DECIMAL ± 0.01	DRAWN	N. Constable	3/8/2023
	CHECKED		
	ENG APPR.		
	CONTACT EMAIL constabn@union.edu		
INTERPRET GEOMETRIC TOLERANCING PER:	COMMENTS:		
MATERIAL			
QUANTITY 1 / DXF File			
DO NOT SCALE DRAWING			

TITLE:

Base Assembly

SIZE	DWG. NO.	REV
A	B0	1
SCALE: 1:3	WEIGHT:	SHEET 1 OF 2

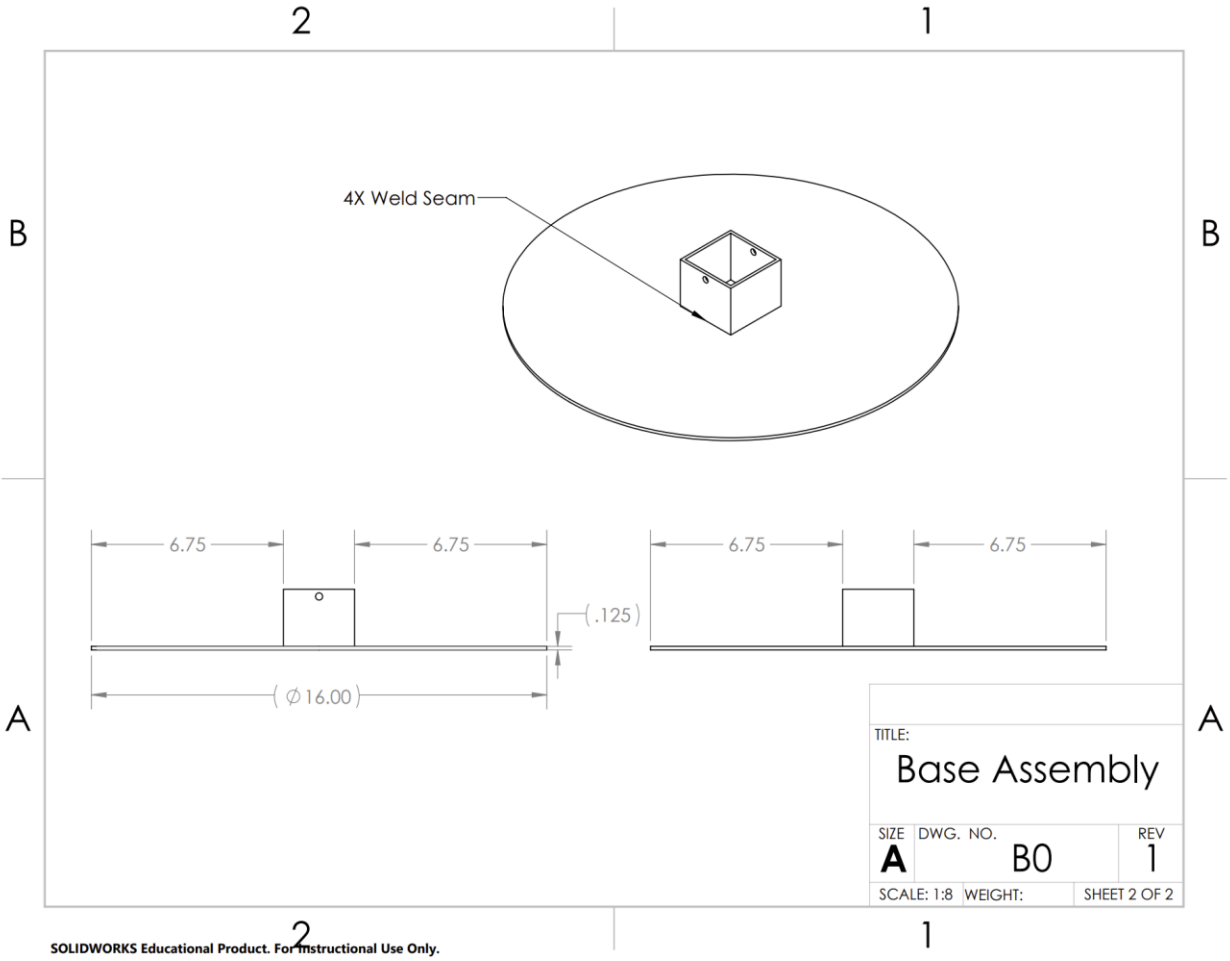
2
1
B
B
4X Weld Seam
6.75
6.75
6.75
6.75
.125
Ø16.00
A
A
TITLE:
Base Assembly
SIZE
A
DWG. NO.
B0
REV
1
SCALE: 1:8
WEIGHT:
SHEET 2 OF 2
2
1
SOLIDWORKS Educational Product. For Instructional Use Only.

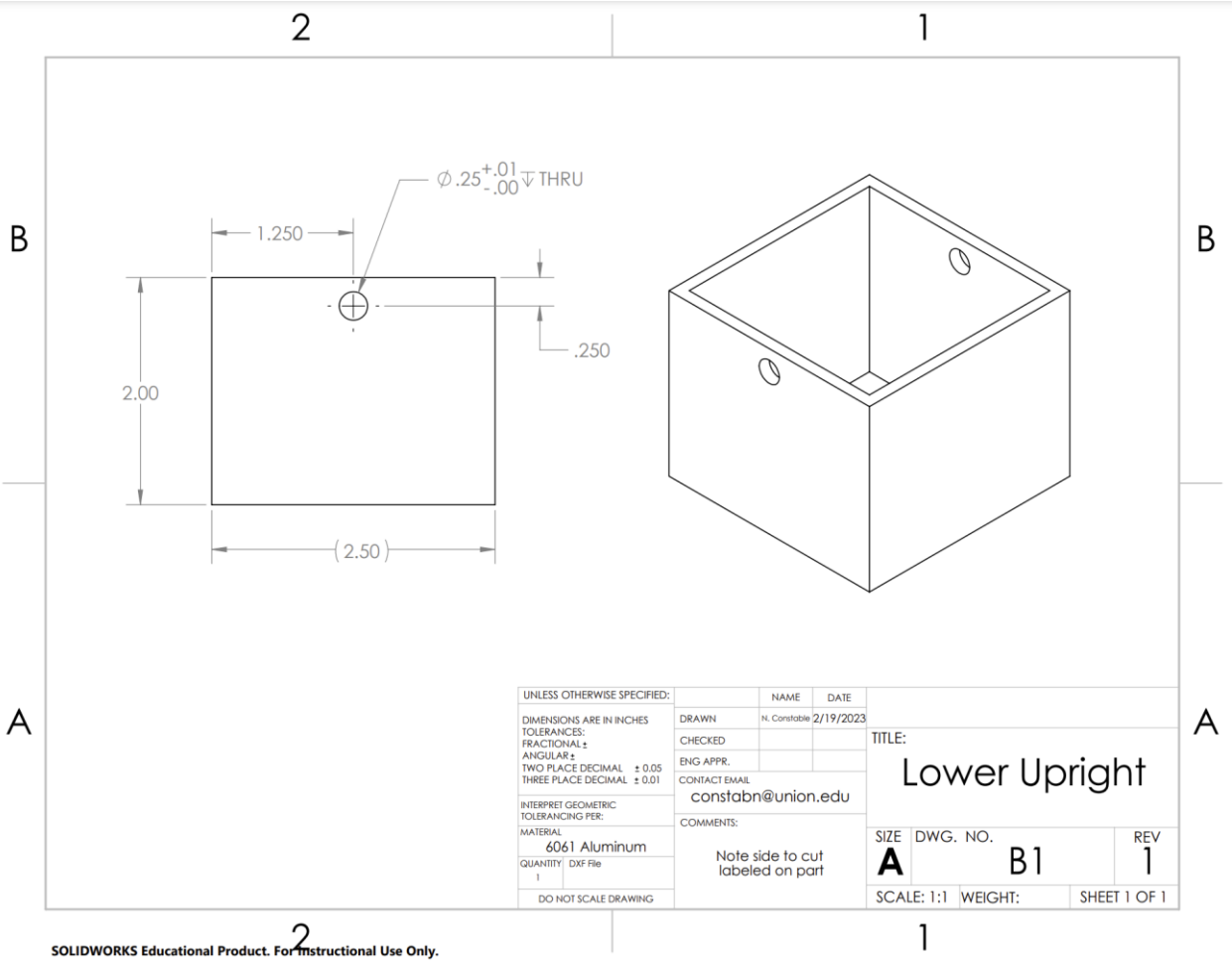
2
1
B
A
Ø.25 +.01 -.00 ↧ THRU
1.250
.250
2.00
2.50
UNLESS OTHERWISE SPECIFIED:
DIMENSIONS ARE IN INCHES
TOLERANCES:
FRACTIONAL ±
ANGULAR ±
TWO PLACE DECIMAL ± 0.05
THREE PLACE DECIMAL ± 0.01
INTERPRET GEOMETRIC TOLERANCING PER:
MATERIAL
6061 Aluminum
QUANTITY 1
DXF File
DO NOT SCALE DRAWING
NAME
DATE
DRAWN
N. Constable 2/19/2023
CHECKED
ENG APPR.
CONTACT EMAIL
constabn@union.edu
COMMENTS:
Note side to cut labeled on part
TITLE:
Lower Upright
SIZE A
DWG. NO. B1
REV 1
SCALE: 1:1
WEIGHT:
SHEET 1 OF 1
SOLIDWORKS Educational Product. For Instructional Use Only.

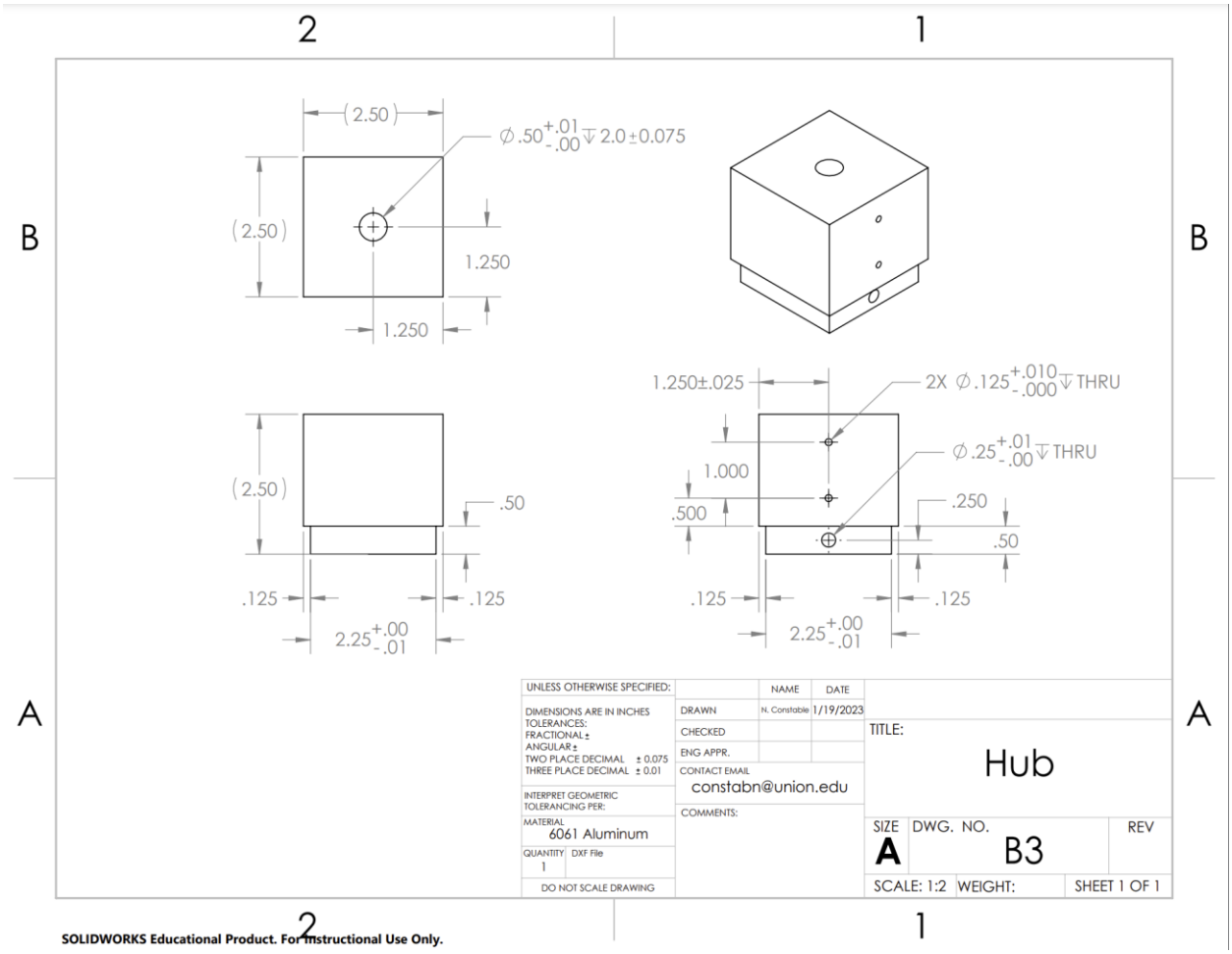
2
1
B
A
(2.50)
(2.50)
Ø.50 +.01 -.00 ↧2.0±0.075
1.250
1.250
(2.50)
.50
.125
.125
2.25 +.00 -.01
1.250±.025
2X Ø.125 +.010 -.000 ↧THRU
Ø.25 +.01 -.00 ↧THRU
1.000
.500
.250
.50
.125
.125
2.25 +.00 -.01
UNLESS OTHERWISE SPECIFIED:
DIMENSIONS ARE IN INCHES
TOLERANCES:
FRACTIONAL ±
ANGULAR ±
TWO PLACE DECIMAL ± 0.075
THREE PLACE DECIMAL ± 0.01
INTERPRET GEOMETRIC TOLERANCING PER:
MATERIAL
6061 Aluminum
QUANTITY 1
DXF File
DO NOT SCALE DRAWING
NAME
DATE
DRAWN
N. Constable 1/19/2023
CHECKED
ENG APPR.
CONTACT EMAIL
constabn@union.edu
COMMENTS:
TITLE:
Hub
SIZE
A
DWG. NO.
B3
REV
SCALE: 1:2
WEIGHT:
SHEET 1 OF 1
SOLIDWORKS Educational Product. For Instructional Use Only.

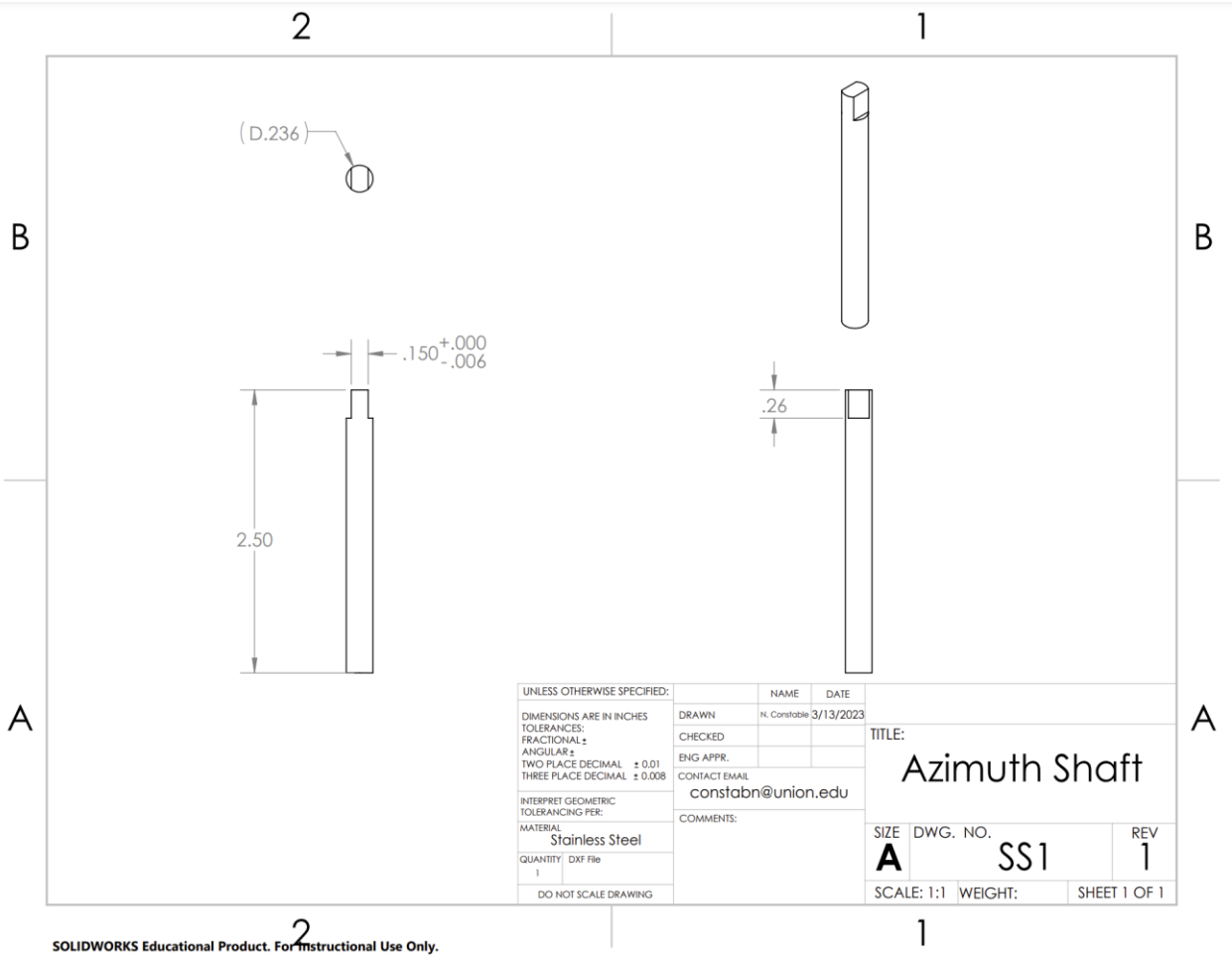
2
1
B
A
(D.236)
.150 +.000 -.006
2.50
.26
UNLESS OTHERWISE SPECIFIED:
DIMENSIONS ARE IN INCHES
TOLERANCES:
FRACTIONAL ±
ANGULAR ±
TWO PLACE DECIMAL ± 0.01
THREE PLACE DECIMAL ± 0.008
INTERPRET GEOMETRIC TOLERANCING PER:
MATERIAL
Stainless Steel
QUANTITY 1
DXF File
DO NOT SCALE DRAWING
NAME
DATE
DRAWN
N. Constable 3/13/2023
CHECKED
ENG APPR.
CONTACT EMAIL
constabn@union.edu
COMMENTS:
TITLE:
Azimuth Shaft
SIZE A
DWG. NO. SS1
REV 1
SCALE: 1:1
WEIGHT:
SHEET 1 OF 1
SOLIDWORKS Educational Product. For Instructional Use Only.

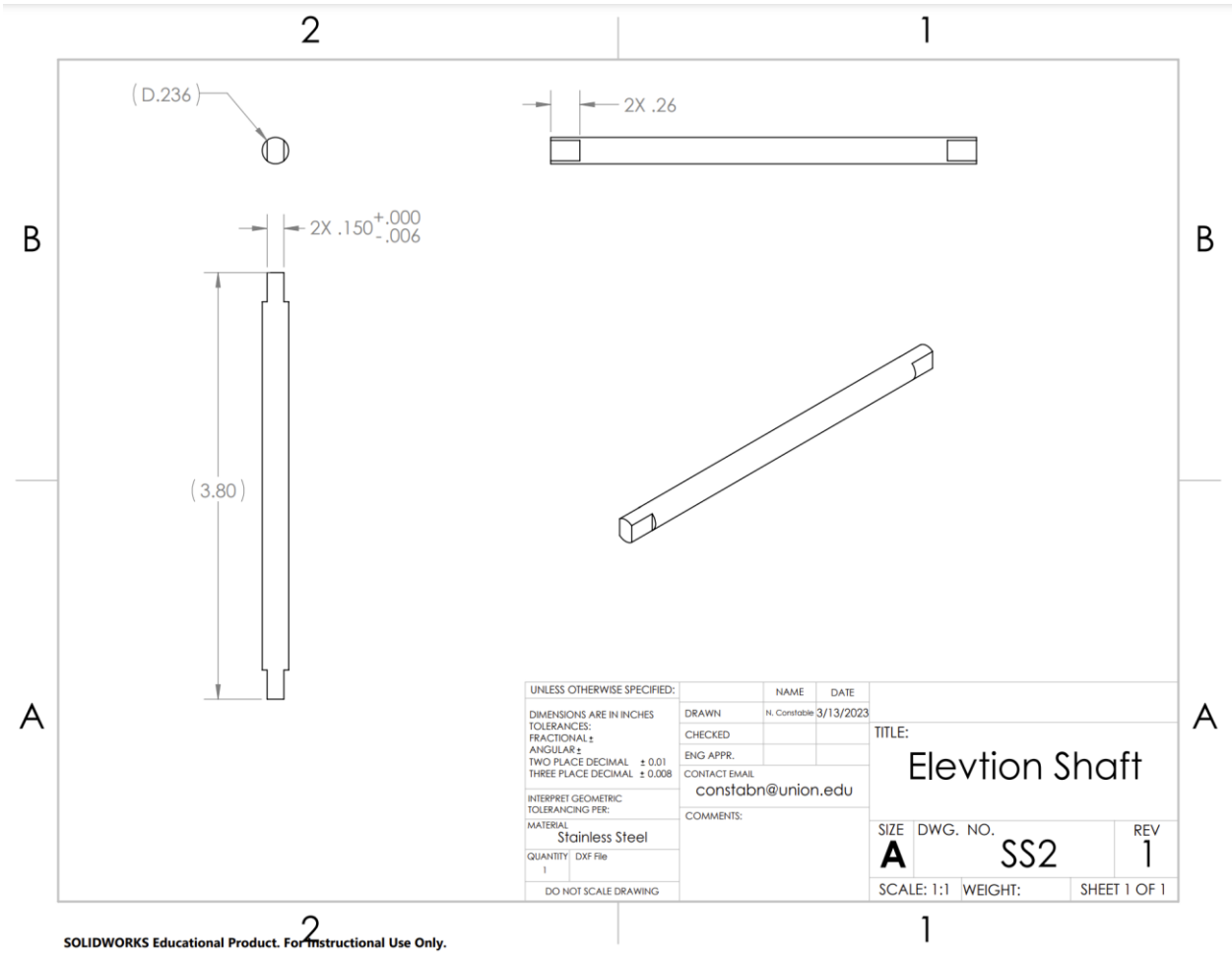
2
1
B
A
(D.236)
2X .26
2X .150 +.000 -.006
(3.80)
UNLESS OTHERWISE SPECIFIED:
DIMENSIONS ARE IN INCHES
TOLERANCES:
FRACTIONAL ±
ANGULAR ±
TWO PLACE DECIMAL ± 0.01
THREE PLACE DECIMAL ± 0.008
INTERPRET GEOMETRIC TOLERANCING PER:
MATERIAL
Stainless Steel
QUANTITY 1
DXF File
DO NOT SCALE DRAWING
NAME
DATE
DRAWN
N. Constable 3/13/2023
CHECKED
ENG APPR.
CONTACT EMAIL
constabn@union.edu
COMMENTS:
TITLE:
Elevtion Shaft
SIZE A
DWG. NO. SS2
REV 1
SCALE: 1:1
WEIGHT:
SHEET 1 OF 1
SOLIDWORKS Educational Product. For Instructional Use Only.

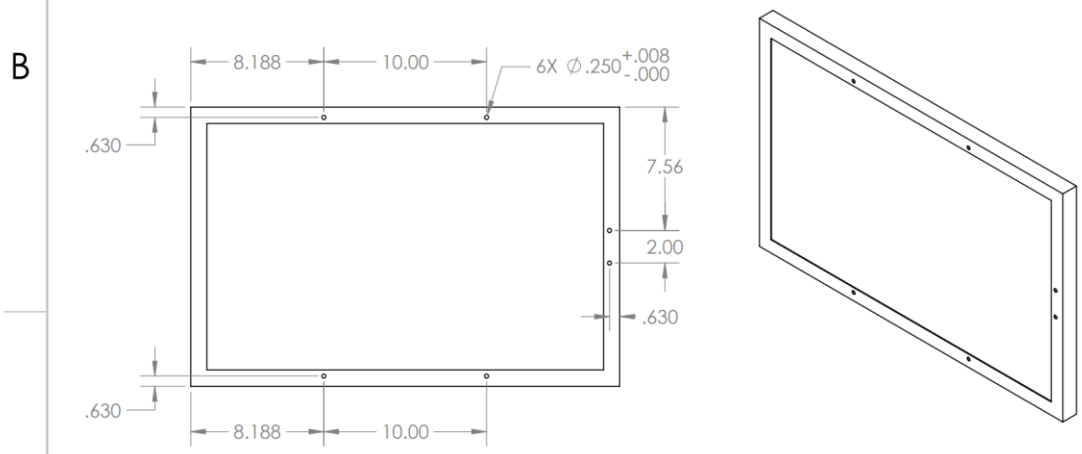

UNLESS OTHERWISE SPECIFIED:		NAME	DATE
DIMENSIONS ARE IN INCHES TOLERANCES: FRACTIONAL ± ANGULAR ± TWO PLACE DECIMAL ± 0.01 THREE PLACE DECIMAL ± 0.004	DRAWN	N. Constable	3/1/2023
	CHECKED		
	ENG APPR.		
	CONTACT EMAIL: constabn@union.edu		
INTERPRET GEOMETRIC TOLERANCING PER:	COMMENTS:		
MATERIAL			
QUANTITY: 1 — DXF File			
DO NOT SCALE DRAWING			

TITLE: Panel

SIZE	DWG. NO.	REV
A	O1	1

SCALE: 1:7 | WEIGHT: | SHEET 1 OF 1

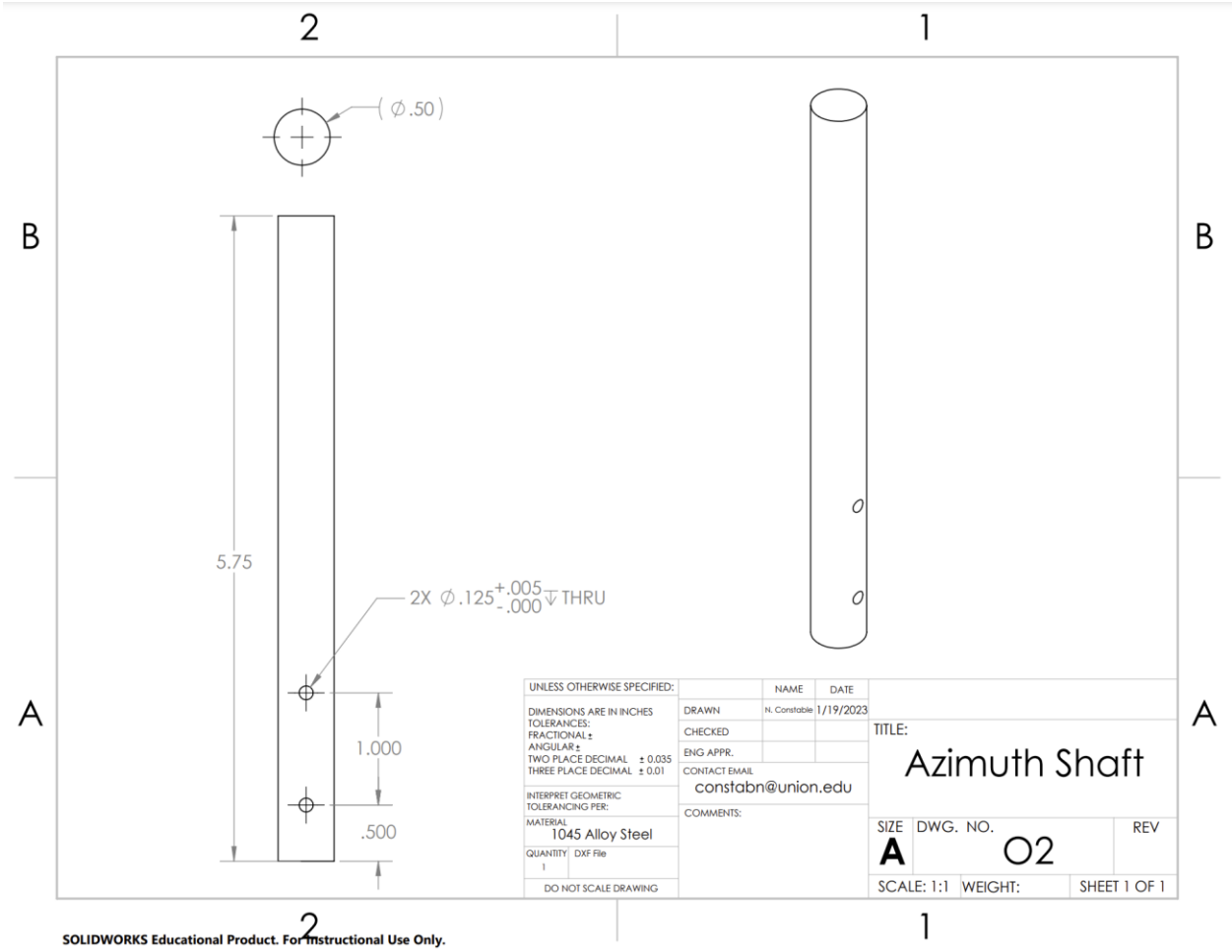
2
1
B
A
Ø.50
5.75
2X Ø.125 +.005 -.000 ↧ THRU
1.000
.500
UNLESS OTHERWISE SPECIFIED:
DIMENSIONS ARE IN INCHES
TOLERANCES:
FRACTIONAL ±
ANGULAR ±
TWO PLACE DECIMAL ± 0.035
THREE PLACE DECIMAL ± 0.01
INTERPRET GEOMETRIC TOLERANCING PER:
MATERIAL
1045 Alloy Steel
QUANTITY 1
DXF File
DO NOT SCALE DRAWING
NAME
DATE
DRAWN
N. Constable
1/19/2023
CHECKED
ENG APPR.
CONTACT EMAIL
constabn@union.edu
COMMENTS:
TITLE:
Azimuth Shaft
SIZE
A
DWG. NO.
O2
REV
SCALE: 1:1
WEIGHT:
SHEET 1 OF 1
SOLIDWORKS Educational Product. For Instructional Use Only.

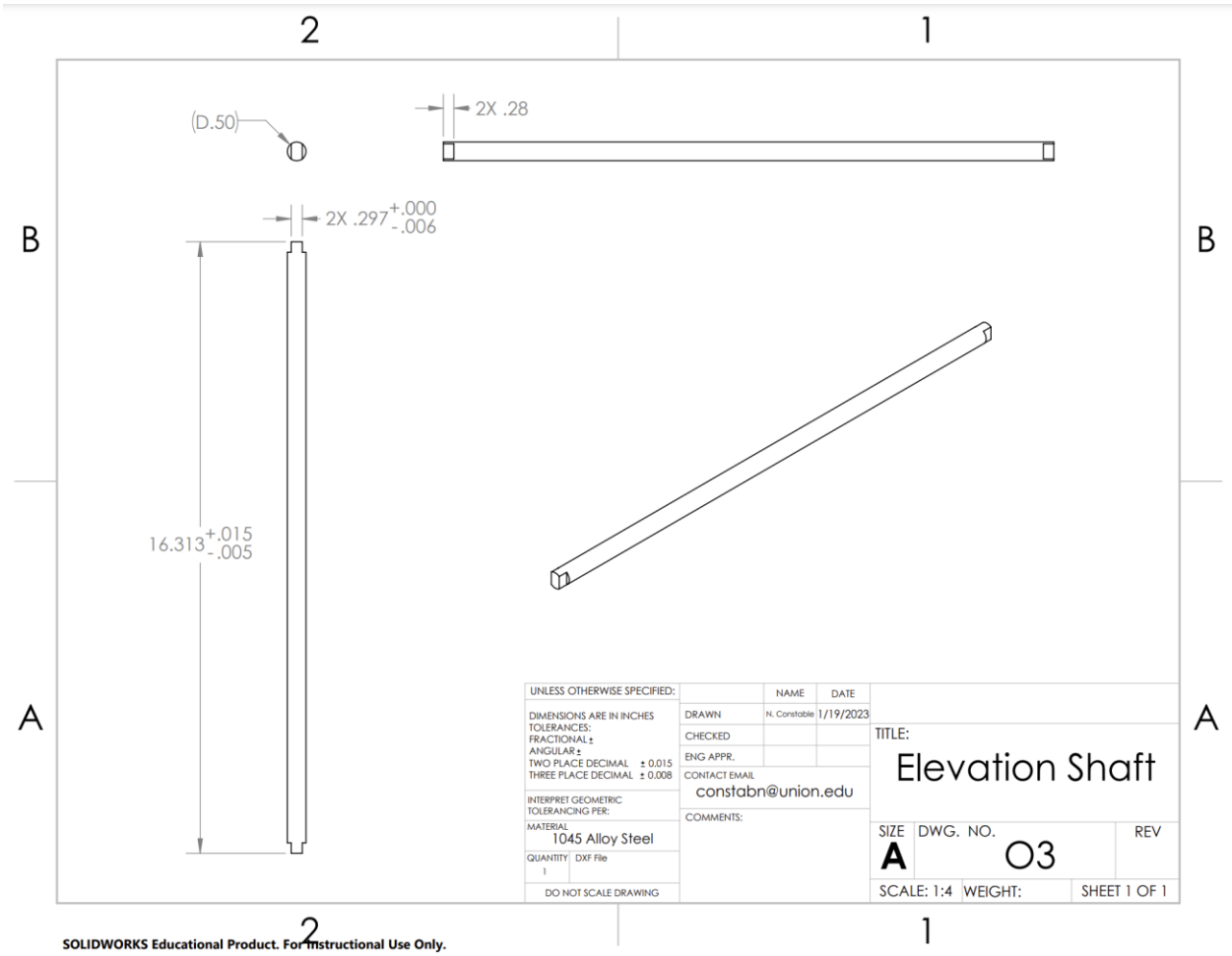
2
1
B
A
(D.50)
2X .28
2X .297 +.000 -.006
16.313 +.015 -.005
UNLESS OTHERWISE SPECIFIED:
DIMENSIONS ARE IN INCHES
TOLERANCES:
FRACTIONAL ±
ANGULAR ±
TWO PLACE DECIMAL ± 0.015
THREE PLACE DECIMAL ± 0.008
INTERPRET GEOMETRIC TOLERANCING PER:
MATERIAL
1045 Alloy Steel
QUANTITY 1
DXF File
DO NOT SCALE DRAWING
NAME
DATE
DRAWN
N. Constable
1/19/2023
CHECKED
ENG APPR.
CONTACT EMAIL
constabn@union.edu
COMMENTS:
TITLE:
Elevation Shaft
SIZE
A
DWG. NO.
O3
REV
SCALE: 1:4
WEIGHT:
SHEET 1 OF 1
SOLIDWORKS Educational Product. For Instructional Use Only.

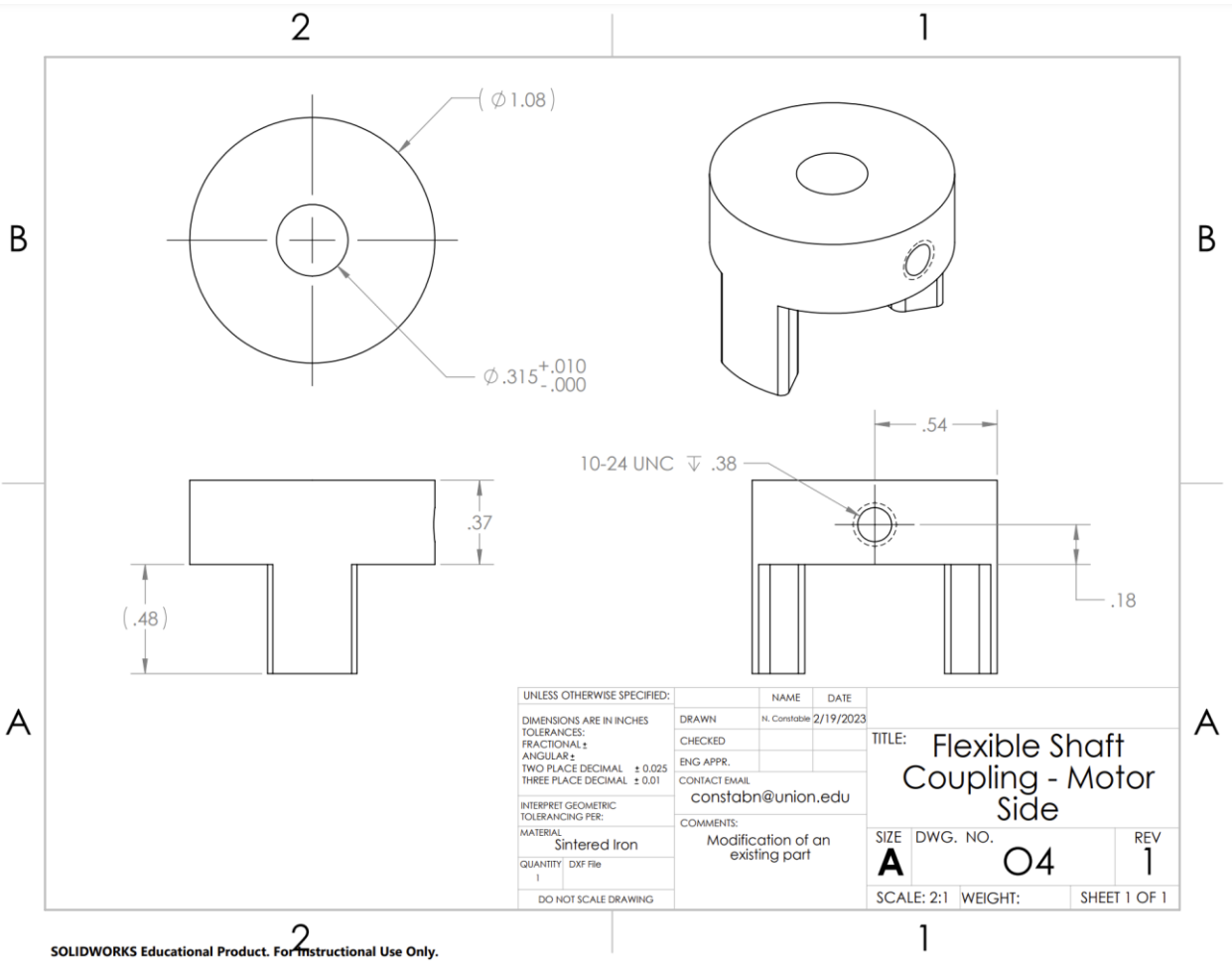
2
1
B
A
(∅1.08)
∅.315 +.010 -.000
.54
10-24 UNC ↧ .38
.37
(.48)
.18
UNLESS OTHERWISE SPECIFIED:
DIMENSIONS ARE IN INCHES
TOLERANCES:
FRACTIONAL ±
ANGULAR ±
TWO PLACE DECIMAL ± 0.025
THREE PLACE DECIMAL ± 0.01
INTERPRET GEOMETRIC TOLERANCING PER:
MATERIAL
Sintered Iron
QUANTITY 1
DXF File
DO NOT SCALE DRAWING
NAME
DATE
DRAWN
N. Constable 2/19/2023
CHECKED
ENG APPR.
CONTACT EMAIL
constabn@union.edu
COMMENTS:
Modification of an existing part
TITLE:
Flexible Shaft Coupling - Motor Side
SIZE
A
DWG. NO.
04
REV
1
SCALE: 2:1
WEIGHT:
SHEET 1 OF 1
SOLIDWORKS Educational Product. For Instructional Use Only.

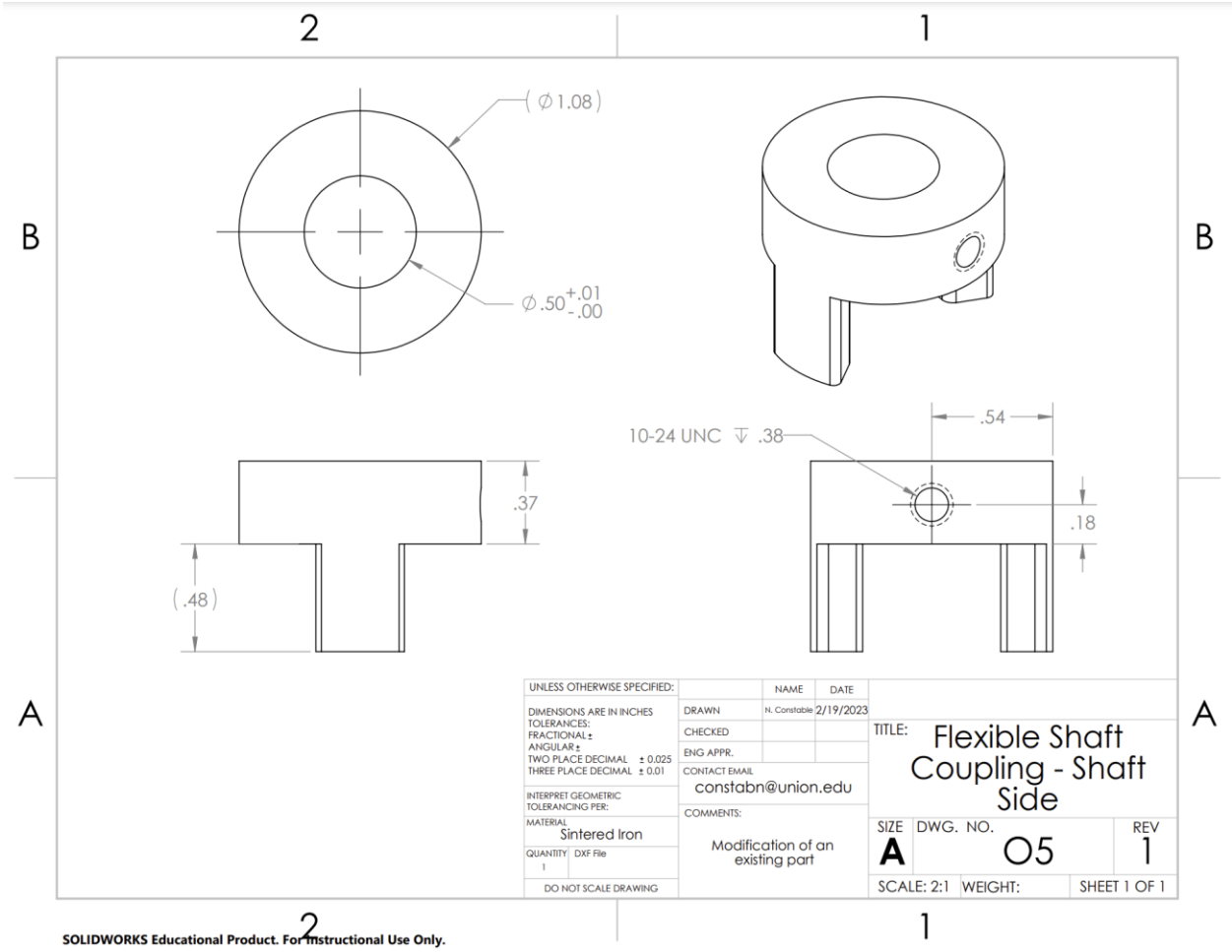
2
1
B
A
(∅1.08)
∅.50 +.01 -.00
.37
(.48)
10-24 UNC ↧ .38
.54
.18
UNLESS OTHERWISE SPECIFIED:
DIMENSIONS ARE IN INCHES
TOLERANCES:
FRACTIONAL ±
ANGULAR ±
TWO PLACE DECIMAL ± 0.025
THREE PLACE DECIMAL ± 0.01
INTERPRET GEOMETRIC TOLERANCING PER:
MATERIAL
Sintered Iron
QUANTITY 1
DXF File
DO NOT SCALE DRAWING
NAME
DATE
DRAWN
N. Constable 2/19/2023
CHECKED
ENG APPR.
CONTACT EMAIL
constabn@union.edu
COMMENTS:
Modification of an existing part
TITLE:
Flexible Shaft Coupling - Shaft Side
SIZE A
DWG. NO. O5
REV 1
SCALE: 2:1
WEIGHT:
SHEET 1 OF 1
SOLIDWORKS Educational Product. For Instructional Use Only.

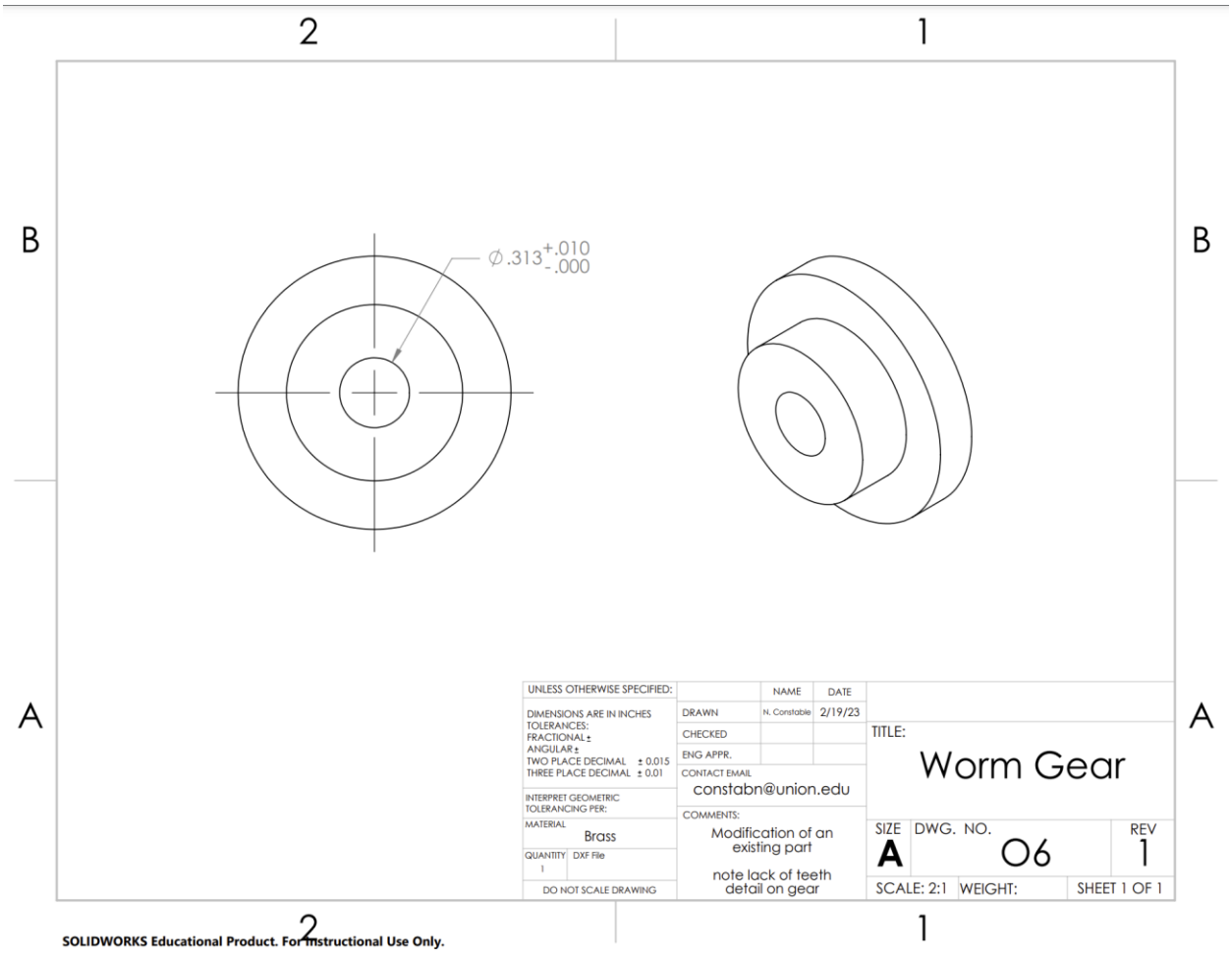
2
1
B
B
A
A
Ø.313 +.010 -.000
UNLESS OTHERWISE SPECIFIED:
DIMENSIONS ARE IN INCHES
TOLERANCES:
FRACTIONAL ±
ANGULAR ±
TWO PLACE DECIMAL ± 0.015
THREE PLACE DECIMAL ± 0.01
INTERPRET GEOMETRIC TOLERANCING PER:
MATERIAL
Brass
QUANTITY 1
DXF File
DO NOT SCALE DRAWING
NAME
DATE
DRAWN
N. Constable
2/19/23
CHECKED
ENG APPR.
CONTACT EMAIL
constabn@union.edu
COMMENTS:
Modification of an existing part
note lack of teeth detail on gear
TITLE:
Worm Gear
SIZE
A
DWG. NO.
O6
REV
1
SCALE: 2:1
WEIGHT:
SHEET 1 OF 1
2
1
SOLIDWORKS Educational Product. For Instructional Use Only.

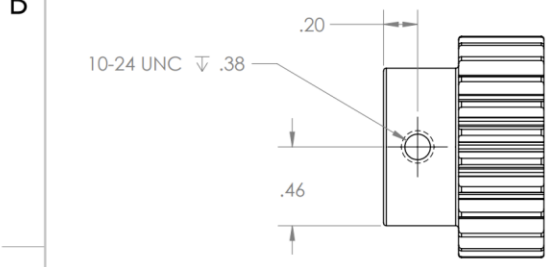

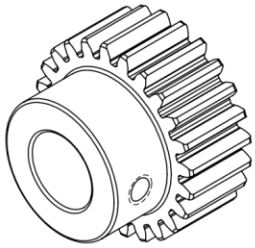

UNLESS OTHERWISE SPECIFIED:		NAME	DATE
DIMENSIONS ARE IN INCHES TOLERANCES: FRACTIONAL ± ANGULAR ± TWO PLACE DECIMAL ± 0.015 THREE PLACE DECIMAL ± 0.01	DRAWN	N. Constable	2/19/2023
	CHECKED		
	ENG APPR.		
	CONTACT EMAIL: constabn@union.edu		
INTERPRET GEOMETRIC TOLERANCING PER:			
MATERIAL: 1117 Carbon Steel	COMMENTS: Modification of an existing part		
QUANTITY: 1 / DXF File			
DO NOT SCALE DRAWING			

TITLE: 1/2in Spur Gear

SIZE	DWG. NO.	REV
A	O7	
SCALE: 2:1	WEIGHT:	SHEET 1 OF 1

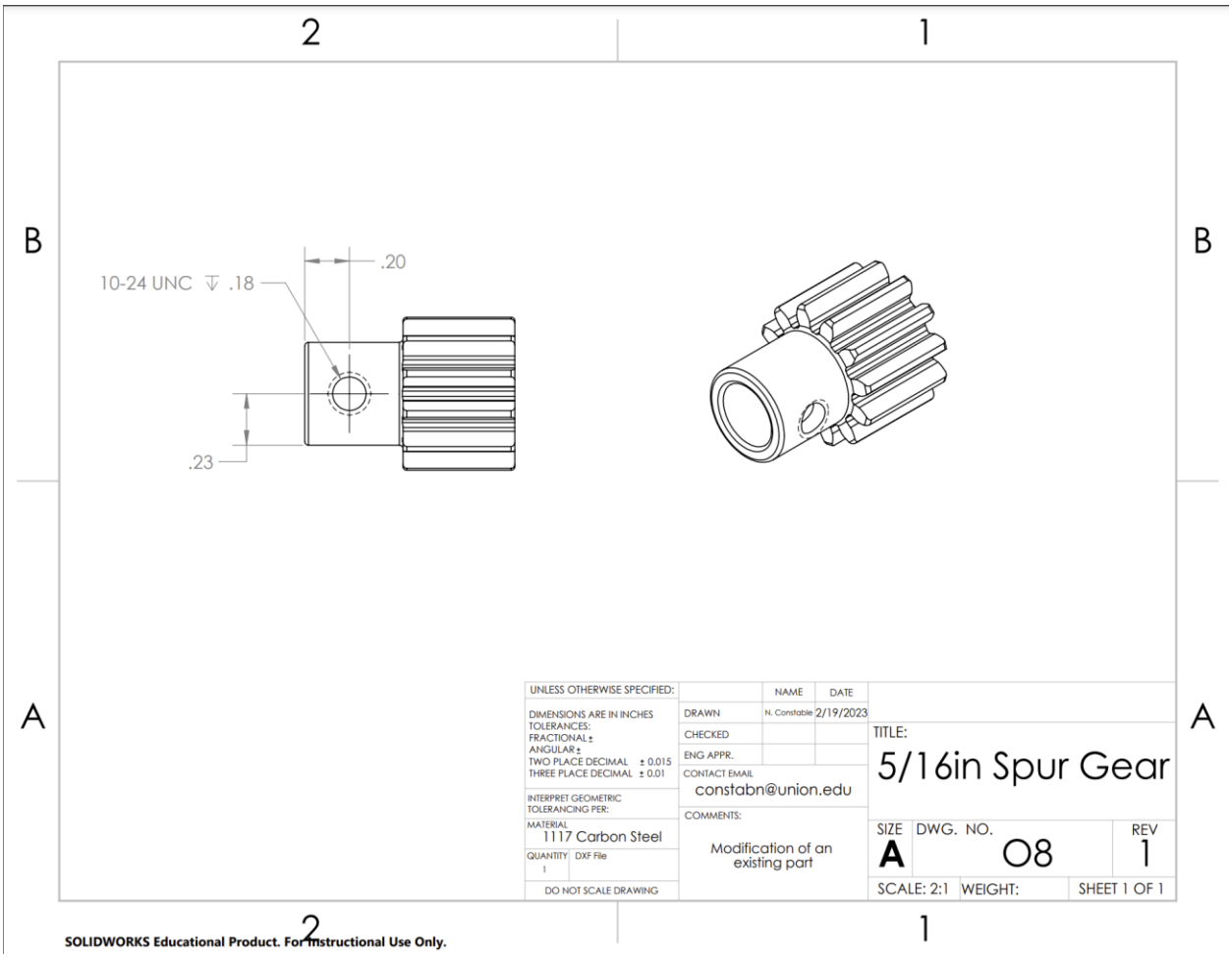
2
1
B
A
10-24 UNC ↧ .18
.20
.23
UNLESS OTHERWISE SPECIFIED:
DIMENSIONS ARE IN INCHES
TOLERANCES:
FRACTIONAL ±
ANGULAR ±
TWO PLACE DECIMAL ± 0.015
THREE PLACE DECIMAL ± 0.01
INTERPRET GEOMETRIC TOLERANCING PER:
MATERIAL
1117 Carbon Steel
QUANTITY
1
DXF File
DO NOT SCALE DRAWING
NAME
DATE
DRAWN
N. Constable
2/19/2023
CHECKED
ENG APPR.
CONTACT EMAIL
constabn@union.edu
COMMENTS:
Modification of an existing part
TITLE:
5/16in Spur Gear
SIZE
A
DWG. NO.
O8
REV
1
SCALE: 2:1
WEIGHT:
SHEET 1 OF 1
SOLIDWORKS Educational Product. For Instructional Use Only.

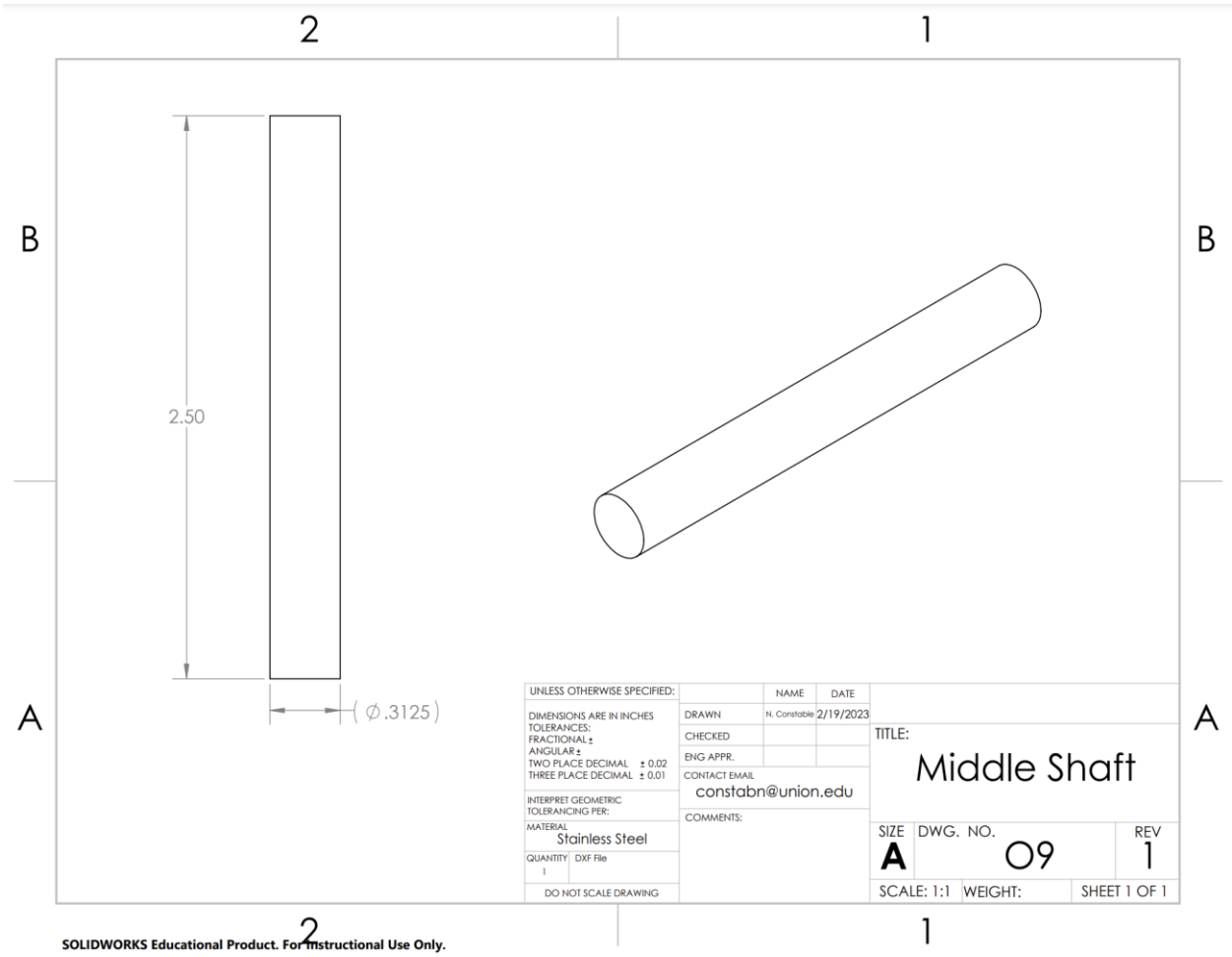
2
1
B
B
A
A
2.50
(∅.3125)
UNLESS OTHERWISE SPECIFIED:
DIMENSIONS ARE IN INCHES
TOLERANCES:
FRACTIONAL ±
ANGULAR ±
TWO PLACE DECIMAL ± 0.02
THREE PLACE DECIMAL ± 0.01
INTERPRET GEOMETRIC TOLERANCING PER:
MATERIAL
Stainless Steel
QUANTITY 1
DXF File
DO NOT SCALE DRAWING
NAME
DATE
DRAWN
N. Constable 2/19/2023
CHECKED
ENG APPR.
CONTACT EMAIL
constabn@union.edu
COMMENTS:
TITLE:
Middle Shaft
SIZE A
DWG. NO. O9
REV 1
SCALE: 1:1
WEIGHT:
SHEET 1 OF 1
2
1
SOLIDWORKS Educational Product. For Instructional Use Only.

Appendix F: Full Arduino Code

```
#include <Arduino.h>
#include <SoftwareSerial.h>

// Driving the two pololu gearmotors on a DRV8833
#define A1_pin 10
#define A2_pin 11
#define B1_pin 13
#define B2_pin 12
//Encoder Pins
#define MA_EA 3   //3
#define MA_EB 4   //2
#define MB_EA 5   //5
#define MB_EB 6   //4
//Motor Position
int pos_A = 0;
int pos_B = 0;

//PID Controller
int prevT = 0;
float eprev = 0;
float eintegral = 0;


// The serial connection to the GPS module
#define rxPin 2
#define txPin 3
SoftwareSerial mySerial = SoftwareSerial(rxPin, txPin);


void setup() {
  Serial.begin(9600);

  // put your setup code here, to run once:
  // Set pins to output so they send information to the motor driver
  pinMode(A1_pin, OUTPUT);
  pinMode(A2_pin, OUTPUT);
  pinMode(B1_pin, OUTPUT);
  pinMode(B2_pin, OUTPUT);

    // Start with motor off
  digitalWrite(A1_pin, LOW);
  digitalWrite(A2_pin, LOW);
  digitalWrite(B1_pin, LOW);
  digitalWrite(B2_pin, LOW);
```

```
  // Set pins to input so they recieve information from the motor driver
  pinMode(MA_EA, INPUT_PULLUP);
  pinMode(MA_EB, INPUT_PULLUP);
  pinMode(MB_EA, INPUT_PULLUP);
  pinMode(MB_EB, INPUT_PULLUP);
  attachInterrupt(digitalPinToInterrupt(MA_EA),readEncoderA,RISING);
  attachInterrupt(digitalPinToInterrupt(MB_EA),readEncoderB,RISING);

  // Sets pin mode for gps module
  pinMode(rxPin, INPUT);
  pinMode(txPin, OUTPUT);

  mySerial.begin(9600);
}

void set_motor(int diff, int speed, int X1_pin, int X2_pin) {
  if (diff > .01) {  // clockwise
    digitalWrite(X1_pin, LOW);
    digitalWrite(X2_pin, HIGH);

  } else if (diff < 0.01) {  // counter clockwise
    digitalWrite(X1_pin, HIGH);
    digitalWrite(X2_pin, LOW);

  } else {
    digitalWrite(X1_pin, LOW);
    digitalWrite(X2_pin, LOW);
  }
}

void motor_feedback() {
  int A_A = digitalRead(MA_EA);
  int A_B = digitalRead(MA_EB);
  int B_A = digitalRead(MB_EA);
  int B_B = digitalRead(MB_EB);
  Serial.print(B_A*5);
  Serial.print(" ");
  Serial.print(B_B*5);
  Serial.println();
}

void readEncoderA(){
  int readA_B = digitalRead(MA_EB);
  if (readA_B>0){
```

```
    pos_A++;
  }
  else{
    pos_A--;
  }
}

void readEncoderB(){
  int readB_B = digitalRead(MB_EB);
  if (readB_B>0){
    pos_B++;
  }
  else{
    pos_B--;
  }
}

void checkLimit(){
  if (pos_A > 1436750){
    digitalWrite(A1_pin, LOW);
    digitalWrite(A2_pin, LOW);
  }
  if (pos_A < 1436750){
    digitalWrite(A1_pin, LOW);
    digitalWrite(A2_pin, LOW);
  }
  if (pos_B > 267000){
    digitalWrite(B1_pin, LOW);
    digitalWrite(B2_pin, LOW);
  }
  if (pos_B < -158042){
    digitalWrite(B1_pin, LOW);
    digitalWrite(B2_pin, LOW);
  }
}

float read_current(float sens_val) {
  float RS = .3;           // Shunt resistor value (in ohms)
  const int ref_volt = 5;     // Voltage supplied to sensor for analog
read
  float current;              // Calculated current value

// Remap the ADC value into a voltage number (5V reference)
  float voltage = (sens_val * ref_volt) / 1023;
  // Serial.print(voltage, 8);
```

```
  // Serial.println(" V");

  current = voltage / RS;

  // Serial.print(current, 8);
  // Serial.println(" A");
  return current;
  delay(500);
}

float read_current5(float sens_val) {
  float RS = .57;
  const int ref_volt = 5;
  float current;

  float voltage = (sens_val * ref_volt) / 1023;
  // Serial.print(voltage, 3);
  // Serial.println(" V");
  current = voltage / RS;
  // Serial.print(current, 3);
  // Serial.println(" A");
  return current;
  delay(500);
}

void loop() {
  float sensor1 = analogRead(A0);  //takes the value of N sensor
  float sensor2 = analogRead(A1);  //takes the value of E sensor
  float sensor3 = analogRead(A2);  //takes the value of S sensor
  float sensor4 = analogRead(A3);  //takes the value of W sensor
  // Serial.println(" ");

  // Serial.print("Sensor 1: ");
  // Serial.println(sensor1);

  // Serial.print("Sensor 3: ");
  // Serial.println(sensor3);

  // Serial.println(" ");

  // Serial.print("Sensor 2: ");
  // Serial.println(sensor2);

  // Serial.print("Sensor 4: ");
  // Serial.println(sensor4);
```

```
  delay(1000);
  //-------------------------------------------------------
  //                    CURRENT READING
  //-------------------------------------------------------
  float current1 = read_current(sensor1);
  float current2 = read_current(sensor2);
  float current3 = read_current5(sensor3);
  float current4 = read_current(sensor4);


  //-------------------------------------------------------
  //                       ELEVATION
  //-------------------------------------------------------
  //map difference in elevation inputs to the 255 scale
  int dif_elev = sensor1 - sensor3;
  int dif_elev_curr = current1 - current3;
  int speed_elev = map(dif_elev, 0, 1023, 0, 255);
  int dif_elev_current = current1 - current3;

  //Set the elevation motor speed to
  set_motor(dif_elev_current, speed_elev, B1_pin, B2_pin);
  checkLimit();
  //-------------------------------------------------------
  //                       AZIMUTH
  //-------------------------------------------------------
  int dif_azim = sensor2 - sensor4;
  int dif_azim_curr = current2 - current4;
  int speed_azim = map(dif_azim, 0, 1023, 0, 255);
  int dif_azim_current = current2 - current4;

  //Set the azimuth motor speed
  set_motor(dif_azim, speed_azim, A1_pin, A2_pin);
  checkLimit();
  //-------------------------------------------------------
  //                       GPS READ
  //-------------------------------------------------------
    if (mySerial.available() > 0){
    //get the byte data from the GPS
    byte gpsData = mySerial.read();
    Serial.write(gpsData);
    }
  motor_feedback();

}
```